

ON THE CRANIAL OSTEOLOGY OF THE SHORT-TAILED OPOSSUM
MONODELPHIS BREVICAUDATA (DIDELPHIDAE, MARSUPIALIA)

JOHN R. WIBLE

Curator, Section of Mammals

ABSTRACT

The Section of Mammals, Carnegie Museum of Natural History houses 54 partial and complete skulls of the short-tailed opossum *Monodelphis*. Described in detail and illustrated are the external surfaces of the bones of the skull for *M. brevicaudata* CM 52729 and the external and internal surfaces of one bone of the basicranium, the petrosal, for *Monodelphis* sp. CM 5024. The disposition of cranial foramina ranging in size from the foramen magnum to tiny emissary and nutrient foramina was studied in all 54 specimens, which in addition to 16 *M. brevicaudata*, includes four *M. dimidiata*, 29 *M. domestica*, two *M. osgoodi*, and three *Monodelphis* sp. Three categories of foramina were identified: (1) foramina bilaterally present in all specimens that show no significant variation; (2) bilateral and midline foramina present in all specimens that show variation in size, number, position, distinctness from other foramina, or elements contributing to their walls; and (3) foramina that are not present in all specimens that also vary in size, number, and position. Comparisons were made with four outgroups, the didelphid *Didelphis albiventris*, the dasyurid *Dasyurus maculatus*, the early Paleocene metatherian *Pucadelphys andinus*, and the Late Cretaceous eutherian *Zalambdalestes lechei*, in order to evaluate the foramina of *Monodelphis* in a phylogenetic context. Of the foramina considered here, four distinguish *Monodelphis*; three distinguish Didelphidae; 15 distinguish Marsupialia; nine distinguish Metatheria; and seven occur across Theria.

KEY WORDS: *Monodelphis*, Didelphidae, Marsupialia, skull, osteology, foramina

INTRODUCTION

Until recently, the bulk of the evidence for our understanding of the basal radiations of marsupial mammals consisted of teeth and jaws (Clemens, 1979). The last few years have witnessed the discovery of well-preserved skulls and even skeletons of basal members of Metatheria (Marshall and Muizon, 1995; Muizon, 1998; Rougier et al., 1998). Didelphidae, the New World opossums, is the extant marsupial family that from a phylogenetic standpoint is generally considered to provide the most appropriate model for studying the anatomy and biomechanics of these basal forms (Wible, 1990; Argot, 2001). However, few detailed, well-illustrated treatments of the didelphid skull or for that matter of any extant marsupial skull are available. In fact, perhaps the most complete description and illustration of a metatherian skull is that of *Pucadelphys andinus* from the early Paleocene of Bolivia (Marshall and Muizon, 1995), referred to Didelphidae by its describers. It is the dearth of similar treatments for extant marsupials that is the impetus for this report. A second impetus is the opportunity to review and standardize anatomical terminology.

A sizeable literature on aspects of didelphid anatomy does exist, with the most comprehensive single source on the didelphid skull likely being Coues (1872), which unfortunately is poorly illustrated and uses terminology that is out of date. Another noteworthy general contribution is the anatomical photographic atlas by Ellsworth (1976), but unfortunately the quality and clarity of the published photographs are uneven, and few features are labelled. More recently, Macrini (2000), in an unpublished masters' thesis, has described the anatomy of the internal surfaces of the skull (e.g., braincase, nasal cavity) of *Monodelphis domestica* based on CT scans; external views of the skull produced from the

Submitted 9 January 2003.

CT scans are published in Macrini (2002:fig. 4). Selected anatomical topics of the didelphid head that have received considerable attention include the basicranium (e.g., Archer, 1976; Maier, 1989; Wible, 1990; Sánchez-Villagra and Wible, 2002) and cranial musculature (e.g., Hiiemae and Jenkins, 1969; Turnbull, 1970; Minkoff et al., 1979). There is also a sizeable literature on aspects of cranial ontogeny in didelphids (e.g., Toeplitz, 1920; Nesslinger, 1956; Maier, 1987a, b; Filan, 1991; Clark and Smith, 1993; Smith, 1994; Rowe, 1996; Abdala et al., 2001; Sánchez-Villagra et al., 2002).

Two didelphids, *Didelphis virginiana* and *Monodelphis domestica*, have become increasingly popular as laboratory models for biomedical research (Tyndale-Biscoe and Janssens, 1988; Saunders and Hind, 1997). Because the latter taxon has been the subject of most recent contributions on aspects of cranial development (e.g., Maier, 1987a, b; Filan, 1991; Clark and Smith, 1993; Smith, 1994), the genus *Monodelphis* was chosen to be the subject of this report, a bone-by-bone description of the exterior of the adult skull. For illustrative purposes, a skull from another species of the genus, *M. breviceaudata*, was chosen for the bulk of the figures. Differences between *M. breviceaudata*, *M. domestica*, and two other species, *M. dimidiata* and *M. osgoodi*, are noted. Fifteen species of *Monodelphis* are recognized by Gardner (1993).

MATERIALS AND METHODS

The Section of Mammals of the Carnegie Museum of Natural History has holdings of 54 skulls of *Monodelphis*, including 16 *M. breviceaudata*, 29 *M. domestica*, 4 *M. dimidiata*, 2 *M. osgoodi*, and 3 *M. sp.* All specimens were examined for this report (see Appendix 1). Three cranial measurements (premaxillary-condylar length, maximum zygomatic breadth, and length of mandible) were taken from 47 of the 54 specimens (see Appendix 2); the remaining seven specimens were damaged in some way, but it was possible to take at least one of these measurements (length of mandible) from them. Regarding age of the specimens, the majority (45 of 54) has all four upper and lower molars in place in the jaws and are considered to be adults. In the remainder, the deciduous third premolar is retained with either the ultimate or penultimate molar not fully erupted (see Appendix 2); these specimens are considered to be juveniles. The third premolar is the only tooth to be replaced in marsupials (Luckett, 1993).

The bone-by-bone descriptions of the exterior of the adult skull are based principally on *Monodelphis breviceaudata* CM 52729, the specimen illustrated in figures 1–6, and 9. The chief exception is the petrosal bone, which is based on an isolated left petrosal of *Monodelphis sp.* CM 5024 (which I provisionally have identified as *M. domestica*) and an isolated right petrosal of *M. breviceaudata* CM 5061; the former is illustrated in figures 7–8. Following the bone-by-bone descriptions is a discussion of the major cranial foramina, their contents, the variations observed among the available sample, and the condition observed in selected outgroups. The descriptions and discussions touch upon some soft-tissue structures of the head, specifically, muscles, nerves, arteries, and veins. The two principal sources for information on soft tissues are the literature (e.g., Tandler, 1899; Hiiemae and Jenkins, 1969; Turnbull, 1970), including some references by the author (e.g., Wible, 1987, 1990; Wible and Hopson, 1995), and unpublished observations based on the study of serially sectioned specimens. The principal collections that house embryological series of marsupials studied by me are as follows: Anatomy Unit, University of Wales, Cardiff, United Kingdom; Duke University Comparative Embryological Collection, Durham, North Carolina; Lehrstuhl für Spezielle Zoologie, Eberhard-Karls-Universität, Tübingen, Germany; and Zentrum der Morphologie, Johann-Wolfgang-Goethe-Universität, Frankfurt am Main, Germany.

Unfortunately, morphologists that have published on the cranial anatomy of extinct and extant metatherians have not employed a common terminology for their descriptions. The reasons for this are many, but largely are the result of history and of unresolved homologies. As a step toward a standardized terminology, Appendix 3 details the sources for the non-dental anatomical terms employed. Whenever possible, the Latin term (or anglicized version thereof) from the fourth edition of the *Nomina Anatomica Veterinaria* (1994) has been used. For the dentition, the abbreviations “I, C, P, M” and “i, c, p, m” are used to refer to upper and lower incisors, canines, premolars, and molars, respectively.

Institutional Abbreviations

AMNH	Department of Mammalogy, American Museum of Natural History, New York, New York.
CM	Section of Mammals, Carnegie Museum of Natural History, Pittsburgh, Pennsylvania.

FMNH	Division of Mammals, Field Museum, Chicago, Illinois.
UKMNH	Division of Mammals, University of Kansas Natural History Museum, Lawrence, Kansas.
WAM	Western Australian Museum, Perth.

DESCRIPTIONS

The cranium of *Monodelphis brevicaudata* CM 52729 is drawn in dorsal, lateral (with and without zygoma), ventral, and occipital views (Figs. 1–2, 4–6, 9) and the mandible in lateral and occlusal views (Figs. 2–3). In addition, the left petrosal of *M. sp.* CM 5024 is drawn in ventral, dorsal, and lateral views (Figs. 7–8). Other useful illustrations of *Monodelphis* already in the literature include line drawings of the cranium of *M. brevicaudata* AMNH 130516 in dorsal, lateral, and ventral views (Novacek, 1993:fig. 9.4), stipple drawings of the right braincase and lower jaw of *M. domestica* in lateral and ventral views (Maier, 1989:fig. 1), stereophotographs of the basicranium of *M. dimidiata* WAM M6824 in ventral and oblique ventral views (Archer, 1976:plate 6A, B), stipple drawings of the right ear region of *M. scalops* (Maier, 1989:fig. 2), and stipple drawings of the right petrosal of *M. sp.* AMNH 133248 in ventral and lateral views (Sánchez-Villagra and Wible, 2002:figs. 3b and 5d).

Nasal

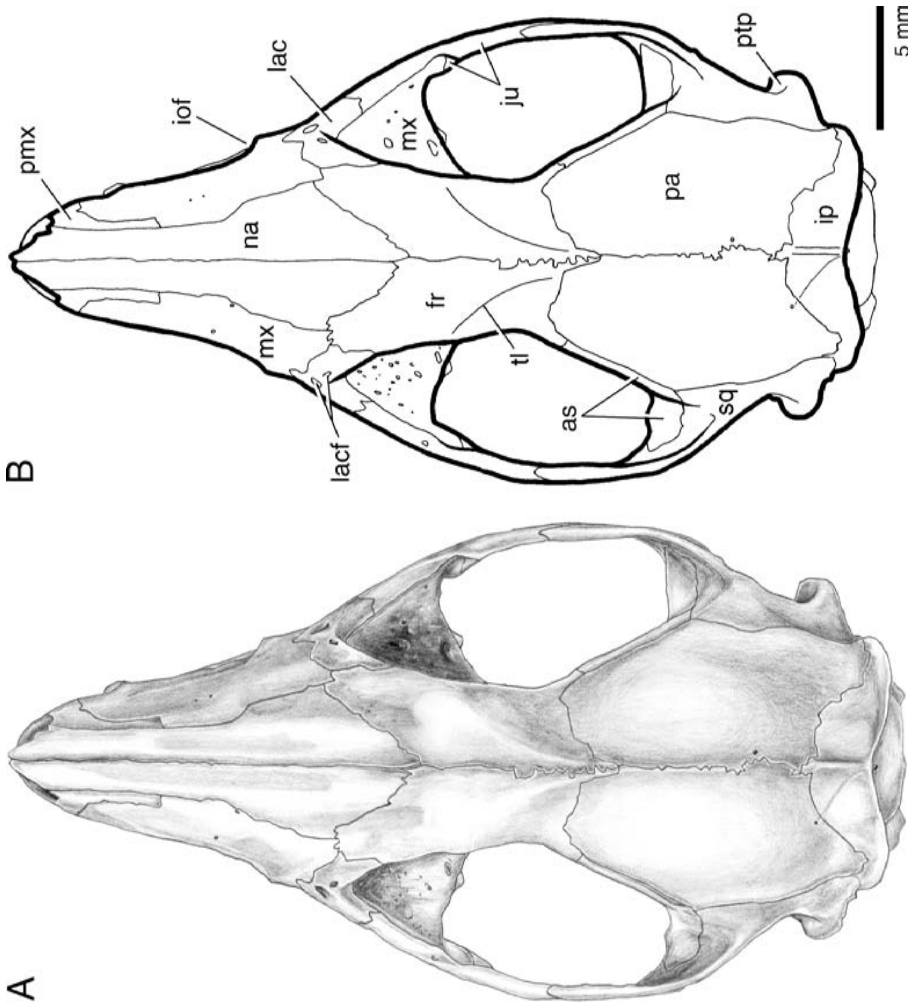
The paired nasal bones occupy the dorsum of the snout and contribute to the dorsal border of the external nasal aperture (Figs. 1–2).

In dorsal view (Fig. 1), the nasals contact, from anterior to posterior, the premaxillae, maxillae, and frontals. The nasals extend from the tip of the rostrum to the level of the M3, a little behind the anterior orbital rim. The rostral two-thirds of the paired nasals are narrow, with essentially parallel sides; the posterior one-third is somewhat diamond-shaped, achieving its maximum width just rostral to the frontomaxillary suture. The frontals overlap the nasals and produce a roughly V-shaped suture. In lateral view (Fig. 2), the anterior nasal spine is well developed, resulting in a considerable nasal overhang of the external nasal aperture. Although the nasal's rim on the external nasal aperture is curved (Fig. 1), there is no anterior nasal notch as occurs in some other taxa (e.g., the Late Cretaceous eutherian *Zalambdalestes*, Wible et al., in press). There are no foramina in the nasals.

Premaxilla

The paired premaxillae are small elements that contain the alveoli for the five upper incisors and, along with the nasals, form the tip of the rostrum (Fig. 2). The premaxillae contact the nasals dorsally and the maxillae posteriorly. The alveolar processes of the premaxillae contain the incisors. The facial processes of the left and right premaxillae form the floor and side walls of the external nasal aperture, the roof being formed by the nasals. The palatal processes of the premaxillae form most of the border for the large incisive foramina (Fig. 5).

In lateral view (Fig. 2), the dorsoventral dimension of the rostral tip of the facial process is very short, and the included root of the I1 must also be short. Posterior to the rostral tip, the dorsoventral dimension increases gradually to its maximum at the level of the I5. The bulk of the contact of the posterior border of the facial process with the maxilla is vertical, starting ventrally just behind the I5 alveolus (to which the maxilla makes a very small contribution posterolaterally). As this suture nears the nasal bone, there is a finger-like projection of the premaxilla (the posterodorsal process) interposed between the maxilla and nasal that reaches to just behind the level of the canine. There is a minute nutrient foramen



bilaterally present in the facial process dorsal to the I3–4 embrasure, near the rim of the external nasal aperture.

In ventral view (Fig. 5), the alveolar and palatal processes of the premaxilla form approximately one-fifth the length of the hard palate. Of the upper five incisors, the I1 alveolus is the largest and just off the midline; the right and left I1 are angled toward each other and their crowns contact. I1 and I2 are separated by a diastema. From the I2 through I5, there is a slight size increase in tooth size; the alveoli are very close and the crowns contact. Behind the I5 is a large depression for the tip of the lower canine. The lateral wall and posterolateral part of the depression are formed by the maxilla, and the remainder by the premaxilla. The posteromedial border of the depression, which is premaxilla, also forms the anteromedial border of the alveolus of the upper canine. The most noteworthy structure in the palatal process is the large, finger-like incisive foramen, which lies medial to the alveoli of I3–5 and the depression for the lower canine. The bulk of this foramen is within the premaxilla; the maxilla forms the posterior border, which is somewhat U-shaped. Forming the foramen's medial border is the medial palatine process of the premaxilla, which increases slightly in breadth posteriorly. Visible through the incisive foramen is the maxilloturbinal.

Maxilla

The paired maxillae are the major elements of the lateral wall of the snout and hard palate, and contain the alveoli for the canine and seven postcanine teeth (three premolars and four molars). On the face (Fig. 2), the maxilla contacts the premaxilla anteriorly and dorsally, the nasal and frontal dorsally, and the lacrimal and jugal posteriorly. On the palate (Fig. 5), the maxilla contacts the premaxilla anteriorly and the palatine posteromedially. The maxilla also contributes to the anterior floor of the orbit.

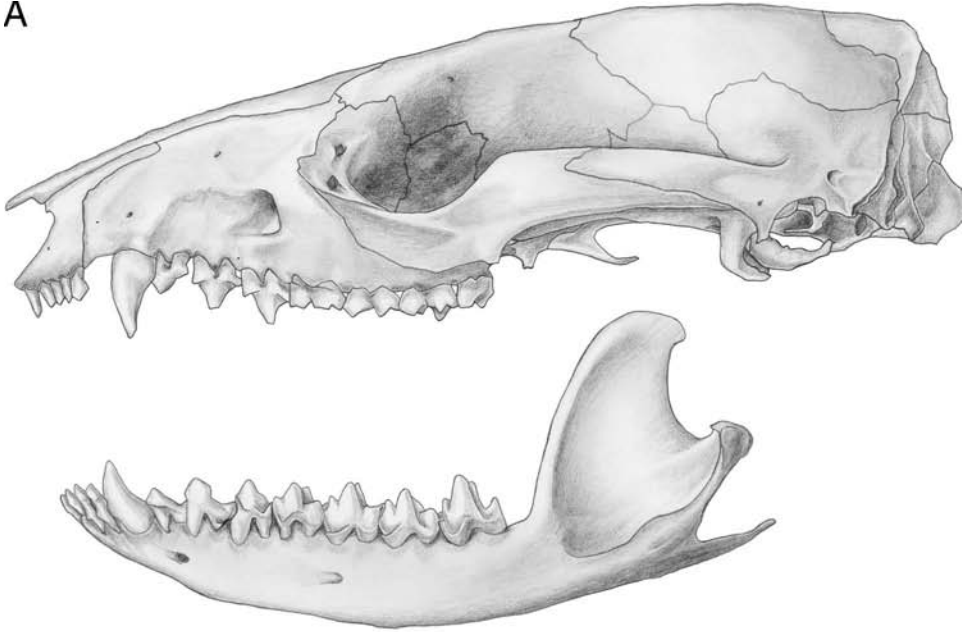
On the face (Fig. 2), the sutures with the premaxilla and nasal have been described above. Posterodorsally, at the level of the M1–M2 embrasure, the maxilla contacts the frontal at a narrow, irregular suture. Ventral to this, the maxilla contacts the lacrimal and then the jugal at gently curved sutures, although that with the lacrimal includes a small, V-shaped process of the maxilla at the level of the upper lacrimal foramen. The most conspicuous feature on the facial process of the maxilla is the large infraorbital foramen. In lateral view, it is a roughly U-shaped aperture, open rostrally, with the base of the U dorsal to the P3–M1 embrasure; in anterior view it is subcircular. Also prominent is the large root of the upper canine, which is visible through the thin bone. It is gently curved, extending posteriorly behind the level of the anterior root of P2 and dorsally above the level of the upper lacrimal foramen. There are also several small nutrient foramina on the face, with the most conspicuous ones posterodorsal and anterior to the canine root, along the course of the nasolacrimal duct, also partially visible through the thin bone.

On the palate (Fig. 5), the suture with the premaxilla has been described above. The intermaxillary suture extends from the level of the canine to the M2 metacone and has a slightly raised crest, more evident posteriorly. The palatines' contribution to the hard palate is small and roughly square, and so the maxilla contacts the palatine at longitudinal and horizontal sutures. The longitudinal suture begins posteriorly in the anteromedial

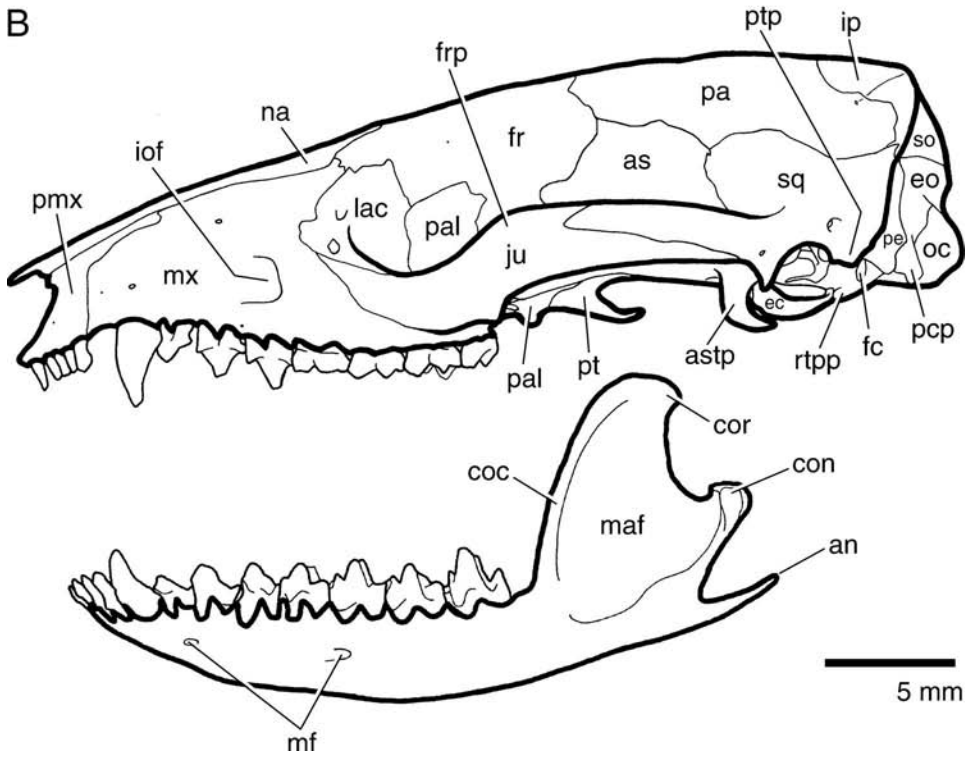
←

Fig. 1.—*Monodelphis brevicaudata* CM 52729, dorsal view of skull (A) with accompanying line drawing (B). Abbreviations: **as**, alisphenoid; **fr**, frontal; **iof**, infraorbital foramen; **ip**, interparietal; **ju**, jugal; **lac**, lacrimal; **lacf**, lacrimal foramen; **mx**, maxilla; **na**, nasal; **pa**, parietal; **pmx**, premaxilla; **ptp**, posttympanic process; **sq**, squamosal; **tl**, temporal line.

A



B



border of the minor palatine foramen and runs more or less forward to the level of the M2 metacone. It turns medially into the horizontal suture, which is interdigitated, with the processes of the palatine reaching nearly to the level of the M2 protocone. The lateral part of the horizontal suture is open, with the palatine forming the posterior border of the elongate major palatine foramen or maxillopalatine vacuity, the most conspicuous feature on the hard palate. The major palatine foramen extends between the level of the P3–M1 and M2–M3 embrasures. Running forward from the anterior edge of the major palatine foramen is a broad, shallow groove for the foramen's contents that reaches nearly to the level of the back of the canine. The minor palatine foramen is oval, on the maxillopalatine suture, posteromedial to M4, and faces anteromedially. The posterolateral border of the foramen is formed by very thin processes of the maxilla and palatine.

The anterior root of the zygoma is formed by the short zygomatic process of the maxilla (Fig. 5). The anterior edge of this process is opposite the M2–M3 embrasure and the posterior edge opposite the M4 paracone. The zygomatic process of the maxilla sends a small lappet posteriorly a short distance along the inner surface of the jugal (Fig. 1). In *Didelphis*, the maxilla has a distinct protuberance dorsal to M4 for attachment of the superficial masseter muscle (Hiimae and Jenkins, 1969; Turnbull, 1970). Such a distinct protuberance is lacking in CM 52729.

The portion of the maxilla housing the roots for M2–4 forms the wedge-shaped floor of the orbit (Fig. 1). In fact, the tips of the medial roots of M3 and 4 are exposed in the orbital floor. The contacts of the maxilla in the orbital floor are with the anterior process of the alisphenoid posteromedially, the palatine medially, the lacrimal anterolaterally, and the jugal laterally (Fig. 4). The maxilla forms the floor and lateral wall of the maxillary foramen, the posterior opening into the infraorbital canal, which is not visible in lateral view. The roof and medial wall of the maxillary foramen are completed by the lacrimal, with a thin sliver of palatine interposed between the maxilla and lacrimal medially.

Palatine

The paired palatine bones have a horizontal process that forms roughly the posterior one-third of the hard palate (Fig. 5) and a perpendicular process that contributes to the medial orbital wall and to the roof and walls of the choanae (Fig. 4).

As noted above with the maxilla, the horizontal processes of the palatines are roughly square and have longitudinal and horizontal sutures with the maxillae (Fig. 5). Because of the thinness of the palatine, it is evident that the palatine overlaps the maxilla along the posterior four-fifths of the longitudinal suture and along the medial one-third of the horizontal suture. Both sutures border sizeable foramina on the hard palate. In the posterior longitudinal suture is the minor palatine foramen, approximately half of which is formed by the palatine in ventral view. In the lateral horizontal suture is the major palatine foramen or maxillopalatine vacuity, of which the palatine forms only the narrow posterior border. Medial to the minor palatine foramen on the right side is a tiny aperture in the palatine that may represent an accessory palatine foramen; the left side has two tiny apertures, both of

←

Fig. 2.—*Monodelphis brevicaudata* CM 52729, left lateral view of skull including mandible (A) with accompanying line drawing (B). Abbreviations: **an**, angular process; **as**, alisphenoid; **astp**, alisphenoid tympanic process; **coc**, coronoid crest; **con**, mandibular condyle; **cor**, coronoid process; **ec**, ectotympanic; **eo**, exoccipital; **fc**, fenestra cochleae; **fr**, frontal; **frp**, frontal process of the jugal; **iof**, infraorbital foramen; **ip**, interparietal; **ju**, jugal; **lac**, lacrimal; **maf**, masseteric fossa; **mf**, mental foramen; **mx**, maxilla; **na**, nasal; **oc**, occipital condyle; **pa**, parietal; **pal**, palatine; **pcp**, paracondylar process of the exoccipital; **pe**, petrosal; **pmx**, premaxilla; **pt**, pterygoid; **ptp**, posttympanic process; **rtpp**, rostral tympanic process of the petrosal; **so**, supraoccipital; **sq**, squamosal.

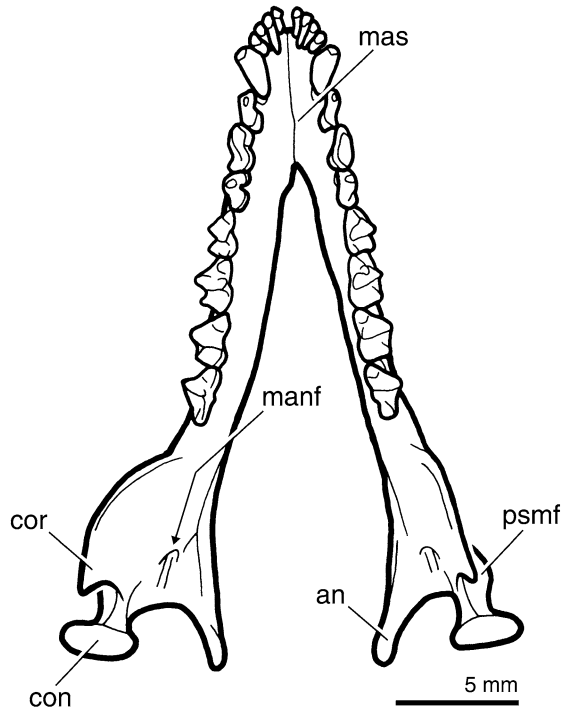


Fig. 3.—*Monodelphis brevicaudata* CM 52729, line drawing of left and right mandibles in occlusal view. Abbreviations: **an**, angular process; **con**, mandibular condyle; **cor**, coronoid process; **manf**, mandibular foramen; **mas**, mandibular symphysis; **psmf**, posterior shelf of the masseteric fossa.

which are slightly more medially positioned than on the right side. As noted above with the intermaxillary suture, the interpalatine suture has a raised crest that in the case of the palatine runs the length of the suture. This crest turns laterally along the posterior border of the horizontal process to form the low postpalatine torus that extends to the minor palatine foramen. Posteromedial to the minor palatine foramen is a small foramen through the postpalatine torus, connecting the hard palate and choanae; this foramen is visible in occipital view (Fig. 9). It likely transmitted structures from the minor palatine foramen to the soft palate.

The lateral surface of the perpendicular process of the palatine lies in the anterior half of the orbitotemporal fossa (Fig. 4). From anterior to posterior, it contacts the lacrimal, frontal, and orbitosphenoid along its dorsal surface, and the maxilla, alisphenoid, pterygoid, and presphenoid along its ventral surface. It is tallest posterior to the lacrimal where it forms roughly the ventral three-fourths of the medial orbital wall, the frontal completing the dorsal fourth. Extending anteriorly and posteriorly from the base of this tallest part of the palatine are narrow anterior and posterior processes. The shorter anterior process extends between the lacrimal and maxilla into the maxillary foramen to the level of the M1–M2 embrasure; the maxillary foramen is at the level of the M2 centrocrista. The posterior process extends into the floor of the sphenorbital fissure, where it contacts the presphenoid and orbitosphenoid. At a level dorsal to the M3–M4 embrasure near the suture with the maxilla, the palatine is pierced by a large, anteromedially directed sphenopalatine foramen. U-shaped in lateral view, in oblique posterolateral view this aperture appears nearly dumbbell shaped, with two foramina merged. Presumably the anterolateral foramen

transmits the sphenopalatine vessels and branches of the maxillary nerve to the hard palate and the posteromedial foramen transmits the caudal nasal nerve and vessels to the nasal cavity. Immediately posterior to the sphenopalatine foramen is a tiny, anterolaterally directed foramen of uncertain function. More posteriorly are three openings that connect the orbital fossa with the choanae. The smaller two are entirely within the palatine: one at the level of the anterior edge of the ethmoidal foramen and the other anterodorsal to that near the suture with the frontal. The largest is elongate, irregular, and situated posterior to the palatine, between that bone and the pterygoid. It is an unossified area that is closed off in some other specimens (e.g., CM 52730, 76730).

The medial surface of the perpendicular process of the palatine forms the lateral wall and contributes to the roof of the choanae (Fig. 5), and extends rostrally into the nasal fossa. At the choanae, the palatine's posterior border is V-shaped and in contact with the pterygoid bone, except along the V's medial leg where the suture contains the irregular opening described above. Along the midline, the palatine abuts the narrow presphenoid bone.

Lacrimal

The paired lacrimal bones form the anterior rim of the orbit and have facial, orbital, and zygomatic processes (Fig. 4).

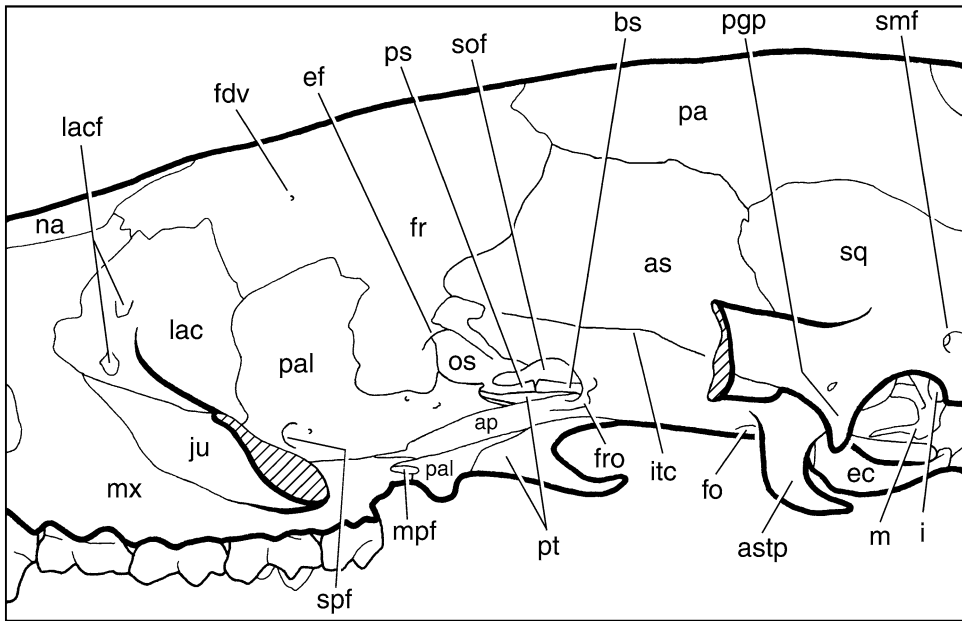
The narrow facial process of the lacrimal is roughly crescentic, but at a level dorsal to the infraorbital foramen is a small tongue-shaped process that is directed anterodorsally (Figs. 1, 4). Contacts of the facial process are with the frontal dorsally, the maxilla anteriorly, and the jugal ventrally. Posterioventrally, the facial process narrows to a short zygomatic process that extends posterolaterally dorsal to the jugal to the level of the M2 metacone (Fig. 4). Two lacrimal foramina lie within the facial process (Figs. 1, 4): the larger anteroventral foramen is immediately dorsal to the jugal suture and is directed anteromedially; the smaller posterodorsal foramen is opposite the top of the tongue shaped process described above and is directed ventrally. The rim of the orbit is rounded and not marked by a distinct crest, except for a portion on the jugal bone behind the zygomatic process of the lacrimal.

The larger orbital process of the lacrimal forms nearly the entire anteromedial wall of the orbit (Fig. 4), the exception being a small slip of palatine that completes the wall inferiorly. In the anteromedial orbital wall, the orbital process of the lacrimal contacts the frontal and palatine posteriorly, and the palatine inferiorly. The orbital process also forms the medial wall and roof of the maxillary foramen; the remaining borders are formed by the maxilla and palatine. Extending posterolaterally from the dorsolateral aspect of the maxillary foramen is the short zygomatic process of the lacrimal, which contacts the maxilla ventrally and the jugal posteriorly. Dorsal to the maxillary foramen on the right side of CM 52729 is a small, anteriorly directed foramen of uncertain function in the orbital process of the lacrimal; on the left side are two smaller foramina rather than a single opening.

Jugal

The paired jugal bones are the principal elements of the zygomatic arches, completing the gap between the zygomatic processes of the maxilla and lacrimal anteriorly and of the squamosal posteriorly (Fig. 2). The jugal also contributes to the ventral rim of the orbit and the face above the upper molars. It extends from the level of the M1 centrocrista anteriorly to the glenoid fossa posteriorly.

The portion of the jugal on the face lies dorsal to the upper molars and with the maxilla forms the anterior root of the zygomatic arch (Fig. 2). In lateral view (Fig. 4), the jugal contacts the maxilla inferiorly at a roughly crescentic suture and the zygomatic process of the lacrimal bone anterodorsally. The surface of the jugal on the face bears a large muscular



5 mm

Fig. 4.—*Monodelphis brevicaudata* CM 52729, line drawing of left orbitotemporal region without zygoma (parallel lines represent cut surfaces). Abbreviations: **ap**, anterior process of the alisphenoid; **as**, alisphenoid; **astp**, alisphenoid tympanic process; **bs**, basisphenoid; **ec**, ectotympanic; **ef**, ethmoidal foramen; **fdv**, foramen for the frontal diploic vein; **fr**, frontal; **fro**, foramen rotundum; **fo**, foramen ovale; **i**, incus; **ju**, jugal; **lac**, lacrimal; **lacf**, lacrimal foramen; **m**, malleus; **mpf**, minor palatine foramen; **mx**, maxilla; **na**, nasal; **os**, orbitosphenoid; **pa**, parietal; **pal**, palatine; **pggp**, postglenoid process; **ps**, presphenoid; **pt**, pterygoid; **smf**, suprameatal foramen; **sof**, sphenorbital fissure; **spf**, sphenopalatine foramen; **sq**, squamosal.

depression that extends anteriorly onto the maxilla posterior to the infraorbital foramen. This cigar-shaped depression houses the zygomaticus and levator labii muscles, based on *Didelphis marsupialis* (Turnbull, 1970). Behind the lacrimal, the dorsal border of the jugal is curved to form the infraorbital margin, which ends posteriorly in a low, but distinct frontal process (dorsal process) providing attachment for the postorbital ligament delimiting the orbital and temporal fossae (Fig. 2). Behind the frontal process in lateral view, the jugal contacts the zygomatic process of the squamosal at a V-shaped suture, the legs of which are posteriorly directed. The superior leg is very short, but the inferior leg reaches all the way to the glenoid fossa. The suture between the jugal and squamosal on the medial surface of the zygoma is diagonal, slanted anterodorsally, and more posteriorly placed. Beginning anteriorly on the zygomatic process of the maxilla and extending nearly to the glenoid fossa is a narrow muscular depression on the inferior margin of the jugal's lateral surface, which is for the superficial and deep masseter, based on *Didelphis* (Hiemae and Jenkins, 1969; Turnbull, 1970). The medial surface of the zygomatic arch, including the maxillary, jugal, and squamosal contributions, is concave and provides attachment anteriorly for the zygomaticomandibularis muscle and posteriorly for the zygomatic part of the temporalis muscle, based on *Didelphis marsupialis* (Turnbull, 1970). In ventral view (Fig. 5), the ventral edge of the jugal bears a blunt crest from the anterior root of the zygoma to just anterior to the glenoid fossa. At the glenoid, the jugal widens to form a broad glenoid

process (Fig. 6). The posterior surface of the glenoid process bears a facet that contributes to the anterolateral corner of the glenoid fossa. The glenoid process of the jugal approximates but does not touch the glenoid process of the alisphenoid.

Frontal

The paired frontal bones form the skull roof medial to the orbits (Fig. 1) and contribute to the medial walls of the orbital and temporal fossae (Fig. 4).

In dorsal view in the skull roof (Fig. 1), the frontals contact the nasals anteriorly at a roughly V-shaped suture, the legs of which are directed anteriorly. Lateral to the frontonasal suture, the anterior edge of the frontal has a narrow contact with the maxilla and the lacrimal. The thinness of the bone shows that the frontal overlaps both the maxilla and lacrimal. Posterior to the lacrimal, the frontal forms the rounded supraorbital margin, the posterior limit of which is indicated by a subtle postorbital process at the anterior end of the temporal line. From the postorbital process, the low temporal line curves posteromedially on the frontal, converging with its member of the opposite side at the frontoparietal suture to form a trace of a sagittal crest. The posterior edge of the frontal has a broad contact with the parietal and, lateral to that, a narrow contact with the alisphenoid. On the midline, a small V-shaped process of the frontals is interposed between the parietals. Because of the thinness of the bone, it is evident that the parietal and alisphenoid considerably overlap the frontal at their sutures. The anterior half of the interfrontal suture is relatively straight, but its posterior half is sinuous.

In lateral view within the orbital and temporal fossae (Fig. 4), the contacts of the frontal from anterior to posterior are with the lacrimal, palatine, orbitosphenoid, and alisphenoid. The suture with the lacrimal within the orbit is roughly vertical and that with the palatine is initially horizontal, then vertical, and then horizontal again. The latter two portions of the frontopalatine suture delimit the ventralmost intrusion of the frontal into the orbitotemporal fossa. Posterior to the frontopalatine suture, the frontal contacts the orbitosphenoid at a short vertical suture, at the top of which the ethmoidal foramen lies, and then at a short concave suture. Posterior to the suture with the orbitosphenoid, the frontal has a very broad contact with the overlapping alisphenoid that trends posterodorsally.

Two foramina are associated with the frontal within the orbitotemporal fossa (Fig. 4). First, wholly within the frontal in the supraorbital margin, anterior to the subtle postorbital process is a small, anterolaterally directed aperture, which I interpret as a foramen for the frontal diploic vein. Second, in the middle of the suture between the frontal and orbitosphenoid lies the ethmoidal foramen. This large oval aperture is nearly vertically directed, and, therefore, only its lateral rim is visible in lateral view. The frontal and orbitosphenoid contribute equally to the borders of the ethmoidal foramen, with the frontal forming the anterior and most of the lateral walls and the orbitosphenoid forming the posterior and most of the medial walls.

The frontal in *Didelphis marsupialis* has a distinct orbitotemporal crest that runs posteroventrally from the postorbital process to the ethmoidal foramen and marks the anterior extent of the origin of the temporalis muscle (Turnbull, 1970). An orbitotemporal crest is not evident in CM 52729.

Parietal

The paired parietals form the bulk of the posterior skull roof (Fig. 1) and arch over the cerebral hemispheres to contribute to the posterior side wall of the braincase (Fig. 2). They also provide the bulk of the attachment area for the temporalis muscle, based on *Didelphis* (Hiemae and Jenkins, 1969; Turnbull, 1970).

The parietal extends from the level of the sphenorbital fissure anteriorly to just in front of the nuchal crest posteriorly (Fig. 1). The thinness of the bone in the posterior skull roof reveals the details of the interosseous contacts. Along its anterior and posterior margins, the parietal overlaps considerably the frontal and interparietal, respectively. Laterally, the parietal is overlapped considerably by the alisphenoid and squamosal. The suture between the parietals, which lies in the low sagittal crest, is relatively straight anteriorly but tightly interdigitated posteriorly. There are several tiny emissary foramina in or near the posterior part of the suture. The largest, shown in Figure 1, is in the right parietal anterior to the interparietal bone. In the left parietal is a small, more laterally situated foramen, just anterior to the interparietal bone. It is directed posterodorsomedially into a groove that extends nearly to the confluence of the sagittal and nuchal crests, mainly on the interparietal bone. This foramen and groove do not exist on the right side, but a corresponding structure (presumably a vascular canal with no external egress) is visible because of the thinness of the parietal and interparietal.

Interparietal

An unpaired, intramembranous interparietal (postparietal) bone is described in postnatal stages of *Monodelphis domestica* by Clark and Smith (1993) and of *Didelphis marsupialis* by Toeplitz (1920). This bone apparently fuses seamlessly with the more posteriorly positioned supraoccipital along the nuchal crest and, therefore, is often labelled in adult didelphids as part of the supraoccipital (e.g., Hershkovitz, 1992:figs. 18, 19; Novacek, 1993:fig. 9.4). With little exception, the adult *Monodelphis* studied here have no indication of a suture separating the interparietal and supraoccipital. There are two juvenile *M. domestica* CM 80019 and 80020 (see Appendix 2), which show an open seam between a small portion of the contact between the interparietal and supraoccipital along the occipital surface of the nuchal crest. This seam can be followed only a short distance dorsal to the mastoid exposure of the petrosal. An even shorter seam immediately dorsal to the mastoid exposure is visible on the right side only of *M. brevicaudata* CM 63510, an adult with fully erupted M4. Based on the ontogenetic reports and on these specimens, I accept that the midline bone lying posterior to the parietal and forming the bulk of the nuchal crest in *Monodelphis* is the interparietal.

In dorsal view in CM 52729 (Fig. 1), the interparietal is shaped somewhat like a moustache. Clear sutures distinguish the interparietal from the parietals and squamosals, but there is no separation from the supraoccipital. The anterior surface of the interparietal contacts the paired parietals. In fact, because of the thinness of the parietals, it is very evident that they overlap the interparietal to a considerable extent. The lateral tips of the interparietal have a narrow contact with the posterodorsal squama of the squamosal. Based on the juveniles, the posterior surface of the interparietal forms the bulk of the nuchal crest and its contact with the supraoccipital lies on the occipital side of the nuchal crest. Also based on the juveniles, it seems likely that posteroventrally, the interparietal had a very narrow contact with the mastoid exposure of the petrosal. On the midline of the interparietal is a distinct, but low sagittal crest, which is better developed than that on the parietals.

Pterygoid

The medial surfaces of the paired pterygoid bones form most of the roof and lateral walls of the nasopharyngeal passage behind the choanae (Fig. 5). The lateral surface of the pterygoid is exposed in the infratemporal fossa and makes a tiny contribution to the orbital mosaic (Fig. 4).

In ventral view (Fig. 5), for descriptive purposes, I divide the pterygoid into two portions: one in the roof and a second in the lateral wall of the nasopharyngeal passage (the entopterygoid crest of Novacek, 1986); these have a narrow connection at the level of the presphenoid-basisphenoid suture. The portion in the roof is anteroposteriorly elongate, roughly cigar-shaped with pointed rather than rounded ends, and lies lateral to the midline. The posterior half underlies the basisphenoid. The anterior half does not underlie another bone; it contacts the presphenoid and basisphenoid medially and is separated from the palatine by an irregular fissure anterolaterally. At the posterolateral edge is a small aperture between the pterygoid and basisphenoid that represents the posterior opening of the pterygoid canal (Fig. 6). Leading to this aperture from behind is a narrow groove on the basisphenoid that can be traced posteriorly between the carotid foramen and the transverse canal foramen.

The portion of the pterygoid in the lateral wall of the nasopharyngeal passage, the entopterygoid crest, is boomerang-shaped with superior and inferior arms that meet at a roughly 45° angle (Fig. 4). The flat superior arm connects to the portion of the pterygoid in the nasopharyngeal roof (Fig. 5) and from that connection runs anteroventrolaterally with the superior aspect of its lateral surface in contact with the alisphenoid and palatine; the inferior aspect does not contact another bone. The superior arm joins the inferior arm posterodorsal to the back of the hard palate. The freestanding inferior arm extends posteriorly into the infratemporal fossa and curves slightly laterally. It is flat proximally, but ends in a thickened, rounded hamular process that has a distinct lateral bend, presumably to accommodate the tendon of the tensor veli palatini muscle. The inferior arm is frequently damaged in museum specimens; it is broken on the right side of CM 52729 and wholly missing on the left side (as apparently is the case in the *Monodelphis breviceaudata* AMNH 130516 illustrated by Novacek, 1993:fig. 9.4B, C). It is from the lateral surface of the pterygoid and adjacent parts of the alisphenoid and palatine that the internal pterygoid muscle arises, based on *Didelphis* (Hiimae and Jenkins, 1969; Turnbull, 1970).

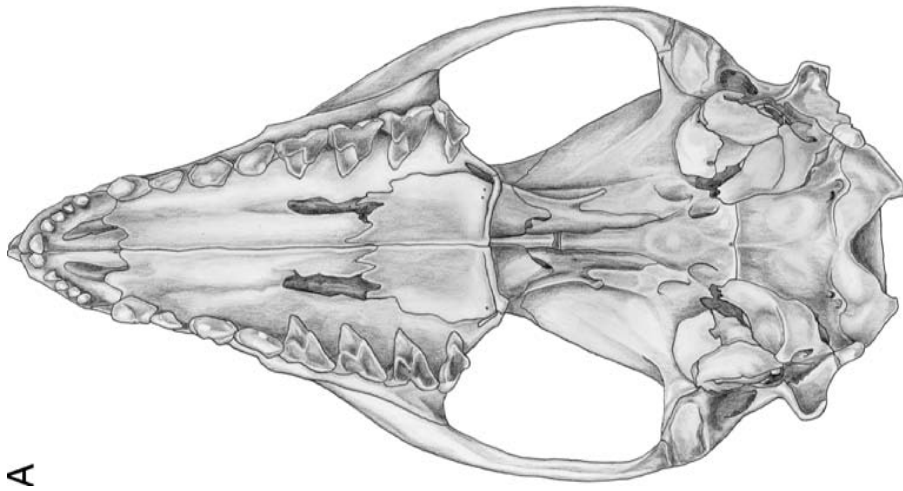
The pterygoid has a minor exposure in the floor of the sphenorbital fissure in the posteroventral aspect of the medial orbit wall (Fig. 4). It is a flat, trapezoidal sliver of bone, longer than wide. It contacts the presphenoid and basisphenoid medially, the alisphenoid posteriorly and laterally, and the palatine anteromedially. Anterolaterally, it is separated from the palatine by an irregular opening. The anterior opening of the pterygoid canal, which is within the sphenorbital fissure and not visible in lateral view, lies between the posterolateral aspect of this lamina of pterygoid and the overlapping alisphenoid. The alisphenoid bears a notch that forms the posterior and lateral borders of this aperture. Extending anteriorly a short distance from the notch is a narrow groove on the pterygoid for the contents of the pterygoid canal.

Vomer

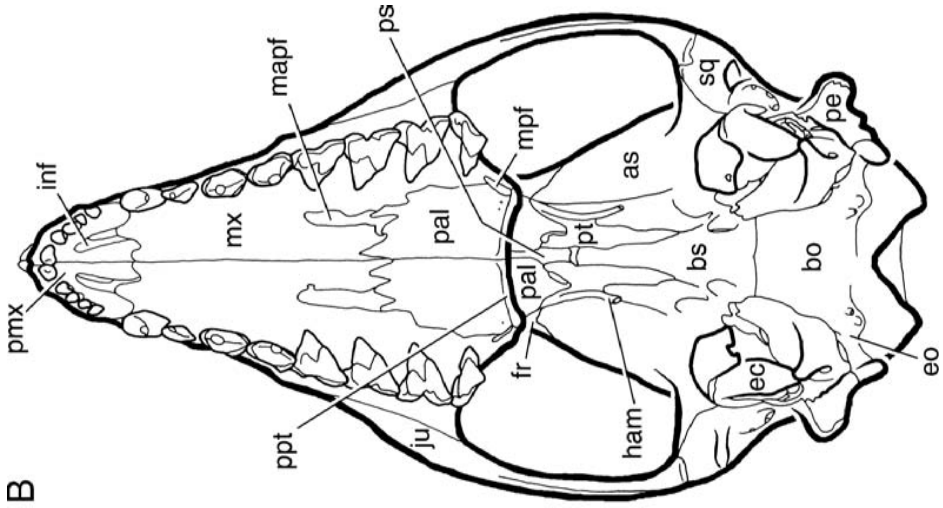
The vomer is not visible in any of the illustrated views. According to Macrini (2000), the vomer is a thin, anteroposteriorly elongate bone that contributes to the anterior portion of the nasal cavity. It articulates with the presphenoid posteriorly, the palatal processes of the maxillae anterodorsally, and the medial palatine processes (vomeric processes) of the premaxillae anteriorly.

Sphenoid Complex

Clark and Smith (1993) identify four bones in the sphenoid complex of *Monodelphis domestica*. The presphenoid and basisphenoid are midline elements in the skull base between the choanae and ear region. Attached to the presphenoid are the paired



A



B

orbitosphenoids, which have a small exposure in the medial orbital wall. Attached to the basisphenoid are the paired alisphenoids, which have a much more substantial contribution to the medial wall of the orbitotemporal fossa. According to Clark and Smith (1993), the presphenoid and orbitosphenoids arise on postnatal day 13 and 14 from three centers of ossification that fuse to form a T-shaped structure by postnatal day 16. I describe the presphenoid as the midline rod and the orbitosphenoids as the arms of the T. The basisphenoid arises from a single center of ossification on postnatal day 5. Each alisphenoid arises from two centers of ossification on postnatal day 4, one between the ophthalmic (V_1) and maxillary (V_2) divisions of the trigeminal nerve, and the other between the maxillary and mandibular (V_3) divisions of the trigeminal nerve; these two centers fuse medial to the foramen rotundum by postnatal day 7 (cf. Maier, 1987a). The basisphenoid and alisphenoid are fused together by postnatal day 25. The landmarks that I employ to demarcate the basisphenoid and alisphenoid in the adult skull are the foramen rotundum, which ontogenetically is entirely within the alisphenoid (Clark and Smith, 1993), and the transverse canal and carotid foramina, which ontogenetically are entirely within the basisphenoid (Wible, unpubl. observ.; Sánchez-Villagra, pers. commun.).

Presphenoid

In ventral view (Fig. 5), the unpaired presphenoid is a rod-shaped element in the midline roof of the nasopharyngeal passage that extends and tapers anteriorly deep into the nasal cavity, where it contributes to the nasal septum, there being no independent ethmoid ossification in marsupials (Broom, 1926). Laterally, within the nasopharyngeal passage, the presphenoid contacts, from anterior to posterior, the palatine and pterygoid; and posteriorly, it contacts the basisphenoid.

In lateral view (Fig. 4), a small quadrangular exposure of the posterodorsal presphenoid is visible in the depths of the sphenorbital fissure, where it contributes to the anteroventral floor. It has sutural contact with the palatine and pterygoid laterally, and the basisphenoid posteriorly. Anterodorsally, it is merged with the left and right orbitosphenoid.

Orbitosphenoid

The paired orbitosphenoid has a small exposure in the medial orbital wall, anterior to the sphenorbital fissure (Fig. 4). In lateral view, the orbitosphenoid is roughly wedge-shaped. It is situated anterodorsal to and is continuous with the presphenoid. For descriptive purposes, the orbitosphenoid can be treated as having anteroventral and posterodorsal parts, with the wedge angled such that the anteroventral part is medial to the posterodorsal one. The anteroventral part contacts the palatine ventrally at a longitudinal suture and the frontal anteriorly at a vertical suture. The posterodorsal part looks somewhat like the front half of a horse with the nose pointing posteriorly. The mane is in contact with the frontal, and the head, neck, and forelimb in contact with the alisphenoid. The anteroventral and posterodorsal parts contribute to the walls of two major apertures: the ethmoidal foramen and sphenorbital fissure. The ventrally directed ethmoidal foramen lies in the suture between the frontal and orbitosphenoid, with the anteroventral part of the orbitosphenoid

←

Fig. 5.—*Monodelphis breviceaudata* CM 52729, skull in ventral view excluding mandibles (A) with accompanying line drawing (B). Abbreviations: **as**, alisphenoid; **bo**, basioccipital; **bs**, basisphenoid; **ec**, ectotympanic; **eo**, exoccipital; **fr**, frontal; **ham**, pterygoid hamulus; **inf**, incisive foramen; **ju**, jugal; **mapf**, major palatine foramen; **mpf**, minor palatine foramen; **mx**, maxilla; **pal**, palatine; **pe**, petrosal; **pmx**, premaxilla; **ppt**, postpalatine torus; **ps**, presphenoid; **pt**, pterygoid; **sq**, squamosal.

forming the medial wall and the posterodorsal part the posterior and posterolateral walls. Running ventrally from the posterior half of the ethmoidal foramen onto the anteroventral part of the orbitosphenoid is a distinct sulcus that curves posteriorly. The large, ovoid, anterolaterally directed sphenorbital fissure has walls made by the orbitosphenoid, alisphenoid, pterygoid, palatine, and presphenoid. The anteroventral part of the orbitosphenoid forms the anterior wall and the posterodorsal part the anterodorsal wall. As is usual in metatherians (Rougier et al., 1998), *Monodelphis* lacks a separate optic foramen for the optic nerve in the orbitosphenoid.

Basisphenoid

The unpaired basisphenoid bone occupies the midline of the basicranium between the presphenoid anteriorly and the basioccipital posteriorly (Fig. 5). It also has a minor exposure laterally deep within the sphenorbital fissure (Fig. 4). The basisphenoid is fused seamlessly with the paired alisphenoids laterally (Fig. 5). Most of what I interpret as the boundary between the basisphenoid and alisphenoid is hidden in ventral view by the underlying pterygoid bone. Posterior to the pterygoid bone, the posterolateral extent of the basisphenoid is marked by the transverse canal and carotid foramina (Fig. 6), which form ontogenetically within the basisphenoid (Wible, unpubl. observ.; Sánchez-Villagra, pers. commun.).

In ventral view (Fig. 5), roughly the anterior half of the exposed basisphenoid is a narrow, gently rounded shaft of bone that lies in the roof of the nasopharyngeal passage between the left and right pterygoids and tapers anteriorly to its suture with the presphenoid. Near the posterior extent of the pterygoids, the basisphenoid widens to encompass two sets of paired foramina (Fig. 6). The more anterolateral set is the transverse canal foramina, the apertures of which are very flattened, almost cigar-shaped, and directed posterolaterally. There is a broad, shallow depression posterolateral to the transverse canal foramen, which likely accommodated the contents of the foramen. The more posteromedial set is the carotid foramina, the apertures of which are ovoid and directed posterolaterally and slightly ventrally. A well-defined, short vascular sulcus on the basisphenoid leads into each carotid foramen from behind. This sulcus is directed toward and in contact with the flat, expanded anteromedial flange of the petrosal (see below). Extending anteriorly from the carotid foramen to the posterior extent of the pterygoid is a raised, rounded ridge. The surface of the basisphenoid between these paired ridges is flat. Running along the lateral aspect of each ridge is a narrow sulcus that ends at a tiny, slit-like foramen between the posterolateral border of the pterygoid and the overlying basisphenoid. This narrow aperture is the posterior opening into the pterygoid canal. The surface of the basisphenoid posteromedial to the carotid foramina is flat, but off the midline is subtly rugous and projects slightly ventrally at its contact with a surface with similar characteristics on the basioccipital. This surface on the basisphenoid-basioccipital suture likely is for the attachment of the longus capitis muscle, based on the dog (Evans, 1993).

In lateral view (Fig. 4), the anterodorsal surface of the basisphenoid is visible in the floor of the sphenorbital fissure. Its shape mirrors that of the ventral surface; that is, it is a rounded shaft. It contacts the presphenoid anteriorly and the pterygoid laterally.

Alisphenoid

The paired alisphenoid bones are situated on either side of the basisphenoid and contribute to the side wall of the braincase, the skull base in front of the ear region, and the auditory bulla (Figs. 5–6). The alisphenoids are fused seamlessly with the basisphenoid. As

stated above, most of the boundary between the alisphenoids and basisphenoid is hidden in ventral view by the underlying pterygoid bones. The medial limit of the alisphenoid lies medial to the foramen ovale and the foramen rotundum, which ontogenetically form in association with the alisphenoid (Maier, 1987a; Clark and Smith, 1993).

In lateral view (Fig. 4), the alisphenoid is roughly pentagonal to which are added two narrow processes, at the anteroventral and posteroventral margins, respectively. The five sides of the pentagon are as follows: anteroventrally, the sphenorbital fissure and the suture with the orbitosphenoid; anterodorsally, the suture with the frontal; posterodorsally, the suture with the parietal; posteroventrally, the suture with the squamosal; and ventrally, the skull margin. A distinct infratemporal crest divides the lateral surface of the pentagon into an inferior one-third facing ventrolaterally into the infratemporal fossa and a superior two-thirds facing laterally into the temporal fossa. This crest marks the ventral limit of the attachment of the temporalis muscle, based on *Didelphis marsupialis* (Turnbull, 1970). Extending anteroventrolaterally from the anteroventral margin of the pentagon is the anterior process of the alisphenoid. This long, straight splint of bone tapers to a point dorsal to the minor palatine foramen. It contacts the basisphenoid, pterygoid, and palatine dorsally, and the pterygoid, palatine, and maxilla ventrally. At the root of the anterior process are the circular, anteriorly directed foramen rotundum (most of which is hidden in lateral view) and, anteromedial to that, the much larger sphenorbital fissure. The alisphenoid entirely encloses the foramen rotundum, but encloses only the posterolateral half of the sphenorbital fissure. Extending ventrally from the posteroventral margin of the pentagon is the alisphenoid tympanic process, which curves posteriorly, cupping the ectotympanic bone and forming the anterior wall of the auditory bulla. Anterior to the base of the alisphenoid tympanic process is the foramen ovale. In the interval between the foramen rotundum anteriorly and the foramen ovale posteriorly, the alisphenoid is gently rounded.

The bulk of the alisphenoid visible in ventral view lies within the infratemporal fossa (Fig. 5). Posterolaterally, the alisphenoid has a triangular glenoid process in contact with the squamosal that provides the anteromedial articular surface of the temporomandibular joint (Fig. 6). Posteromedial to the glenoid process is the inflated, bowl-shaped tympanic process of the alisphenoid (Fig. 6). The posterolateral border of the tympanic process abuts the ectotympanic and anterior process of the malleus; the posteromedial border has a distinct notch that marks the passage of the auditory or eustachian tube. In the posteroventral margin of the tympanic process is a small opening of unknown function on the left side of CM 52729 that is a notch on the right side. Lateral to this notch on the right side, opposite the ventral end of the anterior process of the malleus is a faint notch leading to a short sulcus on the extratympanic surface of the tympanic process. The left side has no notch or sulcus, but only a gap, which is indicated in Figure 6 (“glf”). In other specimens (e.g., *Monodelphis domestica* CM 80016), this notch is closed to a foramen. I interpret this gap, notch, and foramen as for the chorda tympani nerve, a branch of the facial nerve that exits the middle ear and enters the infratemporal fossa. The gap, notch, or foramen for the chorda tympani is a glaserian fissure, which in placentals typically lies near the juncture of the petrosal, ectotympanic, squamosal, and alisphenoid (Klaauw, 1931). The concave inner surface of the alisphenoid tympanic process in CM 52729, which walls an extensive alisphenoid hypotympanic sinus, is expanded posteriorly to contact the petrosal anterodorsal to the tuberculum tympani. Medial to the tympanic process is the elongate foramen ovale, which lies between the alisphenoid and petrosal (Fig. 6). Leaving the anterior end of the foramen ovale and directed ventrolaterally is a sulcus, partly on the skull base and partly on the tympanic process. The foramen ovale is continuous medially with a small aperture between the basisphenoid and petrosal. The walls of this aperture are

rounded, and it transmitted the greater petrosal nerve from the hiatus Fallopii to the pterygoid canal (Wible, unpubl. observ.).

A small area of alisphenoid in the temporal fossa lateral to the parietal and squamosal is visible in dorsal view (Fig. 1). Noteworthy is the alisphenoid's contribution to the dorsal surface of the posterior zygomatic root, which served as attachment area for the temporalis muscle, based on *Didelphis marsupialis* (Turnbull, 1970).

Squamosal

The paired squamosal bones have a flattened squamous portion in the posteroventral side wall of the braincase, a zygomatic process contributing to the posterior half of the zygoma, and the glenoid fossa, the skull's component of the temporomandibular joint (Figs. 1, 2, 4–6).

In lateral view (Fig. 2), the squama of the squamosal is somewhat quadrangular in shape. Because of the thinness of the braincase bones, it is apparent that the bulk of the squama does not contribute to the primary side wall per se; it overlies the parietal anterodorsally, the alisphenoid anteriorly, and the petrosal posteriorly. There is only a narrow area dorsal to the level of the postglenoid process where the squama is the primary wall. Anteriorly, the squama contacts the alisphenoid. Its dorsal border has a gently sinuous contact with the parietal, and the posterodorsal corner has a narrow contact with the interparietal. The posterior border of the squama contacts the mastoid exposure of the petrosal at a suture that contains the posttemporal notch, and forms the ventral one-third of the nuchal crest (Fig. 9). The posteroventral corner of the squama is prolonged ventrally into a stout posttympanic process (Fig. 2), which is buttressed medially by the mastoid process of the petrosal (Fig. 6). The ventral border of the squama is concave between the postglenoid and posttympanic processes, and this area is occupied by the external acoustic meatus. Anterodorsal to the posttympanic process is a large, posterolaterally directed suprameatal foramen (Fig. 4), which connects through the squamosal to the postglenoid foramen on the ventral surface (Fig. 6). Posterior to the suprameatal foramen is a wide depression, which dorsally includes a short, posterodorsally directed sulcus (Fig. 2).

In lateral view (Fig. 2), the zygomatic process of the squamosal lies in the posterior half of the zygoma and is underlain by the glenoid process of the jugal. At the posterior root of the zygomatic process is the prominent, ventrally directed postglenoid process. Dorsal to the postglenoid process is a small, anterolaterally directed, unnamed opening (Fig. 4). Based on CM 76731, I confirm that this opening communicates through the squamosal with the postglenoid foramen on the ventral surface. In dorsal view (Fig. 1), the dorsal edge of the zygoma has a ridge that extends from the frontal process of the jugal to where the posterior root of the zygoma merges with the braincase. Anteriorly, this ridge is very sharp; posteriorly, it is rounded and forms the posterior wall of a triangular depression on the dorsum of the posterior root of the zygoma. The anteromedial portion of this depression is formed by the alisphenoid, the remainder by the squamosal. This depression provides attachment for the temporalis muscle, based on *Didelphis marsupialis* (Turnbull, 1970). In the posterior corner of this depression is a small foramen in the squamosal that is hidden in dorsal view by the ridge running along the dorsal edge of the zygoma. This foramen communicates with the postglenoid foramen.

The most conspicuous features on the squamosal in ventral view are the glenoid fossa at the posterior root of the zygoma and behind that, the postglenoid process and foramen (Fig. 6). The glenoid fossa is ovoid, wider than long, and with the exception of the narrow articular surfaces on the glenoid processes of the jugal and alisphenoid is entirely on

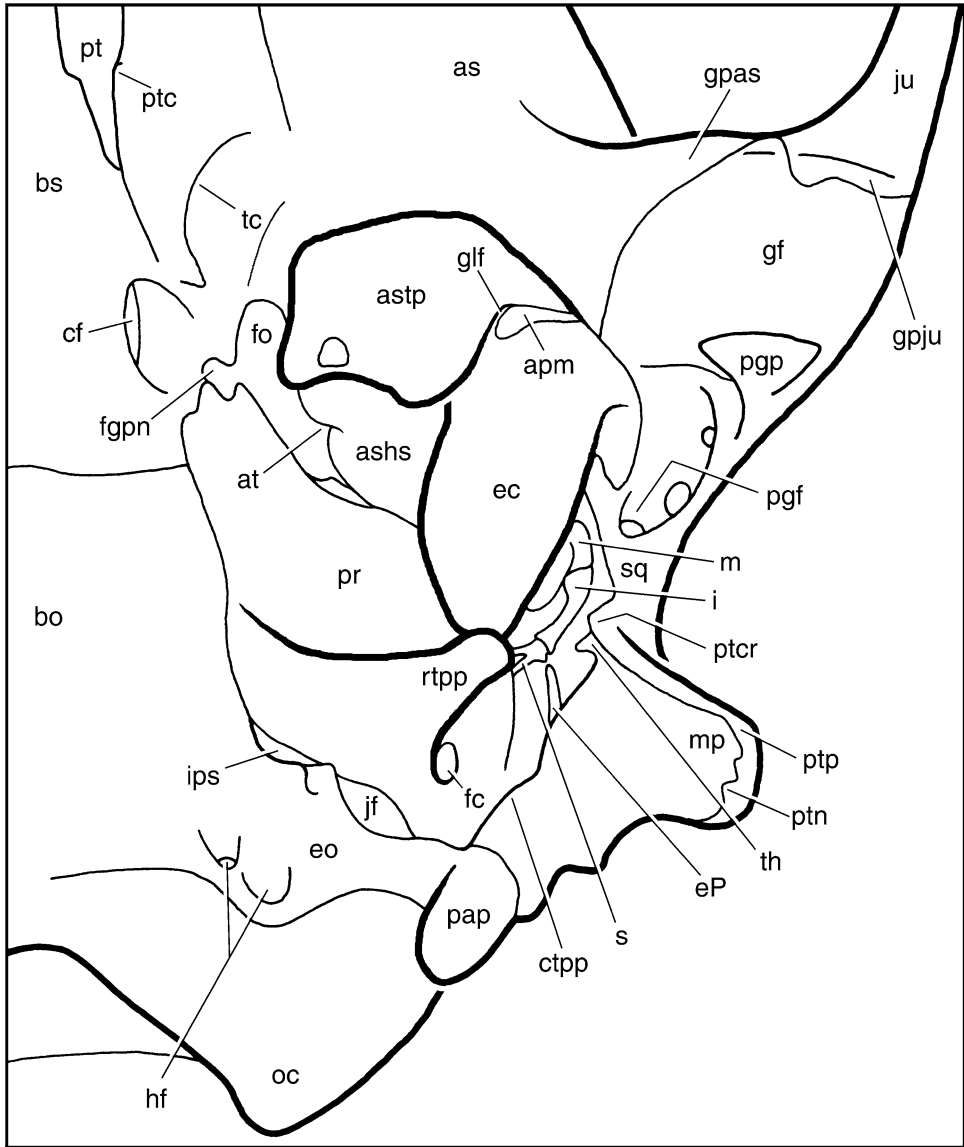


Fig. 6.—*Monodelphis brevicaudata* CM 52729, line drawing of left ear region in ventral view. Abbreviations: **apm**, anterior process of the malleus; **as**, alisphenoid; **ashs**, alisphenoid hypotympanic sinus; **astp**, alisphenoid tympanic process; **at**, groove for the auditory tube; **bo**, basioccipital; **bs**, basisphenoid; **cf**, carotid foramen; **ctpp**, caudal tympanic process of the petrosal; **ec**, ectotympanic; **eo**, exoccipital; **eP**, element of Paaw; **fc**, fenestra cochleae; **fgpn**, foramen for greater petrosal nerve; **fo**, foramen ovale; **gf**, glenoid fossa; **glf**, glaserian fissure; **gpas**, glenoid process of the alisphenoid; **gpju**, glenoid process of the jugal; **hf**, hypoglossal foramen; **i**, incus; **ips**, foramen for the inferior petrosal sinus; **jf**, jugular foramen; **ju**, jugal; **m**, malleus; **mp**, mastoid process; **oc**, occipital condyle; **pap**, paracondylar process of the exoccipital; **pgf**, postglenoid foramen; **pgp**, postglenoid process; **pr**, promontorium; **pt**, pterygoid; **ptc**, pterygoid canal; **ptcr**, posttympanic crest; **ptn**, posttemporal notch; **ptp**, posttympanic process; **rtp**, rostral tympanic process of the petrosal; **s**, stapes; **sq**, squamosal; **tc**, transverse sinus canal; **th**, tympanohyal.

the squamosal. The fossa is also entirely on the posterior zygomatic root and not on the braincase proper. Forming the posteromedial wall of the glenoid fossa is the stout postglenoid process, which in occipital view is U-shaped with the lateral arm of the U more erect than the medial. The ventral limit of the process, the bottom of the U, is asymmetrical in ventral view, with the medial half thinner and the lateral half more bulbous posteriorly.

Posteromedial to the postglenoid process is the large, ovoid postglenoid foramen (Fig. 6). This aperture is entirely within the squamosal; however, underlying the squamosal along the foramen's medial edge is the anterior crus of the ectotympanic. In ventral view, three openings increasing in size posteriorly are visible within the substance of the postglenoid foramen. By far the largest, the posterior opening curves posterodorsally into the squamosal. It represents the true intramural continuation of the postglenoid foramen (that is, the conduit for the sphenoparietal emissary vein), which communicates with the suprameatal foramen on the side wall of the braincase described above. The anterior two openings (postzygomatic foramina of Gregory, 1910) are in the anterior wall of the main postglenoid channel; they are directed anterodorsally into the squamosal (with the anterior one communicating with the small unnamed foramen described above on the posterior zygomatic root dorsal to the postglenoid process, based on CM 76731). The anterior foramen is round and the middle one is ovoid.

Posterior to the postglenoid foramen, the squamosal narrows considerably and then expands chiefly posterolaterally to form the posttympanic process (Fig. 6). The ventral surface of the squamosal between the postglenoid foramen and posttympanic process is dominated by two distinct ridges that meet at roughly 90° to each other. The point at which these ridges meet is a very prominent, sharp, V-shaped process that points ventromedially and overhangs the tympanohyal on the petrosal bone. Wible et al. (in press) called a similar, but more medially expanded version of this process in the Late Cretaceous eutherian *Zalambdalestes* the posttympanic crest, a term that I adopt here. The ridge extending anterolaterally from the posttympanic crest is gently concave and forms the dorsal rim of the external acoustic meatus. The ridge extending posterolaterally from the posttympanic crest is straighter, is buttressed by the mastoid process posteriorly, and connects to the posttympanic process.

Petrosal

The paired petrosal bones enclose the organs of hearing and equilibration, provide attachment for the muscles and ligaments of the middle-ear ossicles, and include grooves, canals, and foramina for components of the cranial vascular and nervous systems. Two divisions of the petrosal are generally recognized: the pars cochlearis, housing the cochlear duct and saccule of the inner ear, and the pars canicularis, housing the utricle and semicircular canals. Because the petrosal has played a prominent role in metatherian phylogenetics (e.g., Archer, 1976; Wible, 1990; Rougier et al., 1998; Sánchez-Villagra and Wible, 2002), detailed descriptions of the various surfaces of the petrosal of *Monodelphis* are included here, based on an isolated left petrosal of *Monodelphis* sp. CM 5024 (which I provisionally identify as *M. domestica*) and an isolated right petrosal of *M. brevicaudata* CM 5061. The former is illustrated in three views in Figures 7–8 (tympanic, dorsal, and lateral) and is the principal basis for the following descriptions, with differences between CM 5024 and 5061 noted. Information on the middle-ear ossicles and neighboring bones is taken from *M. brevicaudata* CM 52729, which is illustrated in ventral and occipital views in Figures 6 and 9. Following the descriptions of the three illustrated views of the isolated petrosal is a section on the principal veins of the petrosal bone.

Tympanic View.—The two divisions of the petrosal are most readily seen in the tympanic or ventral view (Fig. 7A, D); the pars cochlearis is represented by the promontorium and

the flange projecting anteromedially from it, and the pars canicularis by the bone lateral and posterior to the promontorium. The bulbous shape of the promontorium reflects the enclosed coiled cochlear duct, which in adult *Didelphis virginiana* has two and one-fourth turns (Larsell et al., 1935). There are two openings in the outer contour of the promontorium: posterolaterally, the fenestra vestibuli, and posteriorly, the fenestra cochleae. The slightly oval-shaped fenestra vestibuli, which houses the footplate of the stapes, has a stapedial ratio (of Segall, 1970, length/width) of 1.45 in CM 5024 (it was not possible to measure CM 5061, because the footplate of the stapes partially obscures the posterior dimension of the fenestra vestibuli). Other didelphids measured by Segall (1970) are comparable (*Metachirus* and *Didelphis*, 1.3; *Marmosa*, 1.4; *Caluromys* and *Philander*, 1.5). The fenestra vestibuli is not fully visible in the direct ventral view (Fig. 6); it is directed laterally and slightly ventrally, and sits in a shallow vestibular fossula, recessed from the surrounding bone. The more elliptical fenestra cochleae, covered in life by the secondary tympanic membrane, is also not fully visible in ventral view, because its ventromedial aspect is hidden by the back of the rostral tympanic process of the petrosal (see below; Fig. 6). It is this hidden portion of the fenestra cochleae that has a shallow cochlear fossula.

The most noteworthy feature on the promontorium is the rostral tympanic process of the petrosal (rtpp) (Fig. 7A, D). This finger-like process projects ventroanterolaterally from the posteromedial surface of the promontorium and abuts the posterior crus of the ectotympanic (Fig. 6). Extending anteromedially and posterolaterally from the main finger-like process are low ridges (Figs. 6, 7A, D). The anteromedial ridge extends the length of the promontorium and contacts the basioccipital bone, distal to the basioccipital-basisphenoid suture (Fig. 6). The shorter posteromedial ridge forms the dorsomedial lip of the cochlear fossula and fenestra cochleae (Figs. 6, 7A, D).

Projecting anteromedially from the promontorium is a fairly flat shelf of bone, the anteromedial flange, which narrows slightly anteriorly and is directed toward the carotid sulcus and foramen within the basisphenoid (Fig. 6). Although the flange has no sign of a vascular sulcus, the internal carotid artery may have contacted this surface en route to the basisphenoid bone. The medial side of the flange contacted the basioccipital and basisphenoid, and the lateral side formed the posteromedial border for the large foramen ovale. The lateral edge of the flange has a narrow, shallow surface that probably accommodated (or provided attachment area for) the tensor tympani muscle (Fig. 7A, D).

As stated above, the pars canicularis is represented by the bone projecting from the lateral and posterior aspects of the promontorium (Fig. 7A, D). On the pars canicularis are two ridges at roughly right angles to one another that meet at the posterolateral corner of the petrosal. At their juncture is a stout, posterolaterally directed mastoid process, which is covered anterolaterally by the posttympanic process of the squamosal (Fig. 6). The ridge running posteromedially from the mastoid process is the caudal tympanic process of the petrosal (ctpp) (Fig. 7A, D). The cttp in the isolated petrosals (CM 5024 and 5061) decreases in height medially, but this is not the case in the skull (CM 52729). The medial end of the cttp abuts the paracondylar process of the exoccipital bone (Fig. 6). The ridge that runs anteriorly from the mastoid process is the crista parotica (Fig. 7A, D), which in the skull is hidden by the squamosal bone (Fig. 6). The crista parotica is much shorter and thinner than the cttp; it extends to approximately the level of the anterior edge of the fenestra vestibuli. At the posterior end of the crista parotica is a thickening, the ventral end of which has a flat triangular surface facing ventromedially. The thickening is the tympanohyal and the triangular surface is the contact for the stylohyal (not preserved). Posterior to the tympanohyal is the stylomastoid notch by which the facial nerve left the middle ear.

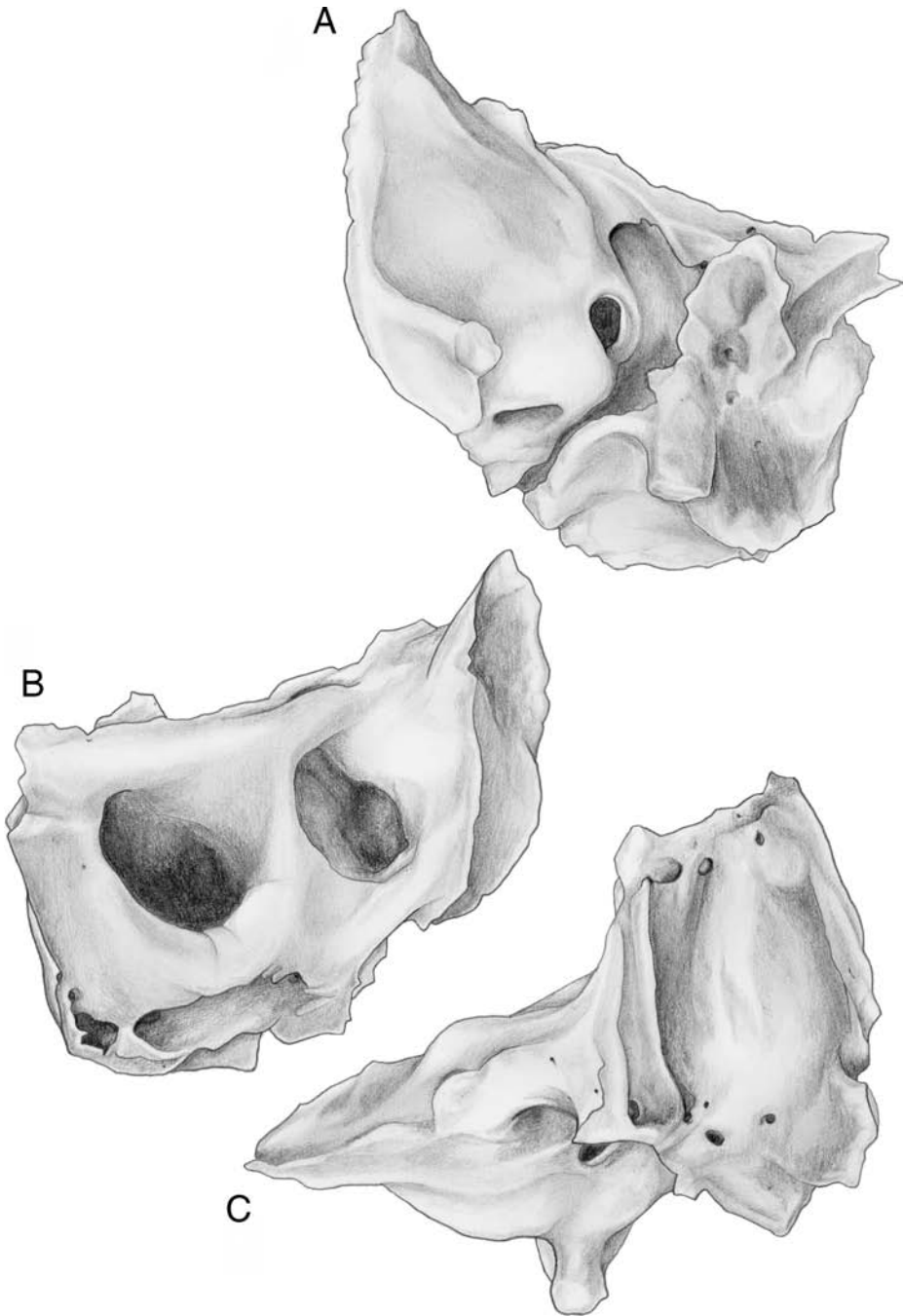


Fig. 7.—*Monodelphis* sp. CM 5024, left petrosal in ventral view (A), dorsal view (B), and lateral view (C), with accompanying line drawing (D), (E), and (F), respectively. Abbreviations: **amf**, anteromedial flange; **av**, aqueductus vestibuli; **br**, broken; **cc**, cochlear canaliculus; **cp**, crista parotica; **cr**, crista petrosa; **crs**, crus commune; **ctpp**, caudal tympanic process of the petrosal; **er**, epitympanic recess; **fai**, foramen acusticum inferius; **fas**, foramen

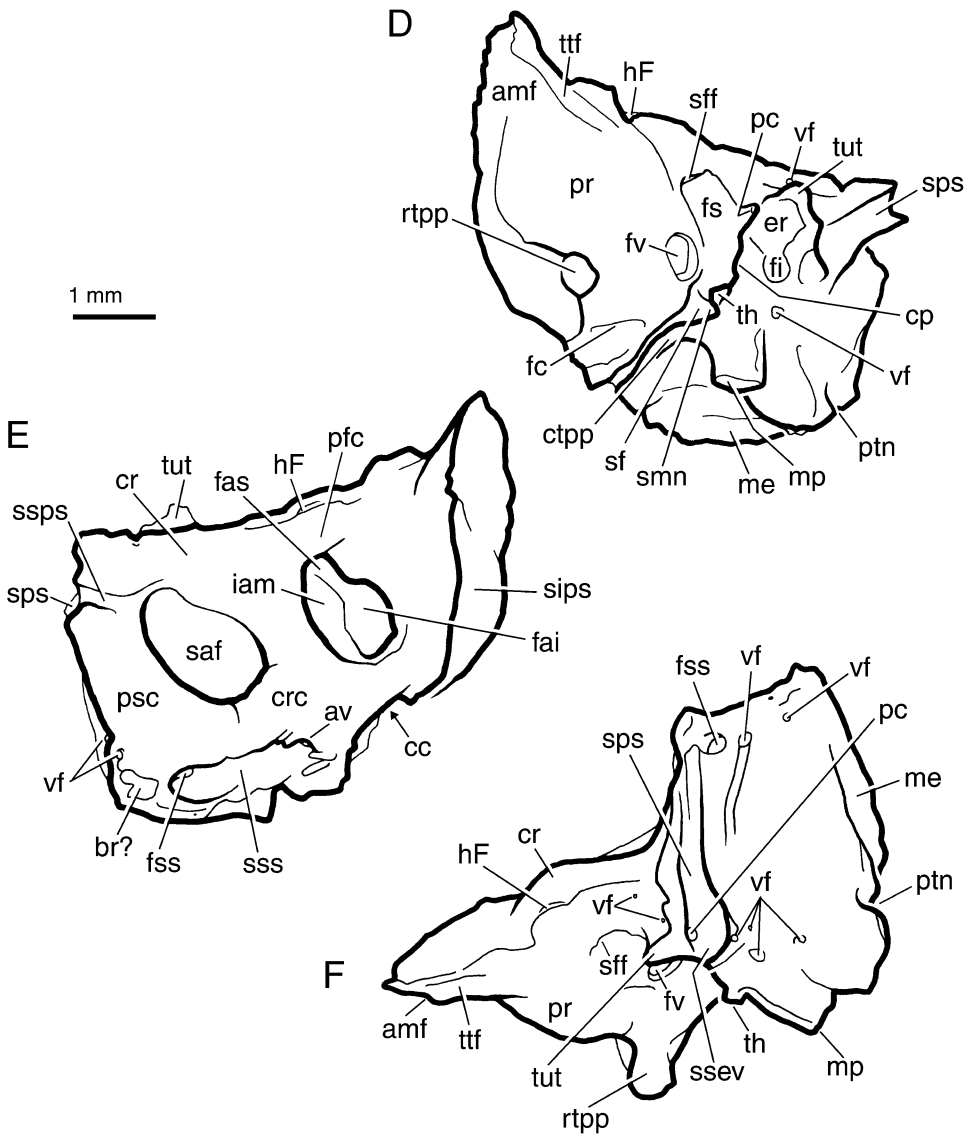


Fig. 7.—Continued.

acusticum superius; **fc**, fenestra cochleae; **fi**, fossa incudis; **fss**, foramen for the sigmoid sinus; **fv**, fenestra vestibuli; **hF**, hiatus Fallopii; **iam**, internal acoustic meatus; **me**, mastoid exposure; **mp**, mastoid process; **pc**, prootic canal; **pfc**, prefacial commissure; **pr**, promontorium; **psc**, posterior semicircular canal; **ptn**, posttemporal notch; **rtp**, rostral tympanic process of the petrosal; **saf**, subarcuate fossa; **sf**, stapedius fossa; **sff**, secondary facial foramen; **sips**, sulcus for the inferior petrosal sinus; **smn**, stylomastoid notch; **sps**, sulcus for the prootic sinus; **ssev**, sulcus for the sphenoparietal emissary vein; **ssps**, sulcus for the superior petrosal sinus; **sss**, sulcus for the superior petrosal sinus; **th**, tympanohyal; **ttf**, tensor tympani fossa; **tut**, tuberculum tympani; **vf**, vascular foramen.

Between the ctp_p and the rear of the promontorium is a deep depression, the bulk of which is not visible in tympanic view (Figs. 6, 7A, D). The narrower medial part of this depression is the post-promontorial tympanic sinus of Wible (1990); the broader, deeper, oval, lateral part is the fossa for the stapedius muscle. The width of the stapedius fossa is roughly three quarters the length of the ctp_p. Projecting anteroventrally from the stapedius fossa is a thin rod of bone in CM 5024 (not illustrated in Figure 7, because it is displaced), 5061, and 52729 that is attached to the muscular process of the stapes by a ligament in CM 52729 (Fig. 6). This is the ossified element of Paaw, which is the functional equivalent of a sesamoid bone in the tendon of the stapedius muscle. The surface of the pars canalicularis posterolateral to the ctp_p is the mastoid exposure, the surface of the petrosal exposed on the occiput.

Between the crista parotica and the fenestra vestibuli is a broad, shallow, anteriorly directed facial sulcus (Fig. 7A, D), so-called because its principal occupant was the facial nerve. Within the sulcus, lateral to the facial nerve ran the much smaller lateral head vein. Opening posteromedially into the lateral aspect of the facial sulcus at the level of the anterior edge of the fenestra vestibuli is the tympanic aperture of the prootic canal. The prootic canal is the route by which the prootic sinus communicated with the lateral head vein (Wible, 1990; Wible and Hopson, 1995). At the level of the tympanic aperture of the prootic canal, the facial sulcus turns anteromedially and after a short course enters the oval secondary facial foramen. The bone immediately anterior to the secondary facial foramen represents the floor of the cavum supracochleare, the space that housed the geniculate ganglion of the facial nerve (Gaupp, 1908). Anterior to this floor, the anteriormost roof of the hiatus Fallopii is visible. The hiatus Fallopii, not fully visible in any of the three views illustrated, is a gap similar in size to the secondary facial foramen. It transmitted the greater petrosal nerve (palatine ramus of the facial nerve).

Lateral to the facial sulcus is a bony shelf of similar dimensions, but whose surface is very irregular (Fig. 7A, D). The lateral edge of this shelf has a ridge that is hidden in the skull by the squamosal and that ends anteriorly in a sharp, anteroventrally directed process. This process is called the tuberculum tympani, because it resembles the structure so identified by Toeplitz (1920) in pouch young *Didelphis marsupialis*. Following Kuhn and Zeller (1987), this is the homologue of the tegmen tympani of placentals. The shelf medial to the lateral ridge has two depressions. Posteriorly is a smaller, circular, deeper depression, the fossa incudis for the short process (crus breve) of the incus. The fossa incudis is bordered medially by the crista parotica and laterally by the squamosal bone. Anterior to and continuous with the fossa incudis is a broader, shallower depression, the epitympanic recess over the mallear-incudal articulation (Klaauw, 1931). The epitympanic recess is bordered medially by a very low ridge, the anterior continuation of the crista parotica, and laterally by the lateral ridge and squamosal.

Dorsal View.—The dorsal or endocranial view (Fig. 7B, E) is dominated by two large openings, the internal acoustic meatus anteromedially and the subarcuate fossa posterolaterally. The smaller internal acoustic meatus for the vestibulocochlear nerve lies in the roof of the pars cochlearis, and the subarcuate fossa, which accommodated the paraflocculus of the cerebellum, is in the roof of the pars canalicularis. The floor of the internal acoustic meatus has a depression that is roughly dumbbell shaped, with the medial and lateral ends of the dumbbell representing the foramen acusticum inferius and superius, respectively. Constricting the central axis of the dumbbell from in front and behind is the low transverse crest. The larger foramen acusticum inferius is kidney-bean shaped and has some tiny perforations that are interpreted as evidence of the spiral cribriform tract (tractus spiralis foraminosus), which transmitted fascicles of the cochlear nerve. In the posterior part of the foramen acusticum inferius is a shallow pit that may represent the foramen singulare

for passage of some bundles of the vestibular nerve. The foramen acousticum superius, largely hidden in dorsal view, has a smaller anterior opening into a canal for the facial nerve and a posterior blind pit, which is interpreted as the cribriform dorsal vestibular area for passage of the remaining bundles of the vestibular nerve. Posterolateral to the internal acoustic meatus is the larger and deeper subarcuate fossa. Components of the semicircular canal system occupy the bone forming the rim of the aperture into the subarcuate fossa. The posterior semicircular canal forms the posterolateral rim, and the crus commune, the conjoined anterior and posterior semicircular canals, forms the posteromedial rim. The aperture into the subarcuate fossa is constricted posteriorly, that is, within the fossa the paraflocculus was expanded and occupied the space dorsal to the posterior semicircular canal and crus commune.

The medial edge of the pars cochlearis has two distinct surfaces (Fig. 7B, E). Anteriorly is the flat roof of the anteromedial flange, which has an incurved lateral wall that produces a distinct pocket. Based on the CT slices in Macrini (2000), this pocket accommodated the basisphenoid and basioccipital bones. Behind this pocket is a broad sulcus for the inferior petrosal sinus, which originated at the cavernous sinus around the hypophysis and left the skull via its own foramen anterior to the jugular foramen.

Anterior to the internal acoustic meatus and subarcuate fossa is a low crest, the crista petrosa (Fig. 7B, E). The medialmost portion of the crista petrosa, the part anterior to the internal acoustic meatus, is the prefacial commissure, the ossified chondrocranial component of the same name. Anterior to and hidden by the prefacial commissure is a narrow gap directed anteromedially, the hiatus Fallopii. The anterior border of the hiatus is formed by a narrow, low ridge that runs nearly the length of the pars cochlearis.

Three vascular sulci are situated in the vicinity of the subarcuate fossa (Fig. 7B, E). At the posterolateral corner of the petrosal is a sulcus running forward toward the crista petrosa along the lateral border of the subarcuate fossa. This short, shallow sulcus for the superior petrosal sinus cannot be traced beyond the anterior rim of the subarcuate fossa. Immediately posterolateral to the sulcus for the superior petrosal sinus is a barely visible sulcus for the prootic sinus, which is described with the lateral view where it is more fully apparent. Posteromedial to the subarcuate fossa, behind the crus commune and posterior semicircular canal, is a well-developed sulcus, the principal occupant of which was the sigmoid sinus. There are foramina at each end of this sulcus. Laterally is an oval aperture directed anterolaterally into a canal, the canal for the sigmoid sinus; medially is the slit-like vestibular aqueduct, which transmitted the endolymphatic duct into the petrosal. CM 5061 differs in that the foramen for the sigmoid sinus is situated more laterally, which creates a longer sulcus for the sigmoid sinus.

Finally, immediately posteroventral to and hidden by the bony bar behind the foramen acousticum inferius is another narrow, slit-like opening, the cochlear canaliculus, which transmitted the perilymphatic duct into the petrosal (Fig. 7B, E).

Lateral View.—The two divisions of the petrosal are also visible in the lateral or squamosal view. In Figure 7C and F, the pars canalicularis lies posterior to and includes the sulcus for the prootic sinus and the tuberculum tympani; the pars cochlearis lies anterior and ventral to these structures. As in the ventral view, the pars cochlearis in lateral view is dominated by the promontorium and two projections from it: ventrally, the rtp, and anteriorly, the anteromedial flange. The lateral edge of the anteromedial flange has a narrow depression that is interpreted as the fossa for the tensor tympani muscle. The dorsal edge of the pars cochlearis includes the low crista petrosa. Ventral to the crista petrosa is another low ridge that runs nearly the length of the pars cochlearis (this ridge is significantly lower in CM 5061 than in CM 5024). Posteriorly, this ridge runs somewhat parallel to the crista petrosa; anteriorly, it is positioned more ventrally and forms the dorsal border of the fossa

for the tensor tympani. Near the midpoint of and largely hidden by this ridge is the hiatus Fallopii (in light of the lower ridge in CM 5061, the hiatus Fallopii is more visible in lateral view). More posteriorly, between this ridge and the tuberculum tympani are two tiny vascular foramina that likely drained venous blood from the petrosal (only the posteroinferior foramen is preserved in CM 5061). The petrosals of juvenile *Monodelphis domestica* studied by the author (reported in Rougier et al., 1992) contain a large amount of venous blood with various points of egress. Ventral to these tiny foramina are two larger apertures on the pars cochlearis of CM 5024 partially visible in lateral view, the secondary facial foramen in front and the fenestra vestibuli behind.

The pars canalicularis is roughly trapezoidal in lateral view (Fig. 7C, F) with posterior, ventral, anterior, and dorsal sides. In the ventral part of the posterior side is the mastoid process and dorsal to it, one-third the way up the posterior side, is a distinct vascular notch, the posttemporal notch (this notch is less distinct in CM 5061). In the skull, this notch is covered laterally by the squamosal to complete a posttemporal foramen, which in CM 52729 does not have a visible aperture (Fig. 9) and apparently did not transmit any substantial structure. There is no indication in CM 5024 and 5061 of a sulcus running anteriorly from the posttemporal notch in contrast to the condition in some other didelphids (see Wible, 1990:fig. 4B; Sánchez-Villagra and Wible, 2002). Running dorsally and slightly anteriorly from the posttemporal notch in figure 7C is a low ridge that delimits the covered and uncovered portions of the pars canalicularis. Posterior to this ridge is the mastoid exposure; anterior to it, the remaining surface of the pars canalicularis is covered by the squamosal bone in the skull.

Anterior to the mastoid process, the ventral side of the pars canalicularis is formed by the tympanohyal, crista parotica, and tuberculum tympani (Fig. 7C, F). Dorsal to the mastoid process and tympanohyal are four small vascular foramina that likely drained venous blood from the petrosal (only two foramina are present in CM 5061).

The anterior side of the pars canalicularis is formed ventrally by the tuberculum tympani, and posterior and dorsal to that by a longitudinal vascular sulcus (Fig. 7C, F). The occupant of this sulcus was a vein, the primary egress of which was the postglenoid foramen in the squamosal bone. The secondary, much smaller egress was the prootic canal, the lateral aperture of which is visible in the ventral portion of the longitudinal sulcus (the lateral aperture in CM 5061 is twice the size of that in CM 5024). The lateral aperture of the prootic canal marks the boundary at which the vein occupying the longitudinal sulcus has two different developmental histories (Gelderen, 1924; Wible, 1990; Wible and Hopson, 1995; Rougier and Wible, in press). The portion of the vein above the prootic canal is the retained prootic sinus, one of the first veins draining the brain to appear embryologically; the portion below the prootic canal, the sphenoparietal emissary vein of Gelderen (1924), is a much later addition developmentally. The dorsal side of the pars canalicularis is characterized by four vascular foramina. The smallest and most dorsal one leads into the substance of the petrosal; the remaining three lead into a canal for the sigmoid sinus that runs the length of the dorsal side. The anteriormost and largest of these three foramina is directed anterolaterally and transmitted the sigmoid sinus into its canal. The foramen posterior to the foramen for the sigmoid sinus is directed ventrolaterally into a sulcus that extends nearly to the level of the posttemporal notch. The posteriormost and smallest foramen appears to be directed laterally. CM 5061 differs from CM 5024 in that the canal for the sigmoid sinus is very short. Instead of a canal in the petrosal, running nearly the length of the lateral surface of the pars canalicularis, there is a sulcus for the sigmoid sinus in the comparable location. The sulcus leads to a foramen near the posterodorsal corner of the lateral surface that after a short bony course opens on the endocranial surface. The

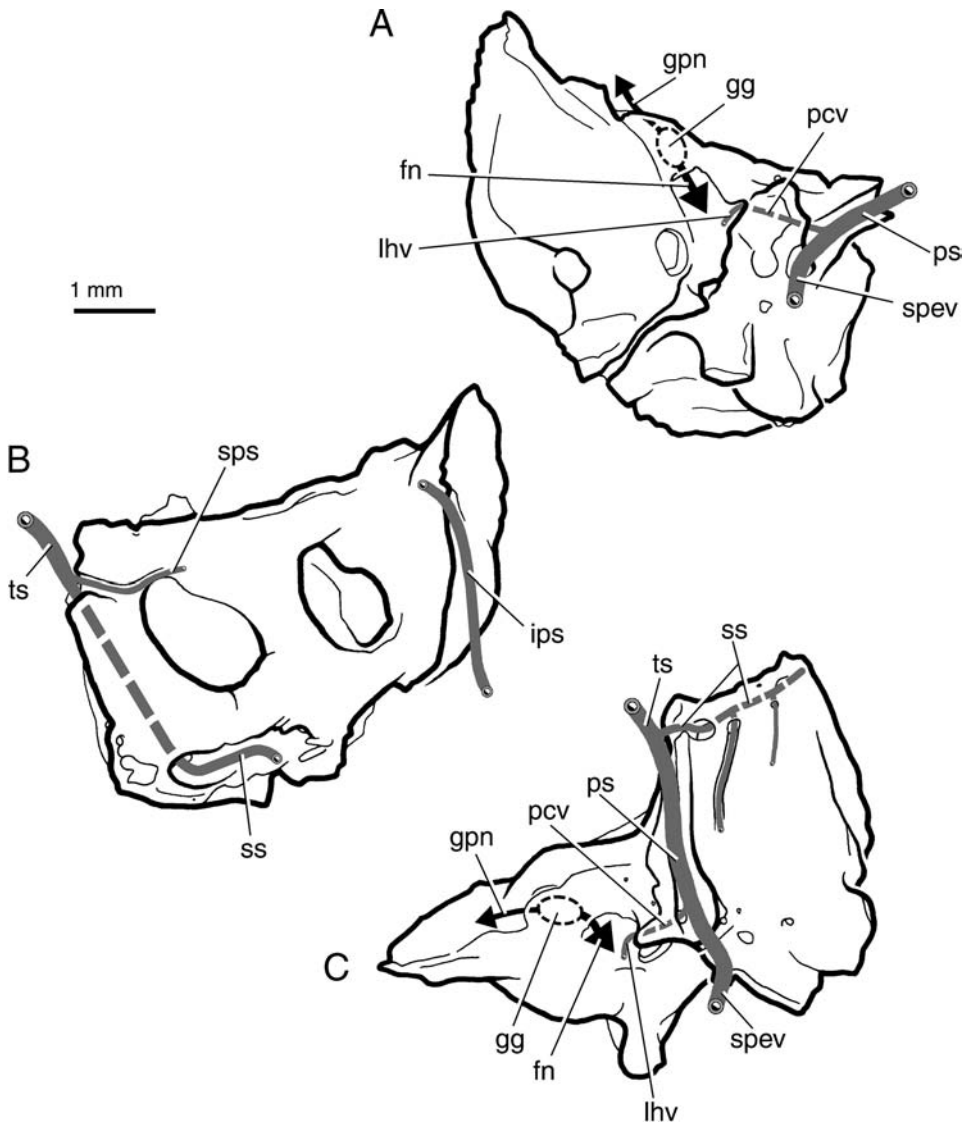


Fig. 8.—*Monodelphis* sp. CM 5024, line drawings of left petrosal with facial nerve and major veins in ventral view (A), dorsal view (B), and lateral view (C). Abbreviations: **fn**, facial nerve; **gg**, geniculate ganglion of the facial nerve; **gpn**, greater petrosal nerve; **ips**, inferior petrosal sinus; **lhv**, lateral head vein; **pcv**, prootic canal vein; **ps**, prootic sinus; **spev**, sphenoparietal emissary vein; **sps**, superior petrosal sinus; **ss**, sigmoid sinus; **ts**, transverse sinus.

sulcus for the sigmoid sinus on the lateral surface in CM 5061 was covered laterally in the skull by the squamosal, thus completing a canal the composition of which differs from that in 5024.

Veins.—As is apparent in the foregoing descriptions, several veins are intimately associated with the petrosal of CM 5024 and 5061. The major foramina, sulci, and canals associated with these veins have been noted above. A comprehensive review of the course

of these veins is included here to document the pathways between the major conduits into and out of the petrosal and skull (Fig. 8). Elsewhere I have published illustrations of the veins of the petrosal in *Didelphis virginiana* (Wible, 1990:fig. 4C, D; Wible and Hopson, 1995:fig. 5). Essentially the same pattern is present in CM 5024 and 5061.

The inferior petrosal sinus runs along the medial edge of the pars cochlearis (Fig. 8B). Anteriorly, the inferior petrosal sinus (sinus petrosus ventralis of Dom et al., 1970) arises from the back of the cavernous sinus, which is situated around the hypophysis above the basisphenoid. The inferior petrosal sinus then runs posteriorly exposed within the floor of the cranial cavity, in the broad sulcus medial to the internal acoustic meatus (Fig. 7B, E). The endocranial position of the inferior petrosal sinus was confirmed in numerous skulls, including CM 52729. This course contrasts with the condition in *Didelphis virginiana*, in which the bulk of the course of the inferior petrosal sinus is not exposed within the cranial cavity, but is within a canal between the petrosal and basioccipital. Just in front of the cochlear canaliculus in *Monodelphis*, the inferior petrosal sinus exits the skull via its own foramen (Fig. 6) and forms the internal jugular vein. Dom et al. (1970) reported that the internal jugular vein in *D. virginiana* is small and drains mainly deep structures of the neck; a similar pattern is likely present in *Monodelphis*.

The other major veins of the petrosal are all distributaries of the transverse sinus. Before addressing the pattern in CM 5024 and 5061, it is instructive to review the pattern in *Didelphis virginiana*, based on Dom et al. (1970), Wible (1990), and Wible and Hopson (1995). According to these authors, the transverse sinus, which runs in the outer edge of the tentorium cerebelli, has three principal distributaries: the superior petrosal sinus (sinus petrosus dorsalis of Dom et al., 1970), the prootic sinus (sinus temporalis of Dom et al., 1970), and the sigmoid sinus. The first distributary is the superior petrosal sinus, which runs forward to the cavernous sinus. An isolated petrosal of *D. virginiana*, CM 23799, shows a well-developed sulcus for the superior petrosal sinus reaching forward to the prefacial commissure. Beyond the origin of the superior petrosal sinus, the transverse sinus divides into the larger prootic sinus and the smaller sigmoid sinus. The prootic sinus runs ventrally in a canal between the petrosal and squamosal and ultimately leaves the skull as the postglenoid vein via the postglenoid foramen in the squamosal. Following Gelderen (1924), Wible (1990) and Wible and Hopson (1995) showed that the vein exiting the postglenoid foramen is composed of two embryologically distinct elements: the ontogenetically older prootic sinus superiorly and the sphenoparietal emissary vein inferiorly. The border between these two is marked by the lateral aperture of the prootic canal, which represents the ontogenetic primary exit of the prootic sinus. The vein within the prootic canal, which connects with the rudimentary lateral head vein, is much reduced in size compared with the prootic sinus and sphenoparietal emissary vein. The remaining distributary of the transverse sinus, the sigmoid sinus, runs medially and then posteriorly, exiting the cranial cavity via the foramen magnum. The isolated petrosal of *D. virginiana* CM 23799 has a deep sulcus for the sigmoid sinus that runs posterior and posteromedial to the posterior semicircular canal and subarcuate fossa.

The isolated petrosals of *Monodelphis* CM 5024 and 5061 by and large conform to the general pattern described above for *Didelphis virginiana*, with bony evidence present for the three distributaries of the transverse sinus. Because the skulls of CM 5024 and 5061 are damaged, it is also possible to document the course of the transverse sinus, which is indicated by a broad sulcus running ventrally and slightly anteriorly from the midline on the endocranial surface of the parietal. This sulcus meets the petrosal posterolateral to the subarcuate fossa, immediately dorsal to the sulcus for the prootic sinus present on the lateral surface of the petrosal (Fig. 8C). From this point of contact, three channels originate. (1) A sulcus for the superior petrosal sinus (Figs. 7B, E, 8B) runs forward along the lateral

contour of the subarcuate fossa in CM 5024 and 5061, differing from that in *D. virginiana* CM 23799 in being weaker and shorter. It is uncertain whether or not this shorter sulcus is truly evidence for a shorter superior petrosal sinus. In contrast to the superior petrosal sinus connecting the transverse and cavernous sinuses reported for *D. virginiana* by Dom et al., (1970), Archer (1976) illustrated the superior petrosal sinus in the dasyurids *Sminthopsis murina* and *Antechinus stuartii* as not extending medial to the level of the internal acoustic meatus and not connecting to the cavernous sinus. (2) The sulcus for the prootic sinus and sphenoparietal emissary vein (Figs. 7C, F, 8C) is essentially identical in *Monodelphis* CM 5024 and 5061 and *D. virginiana* CM 23799, running directly ventrally from the sulcus for the transverse sinus. One difference is that the lateral aperture of the prootic canal is relatively smaller in the latter taxon. (3) The course of the sigmoid sinus (Figs. 7B–C, E–F, 8B–C) exhibits the most pronounced difference among all three isolated petrosals. *D. virginiana* CM 23799 has a sulcus for the sigmoid sinus exposed endocranially, running posterior and posteromedial to the posterior semicircular canal. This is the primitive therian, mammalian, and mammaliaform condition (Kermack et al., 1981; Wible, 1990; Wible et al., 1995, 2001). *Monodelphis* CM 5024 and 5061 differ in that the proximal part of the sigmoid sinus is not exposed endocranially but is enclosed within a canal. The composition and length of the canal differs between CM 5024 and 5061. In the former, the canal is entirely within the petrosal and is longer; in the latter, the canal is between the petrosal and squamosal.

Ectotympanic and Middle-Ear Ossicles

Detailed descriptions of the paired ectotympanic bones and middle-ear ossicles of *Monodelphis* are not included here. The reader is referred to the accounts of *Didelphis virginiana* in Doran (1878), *D. perinigra* in Segall (1969), and *Metachirus* sp. in Fleischer (1973). Photographs of the malleus, incus, and stapes of *M. domestica* are included in Sánchez-Villagra et al. (2002:fig. 10A).

For the sake of completeness, I describe the aspects of the ectotympanic shown in the ventral view (Fig. 6), which exposes most of the outer surface of this irregular U-shaped bone. The anterior leg or crus of the ectotympanic is narrow and has a broad contact with the squamosal, medial to the postglenoid foramen. Anteroventral to the squamosal, the anterior crus has a narrow contact with the alisphenoid tympanic process. At the ventral base of the anterior crus, the anterior surface of the ectotympanic is covered by the anterior process of the malleus, which also contacts the alisphenoid tympanic process. Posterior to the alisphenoid tympanic process, the posterior leg or crus of the ectotympanic is broadened and abuts the rostral tympanic process of the petrosal distally. The sulcus tympanicus, the groove channeling the inner circumference of the ectotympanic to which the tympanum attaches, lies on the extreme medial edge of the bone. Therefore, the expansion of the posterior crus is lateral to the tympanum attachment and contributes to a floor for the external acoustic meatus.

A comment about the stapes is needed in that there is a discrepancy in the literature concerning the presence of an intracural foramen. The photograph of the stapes of *Monodelphis domestica* in Sánchez-Villagra et al. (2002:fig. 10A) shows a well-developed intracural foramen, whereas Archer (1976) reported that the stapes is imperforate in *M. dimidiata* WAM M6785. I checked this feature in the CM *Monodelphis* sample. A perforate stapes as illustrated by Sánchez-Villagra et al. (2002:fig. 10a) occurs in the 14 *M. brevicaudata* and 27 *M. domestica* preserving the bone. In contrast, the stapes is imperforate in the one *M. osgoodi* (5248) preserving the bone and in two *M. dimidiata* (86608, 86609); there is a microperforation in the third *M. dimidiata* (86611) with a stapes.

Occipital Complex

CM 52729 has a single occipital bone that forms the skull base between the ear regions, encircles the foramen magnum, and forms the bulk of the occiput. Developmentally (Clark and Smith, 1993), the occipital is a composite of four bones: unpaired basioccipital and supraoccipital, and the paired exoccipitals. CM 52729 has a remnant of the exoccipital-supraoccipital suture (Fig. 9). However, one juvenile *Monodelphis breviceaudata* (CM 68360) and several juvenile *M. domestica* (CM 80019, 80020, and 80033) preserve sutures delimiting all four bones. Based on these specimens, I describe the basioccipital, exoccipitals, and supraoccipital as separate elements in CM 52729.

Basioccipital

The basioccipital forms the skull base between the petrosals and the anteroventral border of the foramen magnum (Figs. 5–6). It is roughly hexagonal with five straight sides (anterior and paired anterolateral and posterolateral) and a posterior sixth side that is indented by the intercondyloid or odontoid notch (Fig. 5). The anterior side is the horizontal suture with the basisphenoid, which lies at the level of the anterior pole of the petrosal promontorium. The anterolateral side abuts the petrosal promontorium except at its posterior end where there is a gap between the petrosal, basioccipital, and exoccipital for the passage of the inferior petrosal sinus (Fig. 6). The posterolateral side is the fused suture with the exoccipital, which ends posteriorly just lateral to the odontoid notch. The anterior and anterolateral sides project somewhat ventrally. The posterior side is also raised as it bears the medial portion of the left and right occipital condyles, which meet on the midline. Also on the midline of the basioccipital is a raised crest in the form of an inverted Y, which form the medial border of paired oval muscular depressions. Based on the dog (Evans, 1993), these depressions housed the rectus capitis ventralis muscle.

Exoccipital

The paired exoccipitals have two subequal, quadrangular parts: a horizontal one on the skull base (Figs. 5–6) and a vertical one on the occiput (Fig. 9).

In ventral view (Fig. 6), the bulk of the horizontal part bears the occipital condyle, which can be described as two continuous articular surfaces. The smaller anteromedial surface is somewhat teardrop-shaped, with the pointed end on the basioccipital meeting its fellow of the opposite side. The larger posterolateral surface is saddle-shaped and extends onto the occiput. At the posterolateral corner of the horizontal part is a strong, posteroventromedially directed paracondylar process, from which the digastric muscle originates, based on *Didelphis marsupialis* (Turnbull, 1970). The anterior and lateral sides of the paracondylar process are in sutural contact with the petrosal. In fact, the medial end of the petrosal's ctp is raised and contributes to the base of the paracondylar process. Anterolateral to the paracondylar process are two foramina between the exoccipital and petrosal, the jugular foramen and, anteromedial to it, the foramen for the inferior petrosal sinus. Separating the two openings is a narrow, weak abutment of the exoccipital and petrosal. The surface of the exoccipital that contributes to the posteromedial border of both openings projects ventrally. The jugular foramen is oval and directed ventrally; the foramen for the inferior petrosal sinus is narrower and directed posterolaterally. Running posteriorly a short distance from the foramen for the inferior petrosal sinus is a weak sulcus. In the interval between these two foramina and the occipital condyle are two ovoid, anteriorly directed foramina for the hypoglossal nerve. The larger posterior

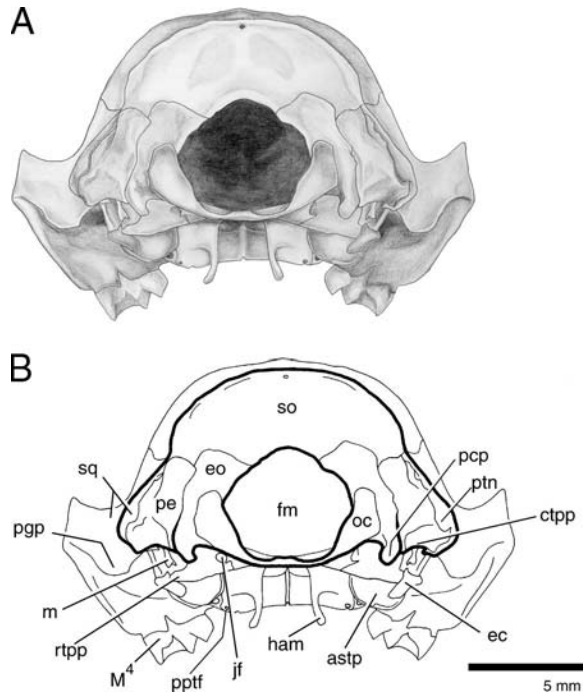


Fig. 9.—*Monodelphis brevicaudata* CM 52729, skull in occipital view excluding mandibles (A) with accompanying line drawing (B). Abbreviations: **astp**, alisphenoid tympanic process; **ctpp**, caudal tympanic process of the petrosal; **ec**, ectotympanic; **eo**, exoccipital; **fm**, foramen magnum; **ham**, pterygoid hamulus; **jf**, jugular foramen; **M⁴**, upper fourth molar; **m**, malleus; **oc**, occipital condyle; **pcp**, paracondylar process of the exoccipital; **pe**, petrosal; **pgp**, postglenoid process; **pptf**, foramen in the postpalatine torus; **ptn**, posttemporal foramen; **rtp**, rostral tympanic process of the petrosal; **so**, supraoccipital; **sq**, squamosal.

foramen is immediately in front of where the two articular surfaces of the occipital condyle meet, and the smaller anterior foramen lies anteromedial to that. Both hypoglossal foramina open into slight depressions.

In occipital view (Fig. 9), the vertical part of the exoccipital forms most of the lateral wall of the foramen magnum. It also bears the posterodorsal part of the saddle-shaped articular surface of the occipital condyle and the back of the paracondylar process. Laterally, the vertical part of the exoccipital contacts the mastoid exposure of the petrosal at a suture that is angled slightly dorsomedially. Dorsally, a remnant of the exoccipital's suture with the supraoccipital is preserved in CM 52729. It is a gently curved contact with the exoccipital convex and the supraoccipital concave. There are no foramina within the vertical part of the exoccipital.

Supraoccipital

The supraoccipital forms roughly the dorsal half of the occiput as well as the cap of the foramen magnum (Fig. 9). Its ventral border has narrow contacts with the paired mastoid exposures of the petrosal laterally and broader contacts with the paired exoccipitals medially. Its dorsal border is fused seamlessly with the interparietal (see above) and contributes to the posterior surface of the nuchal crest. The middle of the supraoccipital has

a gentle bulge over the vermis of the cerebellum. A similar bulge occurs in the dog, and dorsal to it and connected by a crest is a triangular projection, the external occipital protuberance (Evans, 1993). Neither protuberance nor crest occurs in *Monodelphis*. On the midline at the base of the nuchal crest is a small, round opening that contained dried blood in CM 52729 and was probably an emissary foramen. Given the uncertainty of the position of the interparietal-supraoccipital suture on the midline, it is unknown whether this foramen was entirely within the supraoccipital or between the supraoccipital and interparietal.

Mandible

The mandible houses the lower dentition: four incisors, a canine, three premolars, and four molars. It consists of a tooth-bearing horizontal part, or body, and a vertical part, or ramus (Fig. 2). The left and right mandibles are firmly united at the mandibular symphysis, a rough-surfaced fibrous joint. The mandibular symphysis extends from between the roots of the first incisors to the level of the p2–p3 embrasure (Fig. 3).

In lateral view (Fig. 2), the body of the mandible is thin, elongate, and tapered anteriorly; it achieves its maximum depth below m2. It is extremely thin below the incisors and, in fact, the roots of the incisors, canine, and first premolar are all slanted posteroventrally to a considerable degree. Because of the reduction in alveolar space, the root of the second incisor is wedged between that of its neighbors, producing the staggered condition (Hershkovitz, 1982, 1995) whereby the lateral side of the root is covered by a bony buttress that projects above the alveolar line of the adjacent teeth; this condition is not visible in the illustrations because of scale. The bulk of the mandibular body's dorsal surface is tooth bearing, but there is a narrow retromolar space between the last molar and the mandibular ramus (Figs. 2–3). The lateral (labial and buccal) surface of the body bears two subequal mental foramina (Fig. 2), both of which have weak, anterodorsally directed sulci emanating from them. The more anteriorly directed anterior mental foramen lies principally below the posterior root of p1; the more anterodorsally directed posterior mental foramen lies below the anterior root of m2. The medial (lingual) surface bears a subtle, smooth, longitudinal ridge below m3 and m4, which becomes slightly more prominent posterior to the molars on the mandibular ramus. This ridge ends posterodorsal to the mandibular foramen and corresponds in position to the mylohyoid line or crest of the dog (Evans, 1993). However, it apparently does not represent the attachment for the mylohyoid muscle, which is much closer to the ventral margin of the mandibular body and ramus in *Didelphis virginiana* (Hiemae and Jenkins, 1969). Based on *D. virginiana*, this line may represent the anteroventral limit of the attachment of the temporalis muscle. Ventral to and parallel with the “mylohyoid” line are two faint, narrow sulci that may be neurovascular impressions (mylohyoid nerve and vessels). The surface of the mandibular symphysis could not be studied in CM 52729, because the left and right mandibles remain connected. In a *M. brevicaudata* with separate mandibles, CM 76732, the surface of the symphysis is slightly roughened and cigar-shaped.

The ramus of the mandible bears three salient processes (Fig. 2): coronoid, condylar (articular), and angular. The coronoid process, the largest of the three, forms the dorsal part of the ramus and extends upward and outward. It is a large, thin plate of bone with a thickened, convex anterior border, the coronoid crest, and a concave posterior border. The dorsal surface of the coronoid process is rounded and comes to a posteriorly directed point at its posterodorsal limit. The ventral end of the posterior border of the coronoid process turns posteriorly into the condylar process, which buttresses the medial half of the transversely elongated, posterodorsally directed articular surface, the mandibular component of the temporomandibular joint (Fig. 3). The lateral half of the articular surface is buttressed by the posterior shelf of the masseteric fossa (Fig. 3; see below). The articular

surface lies above the occlusal plane, and in dorsal view, is roughly cigar-shaped. The angle of the mandible is the caudoventral part of the ramus. As is generally the case in marsupials, the angular process is medially inflected and, therefore, is best seen in dorsal (or ventral) view (Fig. 3). It is a triangular, posteromedially directed shelf that ends in a finger-like prong, which is concave dorsally and convex ventrally. Attaching to the ventral surface of the angular process is the superficial masseter muscle and to the dorsal surface is the internal pterygoid muscle, based on *Didelphis* (Hiemae and Jenkins, 1969; Turnbull, 1970). In a recent study of the diversity of the marsupial angular process, Sánchez-Villagra and Smith (1997) classified the angular process of *Monodelphis brevicaudata* as rod-like, with the ratio of angular process shelf length to angular process length less than 0.72. The bulk of the lateral surface of the mandibular ramus in CM 52729 (Fig. 2) has a prominent, three-sided depression, the masseteric fossa for the insertion of the deep masseter and zygomaticomandibularis muscles, based on *D. marsupialis* (Turnbull, 1970). The anterior limit of the masseteric fossa is formed by the thickened coronoid crest, which also provides attachment for the temporalis muscle, based on *D. marsupialis* (Turnbull, 1970). The ventral limit of the masseteric fossa is formed by the masseteric line, the posterior part of which is expanded laterally to form the posterior shelf of the masseteric fossa (Marshall and Muizon, 1995), best seen in dorsal view (Fig. 3). On the medial side of the mandibular ramus, dorsal to the base of the angular process is the circular, posteriorly directed mandibular foramen (Fig. 3). The medial surface anterodorsal to the mandibular foramen provides a flat attachment area for the temporalis muscle, based on *D. marsupialis* (Turnbull, 1970). The external pterygoid muscle inserts on the medial side of the ventral-most excursion of the mandibular notch, which separates the coronoid and condylar processes, based on *Didelphis* (Hiemae and Jenkins, 1969; Turnbull, 1970).

Dentition

Detailed descriptions of the dentition of *Monodelphis* are beyond the scope of this report. Reig et al. (1987:figs. 23 A, B, 24) provide detailed drawings of the upper and lower teeth of *M. domestica* FMNH 19504, in labial, occlusal, and lingual views and the upper and lower postcanine teeth of *M. orinoci* UKMNH 123941 in occlusal view. These authors do not describe the *Monodelphis* dentition per se, but numerous dental characters are found in their tables 1 and 2 and in the text.

DISCUSSIONS

As noted in the Introduction, few detailed descriptions of the skull of extant metatherians exist in the literature. Moreover, there are few detailed treatments of the major cranial foramina of extant metatherians, including the identification of contents and observation of variations. Perhaps the most thorough treatment of the major cranial foramina of extant metatherians is that by Archer (1976). This author (1976:figs. 2–4) illustrated the major extracranial arteries and veins in the dasyurids *Sminthopsis murina*, *Planigale maculata*, and *Antechinus stuartii*, based on dissections of latex injected specimens. He then described the basicranium and its major foramina in 17 genera of extant and extinct dasyuromorphians, including *Monodelphis dimidiata* based on WAM M6785 along with four other Recent genera of Didelphidae. Also included in Archer (1976:pp. 219–223) was a glossary of 21 major cranial foramina. Although generally a useful glossary, it is limited in the number of foramina included, the level of detail of contents considered, and the depth of variations described. In addition, some terminology employed by Archer (1976) is peculiar to Metatheria and is requiring of standardization for researchers studying other branches of the mammalian tree.

Following in Archer's (1976) footsteps, I include here a discussion of the major cranial foramina, their contents, and the variations encountered on the extracranial surfaces and on the isolated petrosals of the CM sample of *Monodelphis*. First, considered in alphabetical order are 37 named cranial foramina. For these foramina, I apply either an anglicized name from the fourth edition of the *Nomina Anatomica Veterinaria* (1994) or a name more widely used in the mammalian literature. The sources for the identification of contents of foramina are included. Ideally, identifications are based on studies of *Monodelphis domestica*, either published (e.g., Clark and Smith, 1993; Sánchez-Villagra and Wible, 2002) or my own unpublished observations. Second, considered in alphabetical order by cranial bone are the various small, unnamed foramina, some of which have been noted in the Descriptions. These foramina are of uncertain function, but the majority are likely nutrient or emissary foramina.

In addition to noting the distribution of these foramina in the CM sample of *Monodelphis*, I include observations on four other taxa: the didelphid *Didelphis albiventris* (CM 78203), the dasyurid *Dasyurus maculatus* (CM 50842), the early Paleocene metatherian *Pucadelphys andinus* (based on Marshall and Muizon, 1995), and the eutherian *Zalambdalestes lechei* from the Mongolian Late Cretaceous (based on Kielan-Jaworowska and Trofimov, 1981; Kielan-Jaworowska, 1984; Wible et al., in press). As a rough approximation, following the phylogenetic analysis of Rougier et al. (1998), foramina present in *Monodelphis* and *Didelphis* might be present in didelphids primitively; in these two taxa plus *Dasyurus* might be present in marsupials primitively; in these three taxa plus *Pucadelphys* might be present in metatherians primitively; and in these four taxa plus *Zalambdalestes* might be present in therians primitively. Regarding *P. andinus*, the absence of some of the unnamed foramina reported below should be taken with caution, because the basis is the descriptions by Muizon and Marshall (1995). These authors may not have investigated this extinct taxon to the same level of detail as done here or by Wible et al. (in press).

Named Cranial Foramina

Accessory Palatine Foramen.—In the dog (Evans, 1993), the accessory palatine nerve and artery, off the major palatine nerve and artery respectively, supply the caudal mucosa of the hard palate via foramina on the hard palate that are termed minor palatine foramina. Wible and Rougier (2000) argued that these foramina are best termed accessory palatine foramina, reserving the term minor palatine foramen for the aperture at the back of the palate that transmits the minor palatine nerve and artery to the soft palate. *Monodelphis brevicaudata* CM 52729 (Fig. 5) has a tiny foramen on the right side and two on the left asymmetrically arranged medial to the minor palatine foramen that may have been accessory palatine foramina. The number, size, and position of such apertures varies considerably in the CM sample. Only one specimen, *M. brevicaudata* (63509), has no foramina whatsoever on one side only. The remainder varies from a single tiny opening as on the right side in CM 52729 to a maximum of around 15 on one side in two *M. domestica* (80019, 80028).

Didelphis albiventris CM 78203 has two foramina on each side asymmetrically arranged resembling those in *Monodelphis*. *Dasyurus maculatus* CM 50842 has one small foramen on each side asymmetrically arranged and anteromedial to that more than 20 minute foramina of uncertain function. Foramina are not described for *Pucadelphys andinus* (Marshall and Muizon, 1995), and there are no accessory palatine foramina in *Zalambdalestes lechei* (Wible et al., in press).

Carotid Foramen (Entocarotid Foramen of Archer, 1976).—In *Monodelphis brevicaudata* CM52729 (Fig. 6), the carotid foramen lies entirely within the basisphenoid and, based

on *M. domestica* (Wible, unpubl. observ.), transmitted the internal carotid artery and accompanying vein and sympathetic nerve. This foramen exhibits no variability among the remaining CM specimens.

The carotid foramen is similarly situated in the basisphenoid in *Didelphis albiventris* CM 78203, *Pucadelphys andinus* (Marshall and Muizon, 1995), and *Zalambdalestes lechei* (Wible et al., in press). The carotid foramen is also within the basisphenoid in *Dasyurus maculatus* CM 50842, but it lies nearer the suture with the basioccipital and is recessed dorsally from the basicranial surface.

Condylod Canal.—Archer (1976) described a venous condylar foramen, which carries part of the venous drainage from the sigmoid sinus to the internal jugular vein in dasyurids. However, from Archer's labelled figures in Plate 1, it is apparent that his venous condylar foramen is the posterior hypoglossal foramen of this report. The dog has a condylod canal situated posterolateral to the hypoglossal foramen and transmitting the condylod vein, which connects the sigmoid sinus and the basilar sinus (Evans, 1993). In the ventral condylod fossa of *Monodelphis breviceaudata* CM 52729 (Fig. 6) are two hypoglossal foramina and no additional openings. However, the total absence of a condylod canal posterolateral to the two hypoglossal foramina is unusual in the CM specimens of *Monodelphis*, occurring in only one other *M. breviceaudata* (76730). In the remaining 37 specimens in which this feature could be examined on both sides, condylod canals medial to the paracondylar process are present bilaterally in 9 *M. breviceaudata* (4681, 52370, 65309, 68358, 68360, 68361, 76731, 76733, 76734), 15 *M. domestica* (80016, 80018, 80019, 80021, 80023, 80026–80030, 80035, 80036, 80039, 80040, 101529), one *M. dimidiata* (86608), and the two *M. osgoodi* (5242, 5248). Presence on one side only occurs in two *M. breviceaudata* (63510, 68359), seven *M. domestica* (5010, 80017, 80020, 80031, 80033, 80034, 80038), and one *M. dimidiata* (86609). The sample varies further in the relative size of the condylod canals and the occasional presence of two canals bilaterally or on one side only.

Condylod canals are not present in *Didelphis albiventris* CM 78203, *Dasyurus maculatus* CM 50842, *Pucadelphys andinus* (Marshall and Muizon, 1995), and *Zalambdalestes lechei* (Wible et al., in press).

Ethmoidal Foramen.—According to Archer (1976), the ethmoidal foramen carries a branch of the internal carotid artery (presumably the ophthalmic artery) from the orbit into the nasal cavity in dasyurids. In *Monodelphis domestica* (Wible, unpubl. observ.), in addition to a branch of the ophthalmic artery it also carries the ethmoidal nerve, a branch of the ophthalmic division of the trigeminal nerve. The position of the ethmoidal foramen between the frontal and orbitosphenoid in *M. breviceaudata* CM 52729 (Fig. 4) is repeated in the remaining CM sample.

The ethmoidal foramen is similarly situated between the frontal and orbitosphenoid in *Didelphis albiventris* CM 78203 and *Dasyurus maculatus* CM 50842. It is said to be between the frontal, orbitosphenoid, and alisphenoid in *Pucadelphys andinus* (Marshall and Muizon, 1995) and within the frontal in *Zalambdalestes lechei* (Wible et al., in press).

Foramen for Frontal Diploic Vein (Frontal Foramen of Archer, 1976; Supraorbital Foramen of Marshall and Muizon, 1995).—According to Archer (1976), this foramen transmits the frontal diploic vein from the transverse frontal sinus to a branch of the external jugular vein in dasyurids. In the dog (Evans, 1993), the frontal diploic vein, an emissary vein from the diploë of the frontal bone to the ophthalmic vein, exits via a small unnamed foramen in the orbital surface of the postorbital process of the frontal (for the distribution in other eutherians, see Thewissen, 1989). In *Monodelphis breviceaudata* CM 52729 (Fig. 4), the foramen for the frontal diploic vein is small and lies within the frontal in the supraorbital

margin, anterior to the subtle postorbital process. In the remaining 53 CM *Monodelphis*, at least one bilaterally present foramen for the frontal diploic vein is invariably present. Variations include the size of the foramina and the number present. Double foramina occur bilaterally in one *M. brevicaudata* (76730) and one *M. domestica* (80016), and on one side only in two *M. brevicaudata* (68359, 76731) and four *M. domestica* (80021, 80032, 80036, 80037). The most unusual specimen was *M. domestica* (80040), which had three foramina (one large and two tiny) on the right and five tiny foramina on the left.

The foramen for the diploic vein is present in *Didelphis albiventris* CM 78203, *Dasyurus maculatus* CM 50842, and *Pucadelphys andinus* (Marshall and Muizon, 1995). *D. maculatus* differs in that it has two foramina on the right and three on the left. The diploic vein foramen is lacking in *Zalambdalestes lechei* (Wible et al., in press), but evidently occurs in the slightly older zalambdalestid *Kulbeckia kulbecke* (Archibald and Averianov, 2003).

Foramen for Greater Petrosal Nerve (Median Lacerate Foramen of Marshall and Muizon, 1995).—Based on sectioned specimens of *Monodelphis domestica* (Wible, unpubl. observ.), I identify the small aperture between the basisphenoid and petrosal that is confluent laterally with the much larger foramen ovale in *M. brevicaudata* CM 52729 (Fig. 6) as the foramen for the greater petrosal nerve. It transmits the greater petrosal nerve, a branch of the facial nerve, from the hiatus Fallopii to the posterior opening of the pterygoid canal. Variants in the CM *Monodelphis* sample concern the degree of separation from the foramen ovale, with the majority of specimens exhibiting the pattern of CM 52729. At one extreme are some *M. brevicaudata* (e.g., 8019, 80021) and *M. domestica* (e.g., 63510) in which the foramen for the greater petrosal nerve is nearly closed off from the foramen ovale by prongs extending posteriorly from the sphenoid and anteriorly from the petrosal, and at the other extreme are the two *M. osgoodi* (5242, 5248) with an extremely shallow foramen for the greater petrosal nerve that is barely recognizable as separate from the foramen ovale.

As noted by Marshall and Muizon (1995), Archer (1976) employed the term foramen pseudoovale in two different senses. Where the opening that I would identify as the foramen for the greater petrosal nerve is widely separated from the foramen ovale in the alisphenoid, as in the Tasmanian wolf *Thylacinus cynocephalus*, Archer (1976:pl. 1A) employed the term foramen pseudoovale for the former. Where the opening that I would identify as the foramen for the greater petrosal nerve is confluent with the foramen ovale between the alisphenoid and petrosal, as in the dasyurid *Dasyurus cristicauda*, Archer (1976:pl. 1C) employed the term foramen pseudoovale for the conjoined opening.

A foramen for the greater petrosal nerve is separate from the foramen ovale in *Didelphis albiventris* CM 78203 and *Pucadelphys andinus* (Marshall and Muizon, 1995), but is confluent with the latter opening in *Dasyurus maculatus* CM 50842. In *Zalambdalestes lechei* (Wible et al., in press), the greater petrosal nerve emerged from the cranial cavity via the posteriormost part of the piriform fenestra, the large gap between the petrosal, basisphenoid, and alisphenoid that is closed by membrane in extant forms (MacPhee, 1981).

Foramen for Inferior Petrosal Sinus (Internal Jugular Canal of Archer, 1976; Inferior Petrosal Foramen of Marshall and Muizon, 1995).—According to Archer (1976), this aperture leads the major internal jugular vein from the cranial cavity in dasyurids and does not carry a major artery, contra Gregory (1910) and Patterson (1965) who identified this opening as the posterior carotid canal. The occupant of this canal in didelphids (Dom et al., 1970; Wible, unpubl. observ.) as well as in dasyurids is not the internal jugular vein per se, but the inferior petrosal sinus (Sinus petrosus ventralis), which connects the cavernous sinus and the internal jugular vein. Consequently, I employ the more informative term

foramen for inferior petrosal sinus. In *Monodelphis breviceaudata* CM 52729 (Fig. 6) and the remaining CM sample, this foramen is situated between the exoccipital and petrosal, anterior to the jugular foramen.

A foramen for the inferior petrosal sinus separate from the jugular foramen occurs in *Didelphis albiventris* CM 78203, *Dasyurus maculatus* CM 50842, and *Pucadelphys andinus* (Marshall and Muizon, 1995), but not in *Zalambdalestes lechei* (Wible et al., in press).

Foramen Magnum.—According to Archer (1976), the foramen magnum carries the vertebral arteries, all or part of the sigmoid sinus to the vertebral sinus, cranial nerves, and the posterior part of the brain in dasyurids; presumably, the cranial nerves transmitted are the spinal roots of the accessory nerves, as in the dog (Evans, 1993). In *Monodelphis breviceaudata* CM 52729 (Fig. 9), the bulk of the foramen magnum is enclosed by the paired exoccipitals, with the basioccipital and supraoccipital contributing ventrally and dorsally, respectively. This pattern does not vary among the CM sample, with the following exceptions. Eleven *Monodelphis domestica* (80016, 80021, 80023, 80025–27, 80031, 80036, 80038, 101529, 101531) have a small, rod-shaped ossification that occupies the dorsal margin of the foramen magnum, either entirely separate from or in the process of fusing with the supraoccipital. This element was not reported by Clark and Smith (1993) in their study of cranial osteogenesis in *M. domestica*. It is unknown whether this element has fallen out of the remaining CM skulls or fails to form altogether. One *M. breviceaudata* (68358) has two small, rod-shaped elements in a comparable location, with the right one twice the size of the left.

The supraoccipital contributes to the dorsal border of the foramen magnum in *Didelphis albiventris* CM 78203, *Pucadelphys andinus* (Marshall and Muizon, 1995), and *Zalambdalestes lechei* (Wible et al., in press), whereas the exoccipitals exclude the supraoccipital from the dorsal border in *Dasyurus maculatus* CM 50842.

Foramen Ovale.—The didelphid foramen ovale transmits the mandibular division of the trigeminal nerve (Maier, 1987a; Wible, unpubl. observ.). In *Monodelphis breviceaudata* CM 52729 (Fig. 6), the foramen ovale is located between the alisphenoid and the lateral edge of the anteromedial flange of the promontorium of the petrosal; medially, the foramen ovale is continuous with a smaller opening, the foramen for the greater petrosal nerve, between the anterior edge of the anteromedial flange and the basisphenoid. As mentioned under the foramen for the greater petrosal nerve, variation in the CM sample concerns the degree of continuity between that aperture and the foramen ovale. For more discussion on the marsupial foramen ovale see Gaudin et al. (1996).

The foramen ovale is entirely within the alisphenoid in *Didelphis albiventris* CM 78203 and *Dasyurus maculatus* CM 50842, and between the alisphenoid, squamosal, and petrosal in *Pucadelphys andinus* (Marshall and Muizon, 1995) and *Zalambdalestes lechei* (Wible et al., in press).

Foramen Rotundum.—The foramen rotundum lies entirely within the alisphenoid and transmits the maxillary division of the trigeminal nerve in *Monodelphis domestica* (Clark and Smith, 1993). The only variant in the CM *Monodelphis* sample is on the right side of *M. dimidiata* (86609), in which there is a smaller, anterodorsally directed foramen situated immediately dorsal to the foramen rotundum. The specimen's left side preserves the dried zygomatic branch of the maxillary nerve, which leaves the dorsal margin of the foramen rotundum and is the likely occupant of the foramen on the right side. Archer (1976:p. 280) reported a small foramen of unknown function in *M. dimidiata* WAM M6785 piercing the alisphenoid "adjacent to dorso-lateral margin of foramen rotundum."

A foramen rotundum occurs in *Didelphis albiventris* CM 78203, *Dasyurus maculatus* CM 50842, *Pucadelphys andinus* (Marshall and Muizon, 1995), and *Zalambdalestes lechei*

(Wible et al., in press). In the last three, as in *Monodelphis*, the foramen rotundum lies just posterolateral to the sphenorbital fissure, but in *D. albiventris* it lies more posteriorly, halfway between the sphenorbital fissure and foramen ovale.

Glaserian Fissure.—According to Klaauw (1931:p. 164), the fissura Glaseri develops first as an aperture in the anterior wall of the presumptive auditory bulla transmitting Meckel's cartilage, which disappears later in development; "Later on we find the chorda tympani nerve in it and often also the ramus inferior of the stapedia artery." As the components of the auditory bulla vary in mammals (Klaauw, 1931; Novacek, 1977), so do the components forming the glaserian fissure. In *Monodelphis brevicaudata* CM 52729, I have identified the glaserian fissure as a small notch or gap in the alisphenoid tympanic process, opposite the ventral end of the anterior process of the malleus (Fig. 6). Given that the ramus inferior is not present in marsupials (Wible, 1987), the chorda tympani is the sole occupant of this notch. Rather than a notch or gap, some CM specimens have a small foramen in the alisphenoid tympanic process, which is distributed as follows. In *M. brevicaudata*, a foramen is absent bilaterally (4681, 5061, 52730, 68360, 76731, 76733, 76734) or present on one side only (63509–11, 68358, 68359, 68361, 76730). In *M. domestica*, the foramen is absent bilaterally (5008, 5010, 80021, 80032, 80033, 80035), present on one side only (80017, 80024, 80025, 80032, 80033, 80035), or present bilaterally (80016, 80018, 80023, 80026–31, 80034, 80036–40). In *M. dimidiata*, the foramen is absent bilaterally (86609) or present bilaterally (86611). Finally, the foramen is absent in the one *M. osgoodi* (5242) that could be sampled.

In *Didelphis albiventris* CM 78203, the alisphenoid tympanic process has a deep notch for the chorda tympani nerve. The alisphenoid tympanic process is much larger in *Dasyurus maculatus* CM 50842 than in the didelphids. Near the process's contact with the anterior crus of the ectotympanic, there is a foramen for the chorda tympani on the right side and a notch on the left. An alisphenoid tympanic process is absent in both *Pucadelphys andinus* (Marshall and Muizon, 1995) and *Zalambdalestes lechei* (Wible et al., in press).

Hiatus Fallopii (*Hiatus of Facial Canal of Archer*, 1976).—In *Monodelphis* sp. CM 5024 (Fig. 7), the hiatus Fallopii is the gap in the petrosal at the anterior end of the cavum supracochleare. Based on *Didelphis virginiana* and *M. domestica*, the occupant of the cavum supracochleare is the geniculate ganglion of the facial nerve and the occupant of the hiatus Fallopii is the greater petrosal nerve (Wible, 1990; Sánchez-Villagra and Wible, 2002). Sánchez-Villagra and Wible (2002) identified three character states for the position of the hiatus Fallopii in isolated petrosals of metatherians: dorsal, intermediate, and ventral. In the dorsal state, the floor of the cavum supracochleare extends farther anteriorly than does the roof, whereas in the ventral state, the roof extends farther anteriorly than does the floor. In the intermediate state, the floor and roof extend anteriorly to the same extent. Sánchez-Villagra and Wible (2002) scored the intermediate state for *Monodelphis* sp. AMNH 133248. The two CM isolated petrosals exhibit different states: *Monodelphis* sp. CM 5024 has the intermediate state, whereas *M. brevicaudata* CM 5061 has the ventral state. However, the course of the greater petrosal nerve in both is the same, within the cranial cavity dorsal to the petrosal and exiting via the foramen for the greater petrosal nerve anterior to the petrosal.

The condition of the hiatus Fallopii could not be observed in *Didelphis albiventris* CM 78203 and *Dasyurus maculatus* CM 50842. Sánchez-Villagra and Wible (2002) scored the intermediate condition for *Didelphis* spp. and the ventral condition for *Dasyurus hallucatus*. In *Pucadelphys andinus* (Marshall and Muizon, 1995) and *Zalambdalestes lechei* (Wible et al., in press), the hiatus Fallopii is at the anterior tip of the petrosal, the intermediate condition of Sánchez-Villagra and Wible (2002).

Hypoglossal Foramen (Condylod Foramen of Marshall and Muizon, 1995).—In the dog (Evans, 1993), there is a single hypoglossal foramen in the exoccipital that transmits the hypoglossal nerve and accompanying vein, which connects the condylod and vertebral veins. *Monodelphis breviceaudata* CM 52729 (Fig. 6) has anterior and posterior hypoglossal foramina in the exoccipital, with the latter the larger. Based on *Didelphis virginiana* and *M. domestica*, both these foramina transmit parts of the hypoglossal nerve and accompanying arteries and veins, with the arteries ultimately being branches of the vertebral artery (Wible, unpubl. observ.). In the remaining CM *Monodelphis* sample, all specimens in which the appropriate part of the exoccipital is visible have two hypoglossal foramina, but the relative sizes of the foramina vary. Most specimens of *M. breviceaudata* and *M. domestica* resemble CM 52729 in that the posterior is the larger foramen. However, in the two *M. osgoodi* (5242, 5248) and in some *M. breviceaudata* and *M. domestica*, the anterior is the larger.

Didelphis albiventris CM 78203 has two hypoglossal foramina, with the posterior one more than twice the size of the anterior one. The left side of *Dasyurus maculatus* CM 50842 also has two foramina, with the posteromedial one more than twice the size of the anterolateral; the specimen's right side has an additional small anteromedial foramen. *Pucadelphys andinus* (Marshall and Muizon, 1995) has three small, sub-equal hypoglossal foramina: posterior, anterolateral, and anteromedial. *Zalambdalestes lechei* (Wible et al., in press) has two hypoglossal foramina, with the anterior larger than the posterior.

Incisive Foramen (Anterior Palatine Vacuity of Osgood, 1921).—In *Monodelphis breviceaudata* CM 52729 (Fig. 5) and in the remainder of the CM sample, the elongate incisive foramen is on the anterior hard palate, largely within the premaxilla, but with the maxilla forming the posterior border. Sánchez-Villagra (2001) confirms that the nasopalatine duct communicates with the oral and nasal cavities as well as the vomeronasal organ in adult *M. domestica*, with the site of oral cavity communication being the incisive foramen. It is likely that the incisive foramen in *Monodelphis* also transmits blood vessels and nerves, as in the dog (i.e., the rostral septal branch of the major palatine artery and the septal branch of the caudal nasal nerve; Evans, 1993).

The incisive foramina in *Didelphis albiventris* CM 78203, *Dasyurus maculatus* CM 50842, and *Pucadelphys andinus* (Marshall and Muizon, 1995) resemble those in *Monodelphis* in size and position. They extend between the level of the upper third incisor and upper canine, and are largely within the premaxilla, with the maxilla forming the posterior border. The incisive foramina in *Zalambdalestes lechei* (Wible et al., in press) are very small, with the borders formed equally by the premaxilla and maxilla, and are unusual in that they are directed posteromedioventrally.

Infraorbital Foramen.—The anterior opening of the infraorbital canal on the face is the infraorbital foramen. The major occupant of the didelphid infraorbital canal is the infraorbital nerve, a branch of the maxillary division of the trigeminal nerve, with accompanying infraorbital artery and vein (Sánchez-Villagra and Asher, 2002). Variation in the CM *Monodelphis* sample concerns the position of the infraorbital foramen relative to the teeth; its posterior edge varies from dorsal to between the roots of P3 to dorsal to the posterior root of M1. It is between the roots of P3 in two *M. domestica* (80018, 80024) and one *M. sp.* (5002). It is dorsal to the posterior root of P3 in four *M. breviceaudata* (4681, 63509, 68358, 76731), 23 *M. domestica* (5008, 5010, 5025, 80016, 80017, 80021, 80023, 80025–32, 80034, 80036–40, 101529, 101531), the four *M. dimidiata* (86608–11), and one *M. sp.* (5024). It is dorsal to the P3–M1 embrasure (Fig. 2) in 9 *M. breviceaudata* (5061, 52729, 52730, 63510, 63511, 68359, 68361, 76730); over the anterior root of M1 in one *M. osgoodi* (5248), and over the posterior root of M1 in one *M. osgoodi* (5242). In those specimens retaining the upper deciduous third premolar (see

Appendix 2), the infraorbital foramen is dorsal to the anterior root of that tooth in two *M. domestica* (80033, 80035) and one *M. brevicaudata* (76732); between the roots of that tooth in two *M. domestica* (80019, 80020), and one *M. brevicaudata* (76733); and over the posterior root of that tooth in two *M. brevicaudata* (68360, 76734) and one *M. sp.* (5003).

The infraorbital foramen is dorsal to the anterior root of P3 in *Didelphis albiventris* CM 78203, the posterior root of M1 in *Dasyurus maculatus* CM 50842, P3 in *Pucadelphys andinus* (Marshall and Muizon, 1995), and the P2–P3 embrasure in *Zalambdalestes lechei* (Wible et al., in press).

Internal Acoustic Meatus.—The internal acoustic meatus in the isolated petrosals of *Monodelphis* CM 5024 (Fig. 7) and 5061 follows the pattern described for the dog by Evans (1993). In that form, the meatus is divided by a low transverse crest into dorsal and ventral parts. The dorsal part, the foramen acusticum superius, contains the opening of the facial canal for the facial nerve (the primary facial foramen of this report) and the cribriform dorsal vestibular area for the passage of some bundles of the vestibular nerve from the membranous labyrinth. The ventral part, the foramen acusticum inferius, contains the ventral vestibular area for additional bundles of the vestibular nerve that pass through a deep, tiny depression, the foramen singulare, and the spiral cribriform tract with perforations for the fascicles of the cochlear nerve.

Details of the internal acoustic meatus are not available for *Didelphis albiventris* CM 78203, *Dasyurus maculatus* CM 50842, *Pucadelphys andinus* (Marshall and Muizon, 1995), and *Zalambdalestes lechei* (Wible et al., in press).

Jugular Foramen (Posterior Lacerate Foramen of Archer, 1976).—According to Archer (1976), the jugular foramen in dasyurids transmits cranial nerves (presumably the glossopharyngeal, vagus, and accessory nerves as in didelphids [Wible, unpubl. observ.] and the dog [Evans, 1993]) and occasionally also a very small branch of the sigmoid sinus to the internal jugular vein. A venous channel does not pass through the jugular foramen in *Didelphis virginiana* (Wible, 1990; Wible and Hopson, 1995) and *Monodelphis domestica* (Wible, unpubl. observ.). Because this opening does not transmit the major contributor to the internal jugular vein, Archer (1976) opted for the usage of posterior lacerate foramen rather than jugular foramen. However, I employ the term jugular foramen, because it is more widely used in mammals, including the *Nomina Anatomica Veterinaria* (1994). Based on one juvenile *M. brevicaudata* (CM 68360) and several juvenile *M. domestica* (CM 80019, 80020, and 80033) in which sutures distinguish the basioccipital and exoccipitals, it is apparent that the jugular foramen lies between the exoccipital and the petrosal. No major variation in the jugular foramen was observed in the CM sample.

As in *Monodelphis*, the jugular foramen is small with a separate foramen for the inferior petrosal sinus anterior to it in *Didelphis albiventris* CM 78203, *Dasyurus maculatus* CM 50842, and *Pucadelphys andinus* (Marshall and Muizon, 1995). The jugular foramen is also small in *Zalambdalestes lechei* (Wible et al., in press), but there is no separate foramen for the inferior petrosal sinus.

Lacrimal Foramen.—According to Archer (1976), the lacrimal foramen carries the nasolacrimal duct and does not transmit any major blood vessel in dasyurids. In *Monodelphis brevicaudata* CM 52729 (Figs. 1, 2, 4) and in the remainder of the CM sample, with one exception, there are two lacrimal foramina on the facial process of the lacrimal bone. Each lacrimal foramen transmits a lacrimal canaliculus and accompanying vein; the canaliculi unite within the lacrimal bone to form the lacrimal sac out of which flows the nasolacrimal duct (*M. Sánchez-Villagra*, pers. commun.). The anteroventral foramen is slightly larger than the posterodorsal one. The sole variant is the left side of one *M. osgoodi* (5242) in which only a single large lacrimal foramen occurs. *Sánchez-Villagra*

and Asher (2002) reported more variation in the number of lacrimal foramina in other didelphids; they found that four out of five *Chironectes* and roughly two-thirds of 35 *Didelphis* have only one lacrimal foramen.

Didelphis albiventris CM 78203 and *Dasyurus maculatus* CM 50842 have two lacrimal foramina with the larger anteroventral one on the face and the posterodorsal one on the orbital rim. In contrast, *Pucadelphys andinus* (Marshall and Muizon, 1995) and *Zalambdalestes lechei* (Wible et al., in press) have two lacrimal foramina within the orbit.

Major Palatine Foramen (Maxillary Vacuity of Archer, 1976; Maxillopalatine Vacuity of Hershkovitz, 1992, 1997; Posterior Palatine Vacuity of Osgood, 1921).—In the dog (Evans, 1993), the major palatine nerve and artery, branches off the maxillary artery and nerve, respectively, reach the palate via the major palatine foramen between the maxilla and palatine. In *Monodelphis breviceaudata* CM 52729 (Fig. 5) and the remainder of the CM sample, the major palatine foramen is elongated anteroposteriorly, extending the length of M1 and M2, and largely within the maxilla, with the palatine forming its narrow posterior border. Because of its size, the didelphid major palatine foramen is often referred to as a vacuity (Osgood, 1921; Archer, 1976; Hershkovitz, 1992, 1997).

In *Didelphis albiventris* CM 78203, the major palatine foramen is a large, irregular, assymetrical opening extending between the metacone of M3 and the protocone of M4, nearly completely within the palatine. On the left side of *Dasyurus maculatus* CM 50842, the major palatine foramen is a large opening, extending the length of M2, largely within the maxilla but with the palatine forming the posterior border; on the specimen's right side are two smaller foramina, a posterior one on the maxilla-palatine suture and a smaller anterior one within the maxilla. The major palatine foramen is unknown for *Pucadelphys andinus* (Marshall and Muizon, 1995). In *Zalambdalestes lechei* (Wible et al., in press), one or two major palatine foramina are in the maxilla opposite the penultimate premolar.

Mandibular Foramen.—In didelphids, the mandibular foramen transmits the inferior alveolar nerve off the mandibular division of the trigeminal nerve and accompanying blood vessels (Tandler, 1899; Wible, unpubl. observ.). In *Monodelphis breviceaudata* CM 52729 (Fig. 3) and the remainder of the CM sample, the mandibular foramen is located on the mandular ramus, near the anterior root of the medially inflected angular process.

As in *Monodelphis*, the mandibular foramen is on the mandibular ramus near the anterior root of the medially inflected angular process in *Didelphis albiventris* CM 78203, *Dasyurus maculatus* CM 50842, and *Pucadelphys andinus* (Marshall and Muizon, 1995). In contrast, in *Zalambdalestes lechei* (Kielan-Jaworowska and Trofimov, 1981), the mandibular foramen is situated higher on the mandibular ramus and nearer the anterior border of the coronoid process. However, the mandibular foramen in the Early Cretaceous eutherian *Prokennalestes* resembles that in the metatherians in that it is just dorsal to the anterior root of the posteroventrally directed angular process (Kielan-Jaworowska and Dashzeveg, 1989).

Maxillary Foramen.—The posterior opening of the infraorbital canal within the orbit is the maxillary foramen. In *Monodelphis breviceaudata* CM 52729 and the remainder of the CM sample, with an exception, the maxillary foramen is bordered by the lacrimal dorsally and medially, and the maxilla laterally and ventrally, with a thin prong of palatine interposed between the lacrimal and maxilla. The variant is found in the two specimens of *M. osgoodi* (5242, 5248), in which the contribution of the palatine is considerably expanded, occupying the medial wall and sending a prong into the roof.

The bony borders of the maxillary foramen in *Dasyurus maculatus* CM 50842 and *Pucadelphys andinus* (Marshall and Muizon, 1995) resemble those described for *Monodelphis breviceaudata*. *Didelphis albiventris* CM 78203 differs from the other metatherians studied in that the palatine just barely contributes to the maxillary foramen and does not extend into the infraorbital canal. The maxillary foramen has no palatine

contribution in *Zalambdalestes lechei* (Wible et al., in press); it lies between the maxilla, lacrimal, and frontal.

Mental Foramen.—As in the dog (Evans, 1993), which usually has three mental foramina per side, the mental foramina in *Monodelphis* transmit branches of the inferior alveolar nerve and vessels (Wible, unpubl. observ.). *M. brevicaudata* CM 52729 (Fig. 2) has two mental foramina: the anterior under the posterior root of p1 and the posterior under the anterior root of m2. The CM sample exhibits considerable variability in the position of the mental foramina, some of which may be size related (see below).

Regarding the anterior foramen, the range of variation is between the anterior root of p1 and between the roots of p2. Only one *Monodelphis brevicaudata* (68361) has it below the anterior root of p1. In addition to CM 52729 (Fig. 2), only two other *M. brevicaudata* (63511 left only, 68358), nine *M. domestica* (80017, 80019–21, 80024, 80026, 80029, 80035, 101531), and one *M. sp.* (5003) have it below the posterior root of p1. Eight *M. domestica* (5025, 80018, 80031, 80033, 80034, 80036, 80039, 101529), two *M. dimidiata* (86608, 86610), and one *M. sp.* (5002) have it between p1 and p2. Twelve *M. brevicaudata* (4681, 5061, 52370, 63509, 63511 right only, 68359, 68360, 76730–34), twelve *M. domestica* (5008, 5010, 80016, 80023, 80025, 80027, 80028, 80030, 80032, 80037, 80038, 80040), two *M. dimidiata* (86609, 86611), one *M. osgoodi* (5248), and one *M. sp.* (5024) have it below the anterior root of p2. One *M. brevicaudata* (63510) and one *M. osgoodi* (5242) have it between the roots of p2. Finally, there are two specimens that have double anterior mental foramina on one side only: *M. domestica* (80018) and *M. dimidiata* (86610), between p1 and p2, and below the anterior root of p2.

Regarding the posterior foramen, the range of variation is between the anterior root of m1 to the anterior root of m2. In addition, there is considerably more left-right asymmetry with the posterior foramen. Only one side of one *Monodelphis brevicaudata* (63511) has it below the anterior root of m1. Four *M. brevicaudata* (63509, 63510 left only, 76732, 76733), seven *M. domestica* (5008 right only, 5010, 80016 left only, 80018, 80019, 80025 right only, 80035), the four *M. dimidiata* (86608–11), the two *M. osgoodi* (5242, 5248), and the three *M. sp.* (5002, 5003, 5024) have it between the roots of m1. Six *M. brevicaudata* (4681, 68359 left only, 68360, 68361, 76731, 76734) and 19 *M. domestica* (5008 left only, 5025, 80016 right only, 80020, 80021, 80023, 80024, 80025 left only, 80026, 80027 left only, 80028, 80030, 80033, 80034, 80038, 80039 left only, 80040, 101529, 101531) have it below the posterior root of m1. Three *M. brevicaudata* (5061, 63510 right only, 63511 right only) and four *M. domestica* (80032, 80036 left only, 80037, 80039 right only) have it below the m1–m2 embrasure. In addition to CM 52729 (Fig. 6), only three other *M. brevicaudata* (52370, 68358, 76730) and five *M. domestica* (80017, 80027 right only, 80029, 80031, 80036 right only) have it below the anterior root of m2. One *M. brevicaudata* (68359) has two posterior mental foramen on the right side only at the anterior root of m1 and at the m1–m2 embrasure.

In addition to the anterior and posterior mental foramina, two specimens have a middle mental foramen: *Monodelphis brevicaudata* (4681) at the posterior root of p3 and *M. domestica* (80037) at the anterior root of p3.

There appears to be a stronger correlation between posterior mental foramen position and size. The posterior mental foramen is anteriorly positioned (e.g., between the roots of m1) in six of the nine specimens retaining the lower deciduous third premolar, *Monodelphis brevicaudata* (68360, 76733, 76734), *M. domestica* (80019, 80035), and *M. sp.* (5003), as well as the adult *M. dimidiata* (86608–11) and *M. osgoodi* (5242, 5248), which have the smallest adult skulls (with m4 erupted) in the CM sample (see Appendix 2). The anterior mental foramen in these same specimens ranges from below the posterior root of p1 (5003,

80019, 80035), to between p1 and p2 (80018, 86608, 86610), to below the anterior root of p2 (5248, 68360, 76733, 76734, 86609, 86611), to between the roots of p2 (5242).

Didelphis albiventris CM 78203 has only one mental foramen, below the p1–p2 embrasure. *Dasyurus maculatus* CM 50842, which unlike the didelphids and *Pucadelphys andinus* has only two premolars, has three mental foramina, asymmetrically arranged. On the left they are below the anterior root of the first premolar, the posterior root of the m1, and the m1–m2 embrasure; on the right they are below the posterior root of the first premolar, the posterior root of the second premolar, and the posterior root of the m1. *Pucadelphys andinus* (Marshall and Muizon, 1995) and *Zalambdalestes lechei* (Kielan-Jaworowska and Trofimov, 1981) have two mental foramina: below the p1 and m1 in the former, and below the anterior root of the first premolar and between the roots of the third (penultimate) premolar in the latter.

Minor Palatine Foramen (Postero-Lateral Palatine Foramen of Archer, 1976; Posterolateral Vacuity or Foramen of Hershkovitz, 1992, 1997; Postpalatine Foramen of Marshall and Muizon, 1995).—In the dog (Evans, 1993), the minor palatine nerve and artery, branches of the maxillary nerve and artery, respectively, leave the orbit and reach the palate via an unnamed notch that rarely closes to a foramen in the posterior margin of the maxilla and palatine. In *Monodelphis breviceaudata* CM 52729 (Fig. 5) and in the remainder of the CM sample, the minor palatine foramen is obliquely oriented, posteromedial to the last upper molar, and within the maxillopalatine suture.

The minor palatine foramen in *Didelphis albiventris* CM 78203, *Pucadelphys andinus* (Marshall and Muizon, 1995), and *Zalambdalestes lechei* (Wible et al., in press) resembles that in *Monodelphis*. The foramen in *Dasyurus maculatus* CM 50842 is similarly situated, but the posterior border is partially open, as bony prongs projecting from the maxilla and palatine do not meet.

Parietal Foramen.—A small emissary foramen in the parietal, near the midline, is variably present in humans and some other anthropoid primates (Boyd, 1930, 1934). *Monodelphis breviceaudata* CM 52729 (Fig. 1) has one small emissary foramen near the midline in the right parietal. The presence and number of similar parietal foramina in the remaining CM sample is variable. No foramina occur in four *M. breviceaudata* (5061, 63509, 63511, 76732), eight *M. domestica* (5008, 5025, 80024, 80031, 80033, 80035, 80038, 80039), and the four *M. dimidiata* (86608–11). The remaining specimens have between a single foramen on one side only to the maximum in *M. breviceaudata* CM 76730 of six on the right side and nine on the left.

Didelphis albiventris CM 78203 has three tiny parietal foramina off the midline on each side, whereas *Dasyurus maculatus* CM 50842 has two on each side. Parietal foramina are not described or illustrated for *Pucadelphys andinus* (Marshall and Muizon, 1995) and are absent in *Zalambdalestes lechei* (Wible et al., in press).

Postglenoid Foramen.—According to Archer (1976), the postglenoid foramen in dasyurids carries the postglenoid vein as well as the vein of the suprameatal foramen and the postglenoid artery, a branch of the external carotid that reaches the temporal fossa via the suprameatal foramen. This same pattern occurs in *Didelphis virginiana* (Wible, 1987, 1990) and *Monodelphis domestica* (unpubl. observ.), except that the vein exiting the postglenoid foramen is identified as the sphenoparietal emissary vein, following Gelderen (1924). This is in contrast to the capsuloparietal emissary vein exiting the postglenoid foramen in placentals, which has a different developmental history (Gelderen, 1924; Wible, 1990). In *M. breviceaudata* CM 52729 (Fig. 6), the postglenoid foramen is entirely within the squamosal, although the anterior crus of the ectotympanic approaches the medial margin. Also, three openings are visible within the substance of the postglenoid foramen, with the posterior and largest of these three being the channel for the sphenoparietal

emissary vein; the anterior two are postzygomatic foramina. Checking the number of openings within the substance of the postglenoid foramen in the remaining CM sample was difficult, because soft tissue frequently obstructs this area. In *M. brevicaudata*, some specimens have four openings (63510, 68359, 68631) and others five (63509, 63511, 76734).

The postglenoid foramen of *Dasyurus maculatus* CM 50842 is positioned as that in *Monodelphis*. In *Didelphis albiventris* CM 78203, the foramen is more anteriorly situated, medial to the postglenoid process rather than posterior. The postglenoid foramen also differs positionally in both *Pucadelphys andinus* (Marshall and Muizon, 1995) and *Zalambdalestes lechei* (Wible et al., in press). The aperture in the former is more laterally placed, on the posterior root of the zygomatic arch, and in the latter is more anteriorly placed, within the glenoid fossa, anterior to the postglenoid process.

Posttemporal Notch.—The mammalian posttemporal foramen lies on the occiput usually between the petrosal and squamosal, and transmits the arteria diploëtica magna and accompanying vein (Wible, 1987; Wible and Hopson, 1993, 1995). This aperture and its arterial and venous contents have been identified in the ventrolateral margin of the occiput of *Didelphis virginiana* (Wible, 1990; Wible and Hopson, 1995). In *Monodelphis brevicaudata* CM 52729 (Fig. 9), rather than a distinct posttemporal foramen, there is a notch in the ventrolateral mastoid exposure of the petrosal in the suture with the squamosal (see also Fig. 7). This notch certainly did not transmit any substantial structure, and it is unclear whether it transmitted any vessel at all. In the remaining CM sample, a posttemporal notch is present bilaterally in the mastoid exposure of the vast majority of specimens. However, the notch is present on one side only in two *M. brevicaudata* (5061, 63511) and three *M. domestica* (80032, 80033, 80034), and is absent bilaterally in three *M. domestica* (80016, 80019, 80035) and the two *M. osgoodi* (5242, 5248). In one *M. brevicaudata* (63509), there is a distinct posttemporal foramen entirely within the mastoid exposure on the right side; the left side has only a posttemporal notch.

In *Didelphis albiventris* CM 78203, the posttemporal notch is present, does not appear to be patent, and is situated more dorsally (nearer the supraoccipital bone) than in *Monodelphis*. On the right side of *Dasyurus maculatus* CM 50842, a minute foramen is situated in the middle of the suture between the mastoid exposure and squamosal; on the specimen's left side, this tiny opening is entirely within the petrosal. *Pucadelphys andinus* (Marshall and Muizon, 1995) has a posttemporal foramen in the position of the posttemporal notch of *Monodelphis*. *Zalambdalestes lechei* (Wible et al., in press) has a posttemporal foramen in the position of the notch of *D. albiventris*.

Postzygomatic Foramen (Gregory, 1910).—According to Archer (1976), the postzygomatic foramen in dasyurids carries a vein out of the squamosal root of the zygomatic arch to the postglenoid vein. *Monodelphis brevicaudata* CM 52729 (Fig. 6) has two postzygomatic foramina visible in the anterior wall of the postglenoid foramen. As noted with the postglenoid foramen, checking the number of openings within the substance of that aperture in the CM sample was difficult, because soft tissue frequently obstructs this area. In *M. brevicaudata*, some specimens have three postzygomatic foramina (63510, 68359, 68631) and others four (63509, 63511, 76734).

The left side of *Didelphis albiventris* CM 78203 has three postzygomatic foramina visible within the postglenoid foramen; the specimen's right side has four. The left side of *Dasyurus maculatus* has one tiny postzygomatic foramen within the postglenoid foramen; the specimen's right side has two tiny openings. Postzygomatic foramina are not described in *Pucadelphys andinus* (Marshall and Muizon, 1995) and *Zalambdalestes lechei* (Wible et al., in press).

Marshall and Muizon (1995:figs. 12A, 17) identified the opening on the posterolateral aspect of the postglenoid process in *Pucadelphys andinus* as the postzygomatic foramen; *Monodelphis brevicaudata* CM 52729 (Fig. 4) has a similar aperture discussed with the squamosal bone below that I have not named. Although Archer (1976) did not fully describe the position of the postzygomatic foramen, Gregory (1910) described it as opening “below or within the lip of the postglenoid foramen.” It is the sense of Gregory that I employ the term here.

Primary Facial Foramen.—Following Wible (1990) and Wible and Hopson (1993), the primary facial foramen is the opening on the endocranial surface of the petrosal that transmits the facial nerve from the internal acoustic meatus to the cavum supracochleare. In *Monodelphis* sp. CM 5024 (Fig. 7) and *M. brevicaudata* CM 5061, the primary facial foramen lies within the foramen acusticum superioris, anterior to the dorsal vestibular area.

The primary facial foramen could not be studied in *Didelphis albiventris* CM 78203, *Dasyurus maculatus* CM 50842, and *Zalambdalestes lechei* (Wible et al., in press). The foramen in *Pucadelphys andinus* (Marshall and Muizon, 1995) resembles that in *Monodelphis*.

Prootic Canal (Canal for the Lateral Head Vein of Wible and Hopson, 1995).—According to Wible (1990) and Rougier and Wible (in press), the metatherian prootic canal is a narrow, horizontal canal in the petrosal that connects the groove for the prootic sinus on the lateral surface with the facial sulcus on the ventral surface. As pointed out recently by Rougier and Wible (in press), it is uncertain whether the vein that occupies this canal in metatherians is the prootic sinus or the lateral head vein, because the vein that serves to distinguish these two, the post-trigeminal vein, involutes in early ontogenetic stages. Sánchez-Villagra and Wible (2002) divided the metatherian prootic canal into two characters: the presence/absence of the tympanic aperture and the presence/absence of the lateral aperture. Among extant metatherians, both apertures are found in most didelphids (*Glironia venusta* and *Thylamys* spp. have only the lateral aperture), and some caenolestids, dasyuromorphians, phalangerids, and pseudocheirids. These authors’ observation of both apertures for *Monodelphis* sp. was based on AMNH 133248. *Monodelphis* sp. CM 5024 has both apertures (Fig. 7). In *M. brevicaudata* CM 5061, the ventral aperture cannot be confirmed, because the appropriate area is covered by soft tissue; the lateral aperture is present and is more than double the diameter of the same opening in CM 5024.

The prootic canal in *Didelphis albiventris* CM 78203 and *Pucadelphys andinus* (Marshall and Muizon, 1995) resembles that in *Monodelphis*. The presence/absence of the prootic canal could not be ascertained in *Dasyurus maculatus* CM 50842 because the auditory bulla conceals the middle ear; Sánchez-Villagra and Wible (2002) reported it to be absent in *D. hallucatus*. As in most eutherians, the prootic canal is absent in *Zalambdalestes lechei* (Wible et al., in press); an exception within Eutheria is *Prokennalestes* from the Mongolian Early Cretaceous, which has a short, vertical prootic canal (Wible et al., 2001).

Pterygoid Canal.—In the dog (Evans, 1993), the pterygoid canal lies in the suture between the pterygoid and basisphenoid and transmits the nerve and artery of the pterygoid canal from the skull base to the posteroinferior floor of the orbit. The nerve of the pterygoid canal enters the canal’s basicranial aperture and is composed of sympathetic fibers from the internal carotid (deep petrosal) nerve and parasympathetic fibers from the greater petrosal nerve; the artery enters the orbital aperture and is a branch of the maxillary artery. According to Wible (1984), the metatherian pterygoid canal transmits nerves, but no artery. In *Monodelphis brevicaudata* CM 52729 (Fig. 6) and in the remainder of the CM sample, the basicranial aperture of the pterygoid canal is between the basisphenoid and pterygoid,

anterior to the carotid foramen and medial to the entopterygoid crest; the orbital aperture is between the alisphenoid and pterygoid, in the floor of the sphenorbital fissure.

The pterygoid canal in *Didelphis albiventris* CM 78203 is relatively shorter than that in *Monodelphis*, and the anterior and posterior apertures are slightly different. The anterior aperture is in the floor of the sphenorbital fissure, but between the palatine and alisphenoid; the posterior aperture is between the basisphenoid and pterygoid, but is more anteriorly positioned, just posterior to the level of the foramen rotundum. The apertures of the pterygoid canal in *Dasyurus maculatus* CM 50842 differ from those of the didelphids. The anterior aperture is more anteriorly positioned, just in front of the sphenorbital fissure in the suture between the palatine and alisphenoid; the posterior aperture is more laterally positioned, beneath the entopterygoid process, just posterior to the foramen rotundum. The condition of the pterygoid canal in *Pucadelphys andinus* (Marshall and Muizon, 1995) and *Zalambdalestes lechei* (Wible et al., in press) is unknown.

Secondary Facial Foramen.—Following Wible (1990) and Wible and Hopson (1993), the secondary facial foramen is the opening on the tympanic surface of the petrosal that transmits the facial nerve from the cavum supracochleare into the middle ear. In *Monodelphis* sp. CM 5024 (Fig. 7) and *M. brevicaudata* CM 5061, the secondary facial foramen lies anterior to the fenestra vestibuli and the tympanic aperture of the prootic canal.

The disposition of the secondary facial foramen in *Didelphis albiventris* CM 78203 and *Pucadelphys andinus* (Marshall and Muizon, 1995) is as in *Monodelphis*. The condition in *Dasyurus maculatus* CM 50842 could not be studied because the auditory bulla conceals the middle ear. The secondary facial foramen of *Zalambdalestes lechei* (Wible et al., in press) differs from that of the metatherians in that it is more posteriorly positioned, just in front of the fenestra vestibuli.

Sphenopalatine Foramen.—In the dog (Evans, 1993), there are two openings in the orbital process of the palatine, the sphenopalatine foramen, which transmits the caudal nasal nerve and sphenopalatine artery and vein off the maxillary nerve, artery, and vein, respectively, and the caudal palatine foramen, which transmits the major palatine nerve and artery to the palatine canal. In *Monodelphis brevicaudata* CM 52729 (Fig. 4) and the remainder of the CM sample, only a single opening is present in the orbital process of the palatine serving the function of the two in the dog. I identify the one foramen in *Monodelphis* as the sphenopalatine foramen, following, for example, Archer (1976), the *Nomina Anatomica Veterinaria* (1994), and Marshall and Muizon (1995).

The sphenopalatine foramen of *Didelphis albiventris* CM 78203 and *Pucadelphys andinus* (Marshall and Muizon, 1995) resembles that of *Monodelphis*; it lies anterodorsal to the minor palatine foramen, within the palatine. In *Dasyurus maculatus* CM 50842, the sphenopalatine foramen is also within the palatine, but more anteriorly placed, near the maxillary foramen. In *Zalambdalestes lechei* (Wible et al., in press), the sphenopalatine foramen is anterodorsal to the minor palatine foramen, but between the palatine, frontal, and maxilla.

Sphenorbital Fissure (Optic-Orbital Foramen of Marshall and Muizon, 1995).—In therians, the term sphenorbital fissure has been employed for the large gap in the medial wall of the orbit between the orbitosphenoid and alisphenoid that transmits nerves and vessels from the cavum epiptericum (Gregory, 1910; McDowell, 1958; Archer, 1976). The nervous and vascular contents of this opening vary dramatically among extant therians and may include some combination of the following: the optic, oculomotor, trochlear, ophthalmic, maxillary, and abducens nerves; the ramus infraorbitalis, arteria anastomotica, and ophthalmic artery; and the ophthalmic veins. In marsupials, the usual contents are the optic, oculomotor, trochlear, ophthalmic, and abducens nerves, and the ophthalmic artery and veins (Kuhn and Zeller, 1987; Wible and Rougier, 2000). In *Monodelphis brevicaudata* CM 52729 (Fig. 4) and the remainder of the CM sample, the sphenorbital fissure is situated

between the orbitosphenoid, alisphenoid, pterygoid, palatine, and presphenoid. In contrast to metatherians, eutherians have a separate optic foramen and their sphenorbital fissure is often referred to as the superior orbital fissure to distinguish it from the metatherian condition (Wible et al., in press).

The sphenorbital fissure of *Didelphis albiventris* CM 78203 and *Dasyurus maculatus* CM 50842 differs from that of *Monodelphis* in that there is no contribution from the pterygoid bone. In *Pucadelphys andinus* (Marshall and Muizon, 1995), the sphenorbital fissure lies between the palatine, orbitosphenoid, frontal, and alisphenoid. The corresponding aperture in *Zalambdalestes lechei* (Wible et al., in press) is between the alisphenoid and orbitosphenoid.

Subsquamosal Foramen.—Wible et al. (in press) employed the term subsquamosal foramen for vascular apertures in the squamosal dorsal to the suprameatal bridge. Unfortunately, Archer (1976) used the same term for the suprameatal foramen of this report. Despite the potential confusion, I continue to employ the term subsquamosal foramen in the sense of Wible et al. (in press). *Monodelphis breviceaudata* CM 52729 (Fig. 2) has no subsquamosal foramina, but it is unusual in that absence among the remaining CM sample. In addition to CM 52729, subsquamosal foramina are lacking in two other *M. breviceaudata* (63509, 63510), three of the four *M. dimidiata* (86608–10), and the two *M. osgoodi* (5242, 5248). The remaining twelve *M. breviceaudata* and one *M. dimidiata* (86611), and the 28 *M. domestica* preserving the squamosal have between one and a dozen small subsquamosal foramina.

Didelphis albiventris CM 78203 has six tiny subsquamosal foramina and *Dasyurus maculatus* CM 50842 has but one tiny opening. Subsquamosal foramina are not described or illustrated for *Pucadelphys andinus* (Marshall and Muizon, 1995), and *Zalambdalestes lechei* (Wible et al., in press) has one large subsquamosal foramen, immediately dorsal to the suprameatal bridge.

Suprimeatal Foramen (Subsquamosal Foramen of Archer, 1976).—Based on didelphids (Wible, 1987) and dasyurids (Archer, 1976), the suprimeatal foramen in the metatherian squamosal, dorsal to the external acoustic meatus, carries a temporal branch of the postglenoid artery and accompanying vein to the temporal fossa. Wible (1987) identified this as a ramus temporalis of the stapedia artery system. *Monodelphis breviceaudata* CM 52729 (Fig. 4) has a posterolaterally directed suprimeatal foramen, which is continuous through the squamosal with the postglenoid foramen (Fig. 6). Posterior to the suprimeatal foramen is a depression, which dorsally includes a short, posterodorsally directed sulcus for the ramus temporalis (Fig. 2). The main variant in the CM sample concerns the relative size of the suprimeatal foramen. In three *M. breviceaudata* (68358, 68361, 76732) and one *M. sp.* (5024), the suprimeatal foramen is comparable in size to that of CM 52729. In all the remaining specimens that could be sampled, the 29 *M. domestica*, the four *M. dimidiata*, the two *M. osgoodi*, and the 11 remaining *M. breviceaudata*, 5061, the suprimeatal foramen is roughly twice as big, expanding posteriorly into the area where the depression is present in CM 52729.

Didelphis albiventris CM 78203, *Dasyurus maculatus* CM 50842, *Pucadelphys andinus* (Marshall and Muizon, 1995), and *Zalambdalestes lechei* (Wible et al., in press) have a suprimeatal foramen resembling that in *Monodelphis breviceaudata* CM 52729.

Stylomastoid Notch.—In the dog (Evans, 1993), the stylomastoid foramen is the opening between the petrosal, the osseous bulla, and the tympanohyal cartilage by which the facial nerve leaves the middle ear and by which the stylomastoid artery off the posterior auricular artery enters. Archer (1976) reported for dasyurids that the stylomastoid foramen does not appear to transmit any major vessel; this is the case in *Didelphis virginiana* and *Monodelphis domestica* (Wible, unpubl. observ.). In *M. sp.* CM 5024 (Fig. 7A, D) and the

remainder of the CM sample, there is no stylomastoid foramen, but a notch bordered by the tympanohyal anteriorly and the caudal tympanic process of the petrosal posteriorly.

Didelphis albiventris CM 78203, *Pucadelphys andinus* (Marshall and Muizon, 1995), and *Zalambdalestes lechei* (Wible et al., in press) have a stylomastoid notch resembling that in *Monodelphis* sp. CM 5024. In contrast, *Dasyurus maculatus* CM 50842 has a stylomastoid foramen between the squamosal and petrosal.

Transverse Canal Foramen.—The metatherian transverse canal has been reviewed recently by Sánchez-Villagra and Wible (2002). They reported that most extant metatherians have a transverse canal foramen in the basisphenoid that transmits a vein communicating with the cavernous sinus and that in some forms this vein communicates across the midline with its antimere (see also Archer, 1976). Sánchez-Villagra and Wible (2002) recorded two characters for the transverse canal: the presence/absence and position of the transverse canal foramen, and the presence/absence of an intramural canal between the right and left transverse canal foramina. *Monodelphis* sp. was scored as having the transverse canal foramen anterior to the carotid foramen (as compared with confluent with the carotid foramen or perforating the pterygoid fossa) and with an intramural canal. Their observation of the position of the transverse canal foramen is congruent with that in *M. brevicaudata* CM 52729 (Fig. 6) and the remainder of the CM sample. I did not confirm the presence of an intramural canal.

Didelphis albiventris CM 78203 has a transverse canal foramen resembling that in *Monodelphis*. The foramen in *Dasyurus maculatus* CM 50842 differs from the didelphids in that it is laterally directed rather than posterolaterally directed. The transverse canal foramen is absent in *Pucadelphys andinus* (Marshall and Muizon, 1995) and *Zalambdalestes lechei* (Wible et al., in press).

Unnamed Cranial Foramina

Alisphenoid.—*Monodelphis brevicaudata* CM 52729 (Fig. 6) has a small opening in the ventromedial margin of the tympanic process of the left alisphenoid; on the right side, only a notch exists. Only two other *M. brevicaudata* have comparable openings in the ventromedial aspect of the alisphenoid tympanic process: CM 76732 has a small opening on the right side only and CM 4681 has three small openings on the left side only. It is possible that these are not true foramina, but merely unossified areas in the auditory bulla.

Nearer the glaserian fissure, *Didelphis albiventris* CM 78203 has a deep, narrow notch in the alisphenoid tympanic process. Anterior to this notch on the left side are two tiny foramina and on the right side are three. The function of these structures is unknown. *Dasyurus maculatus* CM 50842 has nothing comparable, and the alisphenoid tympanic process is absent in *Pucadelphys andinus* (Marshall and Muizon, 1995) and *Zalambdalestes lechei* (Wible et al., in press).

Lacrimal.—*Monodelphis brevicaudata* CM 52729 has a small, anteriorly directed foramen in the orbital process of the lacrimal dorsal to the maxillary foramen on the right side and two such openings on the left. A single opening is present bilaterally in the majority of the remaining CM sample, i.e., in 38 of 51 that could be sampled. However, no foramina occur in one *M. domestica* (80028) and one *M. dimidiata* (86610), and are absent on one side only in one *M. brevicaudata* (68360), one *M. dimidiata* (86608), and four *M. domestica* (80024, 80025, 20027, 80031). A third *M. dimidiata* (86609) preserves only the left lacrimal and it has no foramen. As in CM 52729, two foramina on one side and a single on the other are found in three other *M. brevicaudata* (63511, 76733, 76734) and one *M. domestica* (80023). Two foramina are present bilaterally in one *M. sp.* (5003). The two *M. osgoodi* (5242, 5248) present additional variants. Neither specimen has a foramen in the

lacrimal directly over the maxillary foramen; however, CM 5242 has a small foramen within the orbit at the level of the lower lacrimal foramen on the right side only, and CM 5248 has a tiny foramen at the level of the upper lacrimal foramen on the right side only and posterodorsal to that a second tiny foramen that is bilaterally present.

The right side of *Didelphis albiventris* CM 78203 has a foramen in the lacrimal immediately dorsal to the maxillary foramen; it is subequal in size to the upper lacrimal foramen. There is no foramen on the specimen's left side. The left side of *Dasyurus maculatus* CM 50842 has a tiny opening halfway between the maxillary foramen and upper lacrimal foramen; the right side has no foramen. Similar foramina are not reported for *Pucadelphys andinus* (Marshall and Muizon, 1995) and *Zalambdalestes lechei* (Wible et al., in press).

Maxilla.—*Monodelphis breviceaudata* CM 52729 (Fig. 2) has several small foramina on the facial process of the maxilla anterior to the infraorbital foramen. The foramen anterodorsal to the infraorbital foramen, dorsal to P2 is present bilaterally in the remaining 15 specimens of *M. breviceaudata*. Variants include a single foramen on one side and double on the other (4681, 5061), double on both sides (76732–34), and double on one side, triple on the other (63509, 76730). In *M. domestica*, this foramen is absent bilaterally (80028, 80035), absent on one side only (5008, 5010, 5025, 80016, 80018, 80024, 80033, 80038, 101529), present bilaterally (80019–21, 80023, 80026, 80027, 80029–32, 80034, 80036, 80039, 80040), double on one side, single on the other (80017, 80025, 80037), or double bilaterally (101531). A further variant in *M. domestica* is the appearance of a foramen at the level of the infraorbital foramen, dorsal to P3; this is present one side only (80018, 80026, 80033) or present bilaterally (80032). In *M. dimidiata*, the foramen anterodorsal to the infraorbital foramen is present bilaterally (86608, 86611), on one side only (86609), or absent bilaterally (86610). The foramen is absent in the two *M. osgoodi* (5242, 5248) and one *M. sp.* (5024), and present on one side only in the remaining two *M. sp.* (5002, 5003). The left side of *M. osgoodi* (5248) has a foramen dorsal to P3 rather than P2.

Didelphis albiventris CM 78203 has a foramen dorsal to the diastema between the P1 and P2 near the nasal bone; it is subequal in size to the upper lacrimal foramen. The left side of *Dasyurus maculatus* CM 50842 has a tiny opening dorsal to the ultimate premolar–M1 embrasure near the nasal bone; a comparable opening is not present on the right side. Similar foramina in the maxilla are not reported for *Pucadelphys andinus* (Marshall and Muizon, 1995) and *Zalambdalestes lechei* (Wible et al., in press).

Orbitosphenoid.—No foramina are found in the orbitosphenoid in *Monodelphis breviceaudata* CM 52729 (Fig. 4). However, a small foramen occurs in the posteroventral base of the orbitosphenoid, just anterior to the sphenorbital fissure in 31 of the remaining 41 CM specimens that could be sampled. This foramen is present bilaterally in *M. domestica* (80018, 80037, 101529), *M. dimidiata* (86608), and *M. sp.* (5002), and on one side only in *M. breviceaudata* (68359, 68360, 76730–34), *M. domestica* (5008, 80016–19, 80021, 80023, 80025, 80027, 80029–33, 80035, 80036, 80040), *M. dimidiata* (86611), and *M. sp.* (5003). Of the specimens listed, this foramen is double on one side only in one *M. breviceaudata* (68360) and seven *M. domestica* (80016, 80018, 80023, 80025, 80027, 80037, 101529). A foramen in the orbitosphenoid is absent bilaterally in five *M. breviceaudata* (4681, 52730, 63509–11, 68358), four *M. domestica* (5010, 80020, 80026, 80038), and one *M. sp.* (50024).

Similar foramina are not present in *Didelphis albiventris* CM 78203, *Dasyurus maculatus* CM 50842, *Pucadelphys andinus* (Marshall and Muizon, 1995), and *Zalambdalestes lechei* (Wible et al., in press).

Palatine.—In addition to the named foramina in the palatine detailed above, *Monodelphis breviceaudata* CM 52729 has unnamed foramina through the postpalatine

torus and in the orbital process. The small foramen through the postpalatine torus is posteromedial to the minor palatine foramen, connects the hard palate and choanae, and is visible in occipital view (Fig. 9). There are three foramina within the orbital process (Fig. 4): one immediately posterior to the sphenopalatine foramen and two more posteriorly connecting the orbital fossa with the choanae: one at the level of the anterior edge of the ethmoidal foramen and the other anterodorsal to that near the suture with the frontal. Finally, there is an elongate, irregular gap situated posterior to the palatine, between that bone and the pterygoid (Fig. 4).

A foramen through the postpalatine torus is ubiquitous in the remaining 52 CM specimens that could be sampled. Variation in this feature concerns the degree of ventral closure. Both closed foramina and deep notches are present within individuals of *Monodelphis breviceaudata*, *M. domestica*, and *M. dimidiata*. The two *M. osgoodi* (5242, 5248) exhibit the same unusual state: they are the only specimens that have shallow notches. A similar foramen through the postpalatine torus occurs in *Didelphis albiventris* CM 78203 and *Zalambdalestes lechei* (Wible et al., in press); rather than a foramen, *Dasyurus maculatus* CM 50842 has a notch, and neither a foramen nor a notch is reported for *Pucadelphys andinus* (Marshall and Muizon, 1995).

One or more tiny foramina posterior to the sphenopalatine foramen are present bilaterally in 38 of the 41 remaining CM specimens that could be sampled. The three exceptions are two *Monodelphis dimidiata* (86608, 86609) and one *M. sp.* (5003) in which one foramen is present on the right side only. The one remaining *M. dimidiata* that could be sampled (86611) has one foramen present bilaterally. Further variation in this feature concerns the number of foramina, with the maximum of three on the right side and four on the left in *M. domestica* (80018). Multiple foramina on at least one side occur in nine of the 14 *M. breviceaudata* (5061, 52730, 63511, 68360, 68361, 76730–33), and 18 of the 26 *M. domestica* (5008, 80016–18, 80020, 80021, 80023, 80025–28, 80030, 80032, 80034–38). Only the left side of one *M. osgoodi* (5242) could be checked and it had one foramen. *Didelphis albiventris* CM 78203 has a small foramen posterodorsal to and directed towards the sphenopalatine foramen, and *Dasyurus maculatus* CM 50842 has one posterior to and directed towards the sphenopalatine foramen. *Pucadelphys andinus* (Marshall and Muizon, 1995) and *Zalambdalestes lechei* (Wible et al., in press) have no extra foramina in the orbital process of the palatine.

One or more foramina within the orbital process of the palatine at the level of the ethmoidal foramen occur bilaterally in 13 of the 14 *Monodelphis breviceaudata*, all 27 of the *M. domestica*, the one *M. dimidiata* (86611), and the one *M. sp.* (5024) that could be sampled. The sole exception, *M. breviceaudata* (4681), has two foramina on the left side only. Further variation in this feature concerns the number of foramina, with the maximum of five on the right side and three on the left in *M. domestica* (101529). Multiple foramina on at least one side occur in 7 of the 15 *M. breviceaudata* (4681, 5061, 52730, 63510, 63511, 76732, 76733), 14 of the 27 *M. domestica* (5008, 80016–18, 80021, 80025, 80026, 80028, 80030, 80033, 80034, 80037, 101529, 101531), the one *M. dimidiata*, and the one *M. sp.* Only the left side of one *M. osgoodi* (5242) could be checked and it had two foramina. *Didelphis albiventris* CM 78203 has two on the right side and one on the left at the level of the ethmoidal foramen; *Dasyurus maculatus* CM 50842 has none.

A foramen anterodorsal to the previous one considered, near the suture with the frontal occurs bilaterally in all the CM *Monodelphis* specimens that could be sampled: 14 *M. breviceaudata*, 27 *M. domestica*, four *M. dimidiata*, and one *M. sp.* (5024). Only the left side of one *M. osgoodi* (5242) could be checked, and the foramen is present. The only variant is that rather than being situated entirely within the palatine, the foramen is in the suture between the palatine and frontal bilaterally in one *M. breviceaudata* (68359), and on one side

only in one *M. breviceaudata* (76733) and two *M. domestica* (80023, 80032). *Didelphis albiventris* CM 78203 has a similar small foramen within the palatine near the frontal, anterior to the level of the ethmoidal foramen. *Dasyurus maculatus* CM 50842 has a relatively larger aperture within the palatine near the frontal, but it is more anteriorly placed, halfway between the sphenopalatine and ethmoidal foramina.

An elongate, irregular opening in the suture between the palatine and pterygoid occurs in nine of the 15 remaining *Monodelphis breviceaudata*, all 28 *M. domestica*, one of the two *M. dimidiata* (86611), and the one *M. osgoodi* (5242) that could be sampled. A comparable gap is lacking in *Didelphis albiventris* CM 78203, *Dasyurus maculatus* CM 50842, *Pucadelphys andinus* (Marshall and Muizon, 1995), and *Zalambdalestes lechei* (Wible et al., in press).

Parietal.—*Monodelphis breviceaudata* CM 52729 (Fig. 1) has a small foramen in the left parietal just anterior to the interparietal bone that leads into a posterodorsomedially directed groove on the interparietal bone. This foramen is present on one or both sides in 31 of the 48 remaining CM specimens that could be sampled, the exceptions being seven *M. breviceaudata* (4681, 52730, 63509, 68358, 68361, 76730, 76733), nine *M. domestica* (80017, 80019, 80020, 80030, 80033–35, 80037, 80038), and *M. osgoodi* (5242). A foramen is present bilaterally in three *M. breviceaudata* (68359, 68360, 76734), twelve *M. domestica* (5008, 80016, 80018, 80021, 80025, 80027, 80031, 80032, 80036, 80039, 80040, 101531), three *M. dimidiata* (86608, 86610, 86611), and one *M. osgoodi* (5248). The foramen is lacking in the other *M. osgoodi* (5242), but the condition could not be confirmed in the remaining *M. dimidiata* because the parietals were covered with connective tissue. The foramen is present on one side only in four *M. breviceaudata* (63510, 63511, 76731, 76732) and five *M. domestica* (5010, 80024, 80028, 80029, 101529). There are two unusual cases in *M. domestica*; CM 5025 has three foramina on the left and two on the right, and CM 80023 has one in the right side only, but four in the interparietal on the same side and two in the interparietal on the opposite side.

Didelphis albiventris CM 78203 does not have comparable foramina in the parietal, but does have four tiny foramina in the interparietal to the right of the sagittal crest and one to the left, and two tiny foramina in the interparietal anterior to the right nuchal crest and three anterior to the left. As in some *Monodelphis*, *Dasyurus maculatus* CM 50842 has two foramina per side in the parietal that lead into grooves running posterodorsally. Comparable foramina in the parietal are not reported for *Pucadelphys andinus* (Marshall and Muizon, 1995) and *Zalambdalestes lechei* (Wible et al., in press).

Petrosal.—On the right side of *Monodelphis osgoodi* CM 5242, there is a foramen in the anteromedial flange of the petrosal somewhat larger than the anterior hypoglossal foramen that leads into a shallow sulcus directed anteromedially toward the carotid foramen. This foramen leads into a canal that bends dorsomedially and opens endocranially. In light of the canal's position, its endocranial aperture presumably is within or near the sulcus for the inferior petrosal sinus, and its occupant, therefore, may be venous. On the specimen's left side, a foramen in the anteromedial flange exists without a sulcus, but the foramen is roughly one-quarter the size of that on the right side. No other specimen in the CM sample has a foramen in the anteromedial flange. However, the left side of the second *M. osgoodi* CM 5248 has an aperture filled with dried blood between the anteromedial flange of the petrosal and basisphenoid with a sulcus directed anteromedially toward the carotid foramen. On the right side comparable structures do not exist. Several *M. domestica* (e.g., 80018, 80026) have a similarly placed opening bilaterally present between the anteromedial flange and basisphenoid; Archer (1976:p. 281) described a similar opening in *M. dimidiata* WAM M6785. It seems likely that these openings are functioning like the foramina in the anteromedial flange of *M. osgoodi* CM 5242. Given that the suture between the

anteromedial flange and basisphenoid is not a tight one, it is possible that small venous channels may be present more widely in the CM sample than the osteology suggests.

Comparable openings, either within the anteromedial flange or between that and the basisphenoid, are not present in *Didelphis albiventris* CM 78203, *Dasyurus maculatus* CM 50842, *Pucadelphys andinus* (Marshall and Muizon, 1995), and *Zalambdalestes lechei* (Wible et al., in press).

Premaxilla.—*Monodelphis breviceaudata* CM 52729 (Fig. 2) has a tiny foramen bilaterally present in the facial component of the premaxilla dorsal to the I3–4 embrasure, near the rim of the external nasal aperture. In the remaining *M. breviceaudata*, a similar aperture is either absent bilaterally (4681, 63510, 63511, 68358, 68359, 76732, 76733), present on one side only (5061, 52730, 63509, 68360, 68361), or bilaterally present (76730, 76731, 76734). *M. domestica* shows a similar pattern: absent bilaterally (5008, 5010, 80031, 80032, 80034, 80039, 80040, 101529), present on one side only (5025, 80016, 80017, 80019, 80021, 80028–30, 80033, 80038), or bilaterally present (80020, 80023–27, 80035–37, 101531). These foramina are absent in three *M. dimidiata* (86608–10) and present on one side only in the fourth (86611). In the two *M. osgoodi*, foramina are absent in one (5242) and bilaterally present in the other (5248). In the *M. sp.*, the foramina are absent (5002, 5003) or double bilaterally (50024).

Didelphis albiventris CM 78203 has a tiny foramen on the right side only posterodorsal to the I5. *Dasyurus maculatus* CM 50842 has a tiny foramen bilaterally placed dorsal to the I4 and three dorsal to the I5 on the left side only. Similar foramina are not reported for *Pucadelphys andinus* (Marshall and Muizon, 1995) or *Zalambdalestes lechei* (Wible et al., in press).

Squamosal.—*Monodelphis breviceaudata* CM 52729 (Fig. 1) has a triangular depression on the dorsum of the posterior root of the zygoma. In the posterior corner of this depression is a small foramen in the squamosal that communicates with the postglenoid foramen and is hidden in dorsal view by the ridge running along the dorsal edge of the zygoma. One or more foramina are present bilaterally in the remaining 13 *M. breviceaudata*, the 21 *M. domestica*, the one *M. dimidiata* (86609), and the one *M. sp.* (5024) that could be sampled. Two or more foramina are present bilaterally in four *M. breviceaudata* (52730, 63509, 63511, 76730) and seven *M. domestica* (80016, 80017, 80025, 80031, 80032, 80036, 80039). The maximum of four on one side and three on the other occurs in *M. domestica* (80032). Only the left side of one *M. osgoodi* (5042) could be sampled and it had one foramen. *Didelphis albiventris* CM 78203 has three foramina on the right and six on the left; *Dasyurus maculatus* CM 50842 has four on the right and six on the left. None is reported for *Pucadelphys andinus* (Marshall and Muizon, 1995) or *Zalambdalestes lechei* (Wible et al., in press).

Monodelphis breviceaudata CM 52729 (Fig. 4) and the bulk of the CM sample have a small anteriorly directed foramen in the lateral surface of the postglenoid process. This foramen is absent on one side only in two *M. domestica* (80020, 80038). Bilateral double foramina are found in one *M. breviceaudata* (52730). Double foramina on one side and single on the other occur in four *M. domestica* (80016, 80021, 80025, 80040) and one *M. sp.* (50024). Double foramina on one side and triple on the other are found in three *M. breviceaudata* (63509, 63511, 76730). *Didelphis albiventris* CM 78203 and *Pucadelphys andinus* (Marshall and Muizon, 1995) have a similar foramen, whereas *Dasyurus maculatus* CM 50842 has two. *Zalambdalestes lechei* (Wible et al., in press) does not have foramina in a comparable position.

Supraoccipital.—Two sorts of foramina are found on the supraoccipital in the CM sample of *Monodelphis*: foramina on the midline at the base of the nuchal crest and foramina more laterally positioned and generally asymmetrically arranged. *M. breviceaudata* CM 52729

(Fig. 9) has only a small, round opening on the midline at the base of the nuchal crest that contained dried blood and was probably an emissary foramen. Given the uncertainty of the position of the interparietal-supraoccipital suture, it is unknown whether this opening was entirely within the supraoccipital or between the supraoccipital and interparietal. One or more foramina on the midline at the base of the nuchal crest are found in 45 of the remaining 48 CM specimens that could be sampled. The three exceptions, one *M. brevicaudata* (4681) and two *M. domestica* (80034, 80035), do not have a foramen in a comparable position, although the last two have a midline foramen that is located well below the nuchal crest. A single foramen is found in eleven *M. brevicaudata* (52730, 63510, 63511, 68358–61, 76730–32, 76734), 21 *M. domestica* (5010, 5025, 80016, 80017, 80020, 80021, 80024–27, 80029–33, 80036–40, 101531), the four *M. dimidiata* (86608–11), and one *M. osgoodi* (5242). Double foramina are found in two *M. brevicaudata* (63509, 76733), five *M. domestica* (80018, 80019, 80023, 80028, 101529), and one *M. osgoodi* (5248). *Didelphis albiventris* CM 78203 has two foramina on the midline within the supraoccipital. *Dasyurus maculatus* CM 50842 has one on the midline and one off to the right entirely within the supraoccipital. *Pucadelphys andinus* (Marshall and Muizon, 1995) has one on the midline, within the supraoccipital-interparietal suture, and *Zalambdalestes lechei* (Wible et al., in press) has no similar opening.

More laterally positioned foramina are more variable in number and position. As in *Monodelphis brevicaudata* CM 52729 (Fig. 9), more laterally positioned foramina are wholly lacking in three other *M. brevicaudata* (68358, 68359, 76732), six *M. domestica* (5025, 80019, 80033–35, 80039), one of the four *M. dimidiata* (86608), and the two *M. osgoodi* (5242, 5248). The remaining 36 specimens that could be sampled had between a low of one foramen on each side (e.g., *M. brevicaudata* CM 76734) and a high of more than 20 foramina on each side (e.g., *M. brevicaudata* CM 68360). *Didelphis albiventris* CM 78203 has two on the right side and four on the left; *Dasyurus maculatus* CM 50842 has only one on the right side. *Pucadelphys andinus* (Marshall and Muizon, 1995) has one per side, and *Zalambdalestes lechei* (Kielan-Jaworowska, 1984; Wible et al., in press) has numerous small foramina, variable in size and number, near the nuchal crest and somewhat ventral to it.

CONCLUSIONS

Comparisons of the cranial osteology of the CM sample of *Monodelphis* with that of other taxa for the purposes of phylogenetic analysis, as models for interpreting extinct forms, and for standardization of terminology are among the ultimate goals of this contribution. Two sorts of limited comparisons are presented (limited because so few relevant forms have been studied to a comparable level): intrageneric (among four of the 15 species of *Monodelphis* recognized by Gardner, 1993); and with four selected outgroups (the didelphid *Didelphis albiventris*, the dasyurid *Dasyurus maculatus*, the early Paleocene metatherian *Pucadelphys andinus*, and the Late Cretaceous eutherian *Zalambdalestes lechei*).

Intrageneric Comparisons

Four species of *Monodelphis* are represented in the CM collection: *M. brevicaudata*, *M. dimidiata*, *M. domestica*, and *M. osgoodi*. The comparisons that follow are limited for the most part to the named and unnamed cranial foramina that were considered in the Discussions. The caveat is what is unique or unusual among four species may not be when all 15 species recognized by Gardner (1993) and relevant outgroups are examined.

The two specimens of *Monodelphis osgoodi* (the holotype CM 5242 and CM 5248) are the most unique among the CM sample. They are distinguished from the remaining 52 *Monodelphis* specimens by four unique features: (1) rather than a fairly distinct foramen for the greater petrosal nerve, one that is barely distinguishable from the foramen ovale; (2) rather than an infraorbital foramen dorsal to the P3 of the P3–M1 embrasure, one that is dorsal to the M1; (3) rather than a sliver of palatine in the maxillary foramen, a well-developed process that contributes to the medial and dorsal walls of the maxillary foramen; and (4) rather than a foramen through the postpalatine torus, a very shallow notch is present. In addition, they have seven features with a limited distribution among the CM sample: (1) the anterior hypoglossal foramen is larger than the posterior (also in one *M. breviceaudata* and seven *M. domestica*); (2) the posttemporal notch is absent bilaterally (also in a three *M. domestica*); (3) subsquamosal foramina are lacking (also in a three *M. breviceaudata* and three *M. dimidiata*); (4) unnamed foramina in the lacrimal dorsal to the maxillary foramen are lacking (also in one *M. domestica* and one *M. dimidiata*); (5) an unnamed foramen in the maxilla dorsal to the P2 is lacking bilaterally (also in two *M. domestica*, one *M. dimidiata*, and one *M. sp.*); (6) unnamed foramina in the supraoccipital off the midline are lacking (also in three *M. breviceaudata*, six *M. domestica*, and one *M. dimidiata*); and (7) the stapes lacks an intracranial foramen, based on CM 5242 (also in two *M. dimidiata* with the third having a microperforation). In fact, the absence of a well-developed intracranial foramen is unique to *M. osgoodi* and *M. dimidiata* among the CM sample.

Only one other cranial feature is potentially unique to one of the remaining three *Monodelphis* species in the CM sample. A separate, small, midline ossification on the dorsal rim of the foramen magnum may distinguish *M. domestica* from the other species. However, such an element is only known for eleven *M. domestica*. It is uncertain whether this element has fallen out of the remaining 16 *M. domestica* preserving the occiput (or for that matter *M. breviceaudata*, *M. dimidiata*, and *M. osgoodi*) or fails to form altogether. One *M. breviceaudata* (68358) has two small, rod-shaped elements in a comparable location, with the right one twice the size of the left. The four *M. dimidiata* (CM 86608–11) have three features with a limited distribution among the remaining CM sample: (1) an infraorbital foramen situated dorsal to the posterior root of P3 (also in four *M. breviceaudata*, 23 *M. domestica*, and one *M. sp.*), whereas the remaining small *Monodelphis* have the foramen more posteriorly positioned (i.e., *M. osgoodi*); (2) parietal foramina are lacking (also in four *M. breviceaudata* and eight *M. domestica*); and (3) the stapes lacks an intracranial foramen in the three specimens preserving the bone (also in *M. osgoodi* CM 5242).

The cranial foramina considered in the CM sample can be categorized into three groups: (1) foramina bilaterally present in all specimens that exhibit no significant variation (carotid foramen, ethmoidal foramen, foramen for the inferior petrosal sinus, incisive foramen, jugular foramen, major palatine foramen, mandibular foramen, minor palatine foramen, pterygoid canal, sphenopalatine foramen, sphenorbital fissure, stylo mastoid notch, and transverse canal foramen); (2) bilateral or midline foramina that are present in all specimens but exhibiting significant variation in size, number, position, distinctness from other foramina, or elements contributing to its walls (foramen for the frontal diploic vein, foramen for the greater petrosal nerve, foramen magnum, foramen ovale, foramen rotundum, hypoglossal foramen, infraorbital foramen, lacrimal foramen, maxillary foramen, postglenoid foramen, postzygomatic foramen, suprameatal foramen, unnamed foramen through the postpalatine torus, unnamed foramen in the orbital process of the palatine in or near the frontal suture, and unnamed foramen in the dorsum of the posterior zygomatic root of the squamosal); and (3) foramina that are not present in all specimens that also vary in size, number, and position (accessory palatine foramen, condyloid canal, parietal foramen,

posttemporal notch, subsquamosal foramen, glaserian fissure in alisphenoid tympanic process for the chorda tympani, unnamed foramen in the orbital process of the lacrimal, unnamed foramen in the facial process of the maxilla dorsal to P2, unnamed foramen in the orbitosphenoid, unnamed foramina in the palatine near the sphenopalatine foramen and at the level of the ethmoidal foramen, unnamed foramen between the palatine and pterygoid, unnamed foramen in the parietal near the interparietal, unnamed foramen in the anteromedial flange of the petrosal, unnamed foramen in the facial process of the premaxilla, unnamed foramen in the lateral surface of the postglenoid process, and unnamed foramina in the supraoccipital). Finally, some foramina on the petrosal were not widely sampled and are requiring of further investigation (hiatus Fallopii, internal acoustic meatus, prootic canal, secondary facial foramen, and sigmoid sinus canal).

Outgroup Comparisons

Following the phylogenetic analysis of Rougier et al. (1998), cranial foramina present in *Monodelphis* and *Didelphis albiventris* might be present in didelphids primitively; in the two didelphids plus *Dasyurus maculatus* might be present in marsupials primitively; in the three marsupials plus *Pucadelphys andinus* might be present in metatherians primitively; and in the four metatherians plus *Zalambdalestes lechei* might be present in therians primitively. The named and unnamed foramina unique to five taxonomic units are listed below: *Monodelphis*, Didelphidae, Marsupialia, Metatheria, and Theria. Following the foramen and its condition in parentheses are the number of CM *Monodelphis* that exhibit the foramen and condition. The caveat is the very small outgroup sample size and the possibility of preservational bias, with the fossils perhaps not preserving the numerous small foramina that are encountered in the extant taxa.

Monodelphis.—Distinguishing CM *Monodelphis* from the outgroups are: (1) a condyloid canal (at least on one side in 37 of 39 CM *Monodelphis*); (2) two lacrimal foramina on the facial process of the lacrimal (in 53 of 54 CM *Monodelphis*); (3) a small foramen in the posteroventral base of the orbitosphenoid (in 31 of 42 CM *Monodelphis*); and (4) a gap between the palatine and pterygoid (in 40 of 47 CM *Monodelphis*).

Didelphidae.—Distinguishing CM *Monodelphis* and *Didelphis albiventris* CM 78203 from the outgroups are: (1) an elongate major palatine foramen largely within the maxilla, but with the palatine forming the posterior border (in all CM *Monodelphis*); (2) a small foramen in the orbital process of the lacrimal dorsal to the maxillary foramen (at least on one side in 47 of 52 CM *Monodelphis*); and (3) one or more foramina in the orbital process of the palatine at the level of the ethmoidal foramen (bilaterally in 42 of 43 CM *Monodelphis*).

Marsupialia.—Distinguishing CM *Monodelphis*, *Didelphis albiventris* CM 78203, and *Dasyurus maculatus* CM 50842 from the outgroups are: (1) small accessory palatine foramina (in 53 of 54 CM *Monodelphis*); (2) an ethmoidal foramen between the frontal and orbitosphenoid (in all CM *Monodelphis* preserving the foramen); (3) two hypoglossal foramina with the anterior smaller than the posterior (in most CM *Monodelphis*); (4) two lacrimal foramina with at least one on the facial process of the lacrimal (in 53 of 54 CM *Monodelphis*); (5) a parietal foramen (in 34 of 50 CM *Monodelphis*); (6) postzygomatic foramina (in most CM *Monodelphis*); (7) a sphenorbital fissure formed at least by the alisphenoid, orbitosphenoid, palatine, and presphenoid (in all CM *Monodelphis* preserving the fissure); (8) small subsquamosal foramen in the squamosal (in 43 of 49 CM *Monodelphis*); (9) a transverse canal foramen (in all CM *Monodelphis* preserving the foramen); (10) a glaserian fissure in the alisphenoid tympanic process (in all CM *Monodelphis* preserving the alisphenoid tympanic process); (11) a small foramen in the

maxilla dorsal to the premolars or first molar at least on one side (in 49 of 54 CM *Monodelphis*); (12) a small foramen in the palatine posterior to the sphenopalatine foramen (in 39 of 42 CM *Monodelphis*); (13) a small foramen in the palatine (or between the palatine and frontal) anterior to the ethmoidal foramen (in all CM *Monodelphis* preserving the right and left palatine); (14) a small foramen in the facial process of the premaxilla, near the external nasal aperture, at least on one side (in 23 of 44 CM *Monodelphis*); and (15) a small foramen in the dorsal surface of the squamosal at the posterior root of the zygoma (in all CM *Monodelphis* preserving this part of the squamosal).

Metatheria.—Distinguishing CM *Monodelphis*, *Didelphis albiventris* CM 78203, *Dasyurus maculatus* CM 50842, and *Pucadelphys andinus* (Marshall and Muizon, 1995) from the outgroup are: (1) a partial or complete foramen for the greater petrosal nerve (in all CM *Monodelphis* preserving the region); (2) a separate foramen for the inferior petrosal sinus (in all CM *Monodelphis* preserving the region); (3) an elongate incisive foramen largely in the premaxilla, but with the maxilla forming the posterior border (in all CM *Monodelphis* preserving the region); (4) a maxillary foramen between the lacrimal, maxilla, and palatine (in all CM *Monodelphis* preserving the region); (5) a narrow, horizontal prootic canal (in all CM *Monodelphis* preserving the region); (6) a secondary facial foramen well anterior to the fenestra vestibuli (in all CM *Monodelphis* preserving the region) (condition not known for *D. maculatus* CM 50842); (7) a sphenopalatine foramen within the palatine (in all CM *Monodelphis* preserving the region); (8) a foramen on the midline posteroventral to the nuchal crest (in 45 of 48 CM *Monodelphis*); and (9) a sphenorbital fissure that transmits the optic nerve (an exception within Metatheria has been reported recently in Late Cretaceous *Deltatheridium* by Rougier et al., in press).

Theria.—Present in CM *Monodelphis*, *Didelphis albiventris* CM 78203, *Dasyurus maculatus* CM 50842, *Pucadelphys andinus* (Marshall and Muizon, 1995), and *Zalambdalestes lechei* (Kielan-Jaworowska and Trofimov, 1981; Kielan-Jaworowska, 1984; Wible et al., in press) are: (1) a carotid foramen in the basisphenoid (in all CM *Monodelphis* preserving the region); (2) a foramen rotundum with the anterior aperture separate from the sphenorbital fissure (in all CM *Monodelphis* preserving the region); (3) a minor palatine foramen between the palatine and maxilla with a thin posterior bridge (in all CM *Monodelphis* preserving the region); (4) a postglenoid foramen in the squamosal (in all CM *Monodelphis* preserving the region); (5) a posttemporal notch or foramen (at least on one side in all CM *M. brevicaudata* and *M. domestica* preserving the region); (6) a suprameatal foramen (in all CM *Monodelphis* preserving the region); and (7) small foramina in the supraoccipital ventral to the nuchal crest (in 35 of 44 CM *Monodelphis*). *Z. lechei* differs from the remaining taxa in two features for which other basal eutherians present the metatherian condition: (1) a foramen for the frontal diploic vein (at least on one side in all CM *Monodelphis* preserving the region and in the zalambdalestid *Kulbeckia kulbecke*, Archibald and Averianov, 2003); and (2) a mandibular foramen just dorsal to the anterior root of the mandibular angle (in all CM *Monodelphis* preserving the region and in *Prokennalestes*, Kielan-Jaworowska and Dashzeveg, 1989).

ACKNOWLEDGMENTS

The completion of this paper owes a debt of gratitude to all the employees of the Section of Mammals, Carnegie Museum of Natural History: Gina Scanlon completed all the exquisite artwork; Suzanne McLaren helped with database searches; Tim McCarthy helped prepare specimens; and Lisa Miriello helped in measuring and tracking down specimens. I am also grateful to Ted Macrini for a copy of his unpublished master's thesis and Marcelo Sánchez-Villagra for his unpublished observations. I also thank Tim Gaudin, Bob Presley, and Guillermo Rougier for review of the manuscript and discussion of issues raised herein. Funding for this report was provided by the National Science Foundation (NSF Grant DEB-0129127).

LITERATURE CITED

- ABDALA, F., D. A. FLORES, AND N. P. GIANNINI. 2001. Postweaning ontogeny of the skull of *Didelphis albiventris*. *Journal of Mammalogy*, 82:190–200.
- ARCHER, M. 1976. The basicranial region of marsupicarnivores (Marsupialia), interrelationships of carnivorous marsupials, and affinities of the insectivorous peramelids. *Zoological Journal of the Linnean Society*, 59:217–322.
- ARCHIBALD, J. D., AND A. O. AVERIANOV. 2003. The Late Cretaceous placental *Kulbeckia*. *Journal of Vertebrate Paleontology*, 23:404–419.
- ARGOT, C. 2001. Functional-adaptive anatomy of the forelimb in Didelphidae, and the paleobiology of the Paleocene marsupials *Mayulestes ferox* and *Pucadelphys andinus*. *Journal of Morphology*, 24:51–79.
- BOYD, G. I. 1930. The emissary foramina of the cranium in man and the anthropoids. *Journal of Anatomy*, 65:108–121.
- . 1934. The emissary foramina of the cranium in primates. *Journal of Anatomy*, 69:113–117.
- BROOM, R. 1926. On the mammalian presphenoid and mesethmoid bones. *Proceedings, Zoological Society of London*, 17:257–264.
- CLARK, C. T., AND K. K. SMITH. 1993. Cranial osteogenesis in *Monodelphis domestica* (Didelphidae) and *Macropus eugenii* (Macropodidae). *Journal of Morphology*, 215:119–149.
- CLEMENS, W. A. 1979. Marsupialia. Pp. 192–220, in *Mesozoic Mammals, the First Two-thirds of Mammalian History* (J. A. Lillegraven, Z. Kielan-Jaworowska, and W. A. Clemens, eds.). University of California Press, Berkeley.
- COOPER, J. G., AND K. P. BHATNAGAR. 1976. Comparative anatomy of the vomeronasal organ complex in bats. *Journal of Anatomy*, 122:571–601.
- COUES, E. 1872. On the osteology and myology of *Didelphys virginiana*, with an appendix on the brain by Jeffries Wyman. *Memoirs of the Boston Society of Natural History*, 2:41–154.
- DE BEER, G. R. 1937. *The Development of the Vertebrate Skull*. Clarendon Press, Oxford.
- DOM, R., B. L. FISHER, AND G. F. MARTIN. 1970. The venous system of the head and neck of the opossum (*Didelphis virginiana*). *Journal of Morphology*, 132:487–496.
- DORAN, A. H. G. 1878. Morphology of the mammalian ossicula auditus. *Transactions of the Linnean Society of London*, 2nd Series Zoology, 1:391–497.
- ELLSWORTH, A. H. 1976. *The North American Opossum: An Anatomical Atlas*. Robert E. Krieger Publishing Company, Huntington, NY.
- EVANS, H. E. 1993. *Miller's anatomy of the dog*. W. B. Saunders, Philadelphia.
- FILAN, S. L. 1991. Development of the middle ear region in *Monodelphis domestica* (Marsupialia, Didelphidae): marsupial solutions to an early birth. *Journal of Zoology*, London, 225:577–588.
- FLEISCHER, G. 1973. Studien am Skelett des Gehörorgans der Säugetiere, einschließlich des Menschen. *Säugetierkundliche Mitteilungen*, 21:131–239.
- GARDNER, A. L. 1993. Order Didelphimorphia. Pp. 15–23, in *Mammal Species of the World, A Taxonomic and Geographic Reference* (D. E. Wilson and D. M. Reeder, eds.). Smithsonian Institution Press, Washington, D. C.
- GAUDIN, T. J., J. R. WIBLE, J. A. HOPSON, AND W. D. TURNBULL. 1996. Reexamination of the morphological evidence for the Cohort Epitheria (Mammalia, Eutheria). *Journal of Mammalian Evolution*, 3: 31–79.
- GAUPP, E. 1902. Über die Ala temporalis des Säugetierschädels und die Regio orbitalis einiger anderer Wirbeltierschädels. *Anatomische Hefte*, 19:155–230.
- . 1905. Neue Deutungen auf dem Gebiete der Lehre vom Säugetierschädel. *Anatomischer Anzeiger*, 27:273–310.
- . 1908. Zur Entwicklungsgeschichte und vergleichenden Morphologie des Schädels von *Echidna aculeata* var. *typica*. *Semon's Zoologische Forschungsreisen in Australien. Denkschriften der medicinisch-naturwissenschaftliche Gesellschaft zu Jena*, 6:539–788.
- GELDEREN, C. VAN. 1924. Die Morphologie der Sinus durae matris. Zweiter Teil. Die vergleichende Ontogenie der neurokranialen Venen der Vögel und Säugetiere. *Zeitschrift für Anatomie und Entwicklungsgeschichte*, 74:432–508.
- GREGORY, W. K. 1910. The orders of mammals. *Bulletin of the American Museum of Natural History*, 27:1–524.
- HERSHKOVITZ, P. 1982. The staggered marsupial lower third incisor (I3). *Geobios, Mém. Special*, 6:191–200.
- . 1992. The South American gracile mouse opossums, genus *Gracilianus* Gardner and Creighton, 1989 (Marmosidae, Marsupialia): a taxonomic review with notes on general morphology and relationships. *Fieldiana, Zoology*, 70:56 pp.
- . 1995. The staggered marsupial third lower incisor: hallmark of cohort Didelphimorphia, and description of a new genus and species with staggered i3 from the Albian (Lower Cretaceous) of Texas. *Bonner Zoologische Beiträge*, 45:153–169.

- . 1997. Composition of the family Didelphidae Gray, 1821 (Didelphoidea: Marsupialia), with a review of the morphology and behavior of the included four-eyed pouched opossums of the genus *Philander* Tiedemann, 1808. *Fieldiana, Zoology*, 86:103 pp.
- HIEMAE, K., AND F. A. JENKINS, JR. 1969. The anatomy and internal architecture of the muscles of mastication in *Didelphis marsupialis*. *Postilla*, 140:1–49.
- KERMACK, K. A., F. MUSSETT, AND H. W. RIGNEY. 1981. The skull of *Morganucodon*. *Zoological Journal of the Linnean Society*, 71:1–158.
- KIELAN-JAWOROWSKA, Z. 1981. Evolution of the therian mammals in the Late Cretaceous of Asia. Part IV. Skull structure in *Kennalestes* and *Asioryctes*. *Palaeontologia Polonica*, 42:25–78.
- . 1984. Evolution of the therian mammals in the Late Cretaceous of Asia. Part V. Skull structure in *Zalambdalestidae*. *Palaeontologia Polonica*, 46:107–117.
- KIELAN-JAWOROWSKA, Z., AND D. DASHZEVEG. 1989. Eutherian mammals from the Early Cretaceous of Mongolia. *Zoologica Scripta* 18:347–355.
- KIELAN-JAWOROWSKA, Z., AND B. A. TROFIMOV. 1981. A new occurrence of the Late Cretaceous eutherian mammal *Zalambdalestes*. *Acta Palaeontologica Polonica*, 26:3–7.
- KLAAUW, C. J. VAN DER. 1923. Die Skelettstückchen in der Sehne des Musculus stapedius und nahe dem Ursprung der Chorda tympani. *Zeitschrift für Anatomie und Entwicklungsgeschichte*, 69:32–83.
- . 1931. The auditory bulla in some fossil mammals. *Bulletin of the American Museum of Natural History*, 62:1–352.
- KUHN, H.-J., AND U. ZELLER. 1987. The cavum epiptericum in monotremes and therian mammals. Pp. 51–70, in *Morphogenesis of the Mammalian Skull* (H.-J. Kuhn and U. Zeller, eds.). *Mammalia depicta*, 13. Verlag Paul Parey, Hamburg.
- LARSELL, O., E. McCRADY, JR., AND A. A. ZIMMERMANN. 1935. Morphological and functional development of the membranous labyrinth in the opossum. *Journal of Comparative Neurology*, 63:95–118.
- LILLEGRAVEN, J. A., AND G. KRUSAT. 1991. Cranio-mandibular anatomy of *Haldanodon expectatus* (Docodonta; Mammalia) from the Late Jurassic of Portugal and its implications to the evolution of mammalian characters. *Contributions to Geology, University of Wyoming*, 28:39–138.
- LUCKETT, W. P. 1993. An ontogenetic assessment of dental homologies in theria mammals. Pp. 182–204, in *Mammal Phylogeny, Mesozoic Differentiation, Multituberculates, Monotremes, Early Therians, and Marsupials* (F. S. Szalay, M. J. Novacek, and M. C. McKenna, eds.). Springer Verlag, New York.
- MACPHEE, R. D. E. 1981. Auditory region of primates and eutherian insectivores. *Contributions to Primatology*, 18:282 pp.
- MACRINI, T. E. 2000. High resolution X-ray computed tomography (CT) of the skull of the extant opossum (*Monodelphis domestica*) and a comparison of its ontogeny to synapsid phylogeny. Unpublished M.S. thesis, University of Texas, Austin, 158 pp. with CD-ROM.
- . 2002. Quantitative comparison of ontogenetic and phylogenetic character changes in the synapsid mandible and auditory region. *Journal of Mammalian Evolution*, 9:185–208.
- MAIER, W. 1987a. The ontogenetic development of the orbitotemporal region in the skull of *Monodelphis domestica* (Didelphidae, Marsupialia), and the problem of the mammalian alisphenoid. Pp. 71–90, in *Morphogenesis of the Mammalian Skull* (H.-J. Kuhn and U. Zeller, eds.). *Mammalia depicta*, 13. Verlag Paul Parey, Hamburg.
- . 1987b. Der Processus angularis bei *Monodelphis domestica* (Didelphidae; Marsupialia) und seine Beziehungen zum Mittelohr: Eine ontogenetische und evolutionsmorphologische Untersuchung. *Gegenbaurs Morphologisches Jahrbuch*, 133:123–161.
- . 1989. Morphologische Untersuchungen am Mittelohr der Marsupialia. *Zeitschrift für zoologische Systematische und Evolutionsforschung*, 27:149–168.
- MARSHALL, L. G., AND C. DE MUIZON. 1995. Part II. The skull. Pp. 21–90, in *Pucadelphys andinus* (Marsupialia, Mammalia) from the Early Paleocene of Bolivia (L. G. Marshall, C. de Muizon, and D. Sigogneau-Russell, eds.). *Mémoires du Muséum National d'Histoire Naturelle*, 165.
- MCDOWELL, S. B., JR. 1958. The Greater Antillean insectivores. *Bulletin of the American Museum of Natural History*, 115:113–214.
- MINKOFF, E. C., P. MIKKELSEN, W. A. CUNNINGHAM, AND K. W. TAYLOR. 1979. The facial musculature of the opossum (*Didelphis virginiana*). *Journal of Mammalogy*, 60:46–57.
- MUIZON, C. DE. 1998. *Mayulestes ferox*, a borhyaenoid (Metatheria, Mammalia) from the early Palaeocene of Bolivia. *Phylogenetic and palaeobiologic implications*. *Geodiversitas*, 20:19–142.
- NESSLINGER, C. L. 1956. Ossification centers and skeletal development in the postnatal Virginia opossum. *Journal of Mammalogy*, 37:382–394.
- NOMINA ANATOMICA VETERINARIA, 3RD EDITION. 1994. Adolf Holzhausen's Successors, Vienna.
- NOVACEK, M. J. 1977. Aspects of the problem of variation, origin and evolution of the eutherian auditory bulla. *Mammal Review*, 7:131–149.

- . 1986. The skull of leptictid insectivorans and the higher-level classification of eutherian mammals. *Bulletin of the American Museum of Natural History*, 183:1–112.
- . 1993. Patterns of skull diversity in the mammalian skull. Pp. 438–545, in *The Skull*, Vol. 2, *Patterns of Structural and Systematic Diversity* (J. Hanken and B. K. Hall, eds.). University of Chicago Press, Chicago.
- OSGOOD, W. H. 1921. A monographic study of the American marsupial, *Caenolestes*. *Field Museum of Natural History, Zoological Series*, 14:1–156.
- PATTERSON, B. 1965. The auditory region of the borhyaenid marsupial *Cladosictis*. *Breviora*, 217:1–9.
- REIG, O. A., J. A. W. KIRSCH, AND L. G. MARSHALL. 1987. Systematic relationships of the living and Neoceneozoic American “opossum-like” marsupials (suborder Didelphimorphia), with comments on the classification of these and of the Cretaceous and Paleogene New World and European metatherians. Pp. 1–89, in *Possums and Opossums: Studies in Evolution*, Vol. 1 (M. Archer, ed.). Surrey Beatty & Sons Pty Limited, Chipping Norton.
- ROUGIER, G. W., AND J. R. WIBLE. In press. Major changes in the mammalian ear region and basicranium. In *Amniote Paleobiology* (M. T. Carrano, T. J. Gaudin, R. W. Blob, and J. R. Wible, eds.). University of Chicago Press, Chicago.
- ROUGIER, G. W., J. R. WIBLE, AND J. A. HOPSON. 1992. Reconstruction of the cranial vessels in the Early Cretaceous mammal *Vincelestes neuquentianus*: implications for the evolution of the mammalian cranial vascular system. *Journal of Vertebrate Paleontology*, 12:188–216.
- ROUGIER, G. W., J. R. WIBLE, AND M. J. NOVACEK. 1998. Implications of *Deltatheridium* specimens for early marsupial history. *Nature*, 396:459–463.
- . In press. New specimen of *Deltatheroides cretacicus* (Metatheria, Deltatheroidea) from the Late Cretaceous of Mongolia. In *Fanfare for an Uncommon Paleontologist: Papers in Honor of Malcolm C. McKenna* (M. R. Dawson, and J. A. Lillegraven, eds.). *Bulletin of Carnegie Museum of Natural History*.
- ROWE, T. 1996. Coevolution of the mammalian middle ear and neocortex. *Science*, 273:651–654.
- SÁNCHEZ-VILLAGRA, M. R. 2001. Ontogenetic and phylogenetic transformations of the vomeronasal complex and nasal floor elements in marsupial mammals. *Zoological Journal of the Linnean Society*, 131: 459–479.
- SÁNCHEZ-VILLAGRA, M. R., AND R. J. ASHER. 2002. Cranio-sensory adaptations in small faunivorous semiaquatic mammals, with special reference to olfaction and the trigeminal system. *Mammalia*, 66:93–109.
- SÁNCHEZ-VILLAGRA, M. R., S. GEMBALLA, S. NUMMELA, K. K. SMITH, AND W. MAIER. 2002. Ontogenetic and phylogenetic transformations of the ear ossicles in marsupial mammals. *Journal of Morphology*, 251: 219–238.
- SÁNCHEZ-VILLAGRA, M. R., AND K. K. SMITH. 1997. Diversity and evolution of the marsupial mandibular angular process. *Journal of Mammalian Evolution*, 4:119–144.
- SÁNCHEZ-VILLAGRA, M. R., AND J. R. WIBLE. 2002. Patterns of evolutionary transformation in the petrosal bone and some basicranial features in marsupial mammals, with special reference to didelphids. *Journal of Zoological Systematics and Evolutionary Research*, 40:26–45.
- SAUNDERS, N. R., AND L. A. HINDS. 1997. *Marsupial Biology: Recent Research, New Perspectives*. University of New South Wales Press, Sydney.
- SEGALL, W. 1969. The auditory ossicles (malleus, incus) and their relationships to the tympanic: in marsupials. *Acta Anatomica*, 73:176–191.
- . 1970. Morphological parallelisms of the bulla and auditory ossicles in some insectivores and marsupials. *Fieldiana, Zoology*, 51:169–205.
- SMITH, K. K. 1994. Development of craniofacial musculature in *Monodelphis domestica* (Marsupialia, Didelphidae). *Journal of Morphology*, 222:149–173.
- TANDLER, J. 1899. Zur vergleichenden Anatomie der Kopfarterien bei den Mammalia. *Denkschriften Akademie der Wissenschaften, Wien, mathematisch-naturwissenschaftliche Klasse*, 67:677–784.
- THEWISSEN, J. G. M. 1989. Mammalian frontal diploic vein and the human foramen caecum. *Anatomical Record*, 223:242–244.
- TOEPLITZ, C. 1920. Bau und Entwicklung des Knorpelschädels von *Didelphis marsupialis*. *Zoologica, Stuttgart*, 27:1–84.
- TURNBULL, W. D. 1970. Mammalian masticatory apparatus. *Fieldiana, Geology*, 18:149–356.
- TYNDALE-BISCOE, C. H., AND P. A. JANSSENS. 1988. *The Developing Marsupial: Models for Biomedical Research*. Springer Verlag, Berlin.
- VOIT, M. 1909. Das Primordialcranium des Kaninchens unter Berücksichtigung der Deckknochen. *Anatomische Hefte*, 38:425–616.
- WIBLE, J. R. 1983. The internal carotid artery in early eutherians. *Acta Palaeontologica Polonica*, 28:281–293.
- . 1984. The ontogeny and phylogeny of the mammalian cranial arterial pattern. Ph.D. dissertation, Duke University, Durham, NC, 705 pp.
- . 1987. The eutherian stapedia artery: character analysis and implications for superordinal relationships. *Zoological Journal of the Linnean Society*, 91:107–135.

- . 1990. Late Cretaceous marsupial petrosal bones from North America and a cladistic analysis of the petrosal in therian mammals. *Journal of Vertebrate Paleontology*, 10:183–205.
- WIBLE, J. R., AND J. A. HOPSON. 1993. Basicranial evidence for early mammal phylogeny. Pp. 45–62, in *Mammal Phylogeny: Mesozoic Differentiation, Multituberculates, Monotremes, Early Therians, and Marsupials* (F. S. Szalay, M. J. Novacek, and M. C. McKenna, eds.). Springer Verlag, New York.
- . 1995. Homologies of the prootic canal in mammals and non-mammalian cynodonts. *Journal of Vertebrate Paleontology*, 15:331–356.
- WIBLE, J. R., M. J. NOVACEK, AND G. W. ROUGIER. In press. New data on the skull and dentition in the Mongolian Late Cretaceous eutherian mammal *Zalambdalestes*. *Bulletin of the American Museum of Natural History*.
- WIBLE, J. R., AND G. W. ROUGIER. 2000. Cranial anatomy of *Kryptobaatar dashzevegi* (Mammalia, Multituberculata), and its bearing on the evolution of mammalian characters. *Bulletin of the American Museum of Natural History*, 247:124 pp.
- WIBLE, J. R., G. W. ROUGIER, M. J. NOVACEK, AND M. C. MCKENNA. 2001. Earliest eutherian ear region: a petrosal referred to *Prokennalestes* from the Early Cretaceous of Mongolia. *American Museum Novitates*, 3322: 44 pp.
- WIBLE, J. R., G. W. ROUGIER, M. J. NOVACEK, M. C. MCKENNA, AND D. DASHZEVEG. 1995. A mammalian petrosal from the Early Cretaceous of Mongolia: implications for the evolution of the ear and mammalian interrelationships. *American Museum Novitates*, 3149:19 pp.

APPENDIX 1

Monodelphis specimens examined; all CM numbers.

Monodelphis brevicaudata—Brazil: female 5061; male 4681. Suriname: female 52729, 63510, 63511, 68358, 68359, 68360, 68361; male 52730, 63509, 76730, 76731, 76732, 76733, 76734.

Monodelphis dimidiata—Argentina: female 86608, 86609, 86610; male 86611.

Monodelphis domestica—Bolivia: female 5008, 5025; male 5010. Brazil: female 80017, 80018, 80019, 80025, 80028, 80030, 80031, 80033, 80034, 80038, 80040, 101531; male 80016, 80020, 80021, 80023, 80024, 80026, 80027, 80029, 80032, 80035, 80036, 80037, 80039, 101529.

Monodelphis osgoodi—Bolivia: male 5242, 5248.

Monodelphis sp.—Bolivia: female 5002, 5003, 5024.

APPENDIX 2

Cranial measurements (mm) of *Monodelphis*; all CM numbers. Length of mandible was taken from the anterior tip of the bone to the condylar process. * = estimated measurement. ^a Specimen retaining the upper and lower deciduous third premolars and the M3 and m4 in crypts. ^b Specimen retaining the upper and lower deciduous third premolars with the M3 in a crypt and the m4 erupted. ^c Specimen retaining the upper and lower deciduous third premolars with the M3 erupted and the m4 erupted. ^d Specimen retaining the upper and lower deciduous third premolars with the M4 in a crypt. ^e Specimen retaining the lower deciduous third premolar and the M4 erupted.

	Premaxillary-Condylar Length	Greatest Zygomatic Breadth	Length of Mandible
<i>M. brevicaudata</i>			
4681	36.9	19.5	27.4
5061	—	19.5	26.7
52729	34.7	18.5	25.7
52730	35.4	20.0	25.7
63509	32.7	17.1*	24.4
63510	31.2	16.7	22.8
63511	—	17.5	25.3
68358	36.2	19.4	26.6
68359	36.3	18.9	26.8
68360 ^e	17.2	14.7	17.6
68361	33.4	17.3	24.2
76730	35.7	18.8	26.1
76731	35.5	18.4	26.5
76732	38.7	20.8	28.7
76733 ^d	30.6	16.5	22.4
76734 ^b	28.6	15.2	20.3

APPENDIX 2

Continued.

	Premaxillary-Condylar Length	Greatest Zygomatic Breadth	Length of Mandible
<i>M. dimidiata</i>			
86608	24.3	12.3	17.1
86609	29.7	15.7	21.4
86610	24.8	12.2	17.2
86611	24.8	12.2	16.4
<i>M. domestica</i>			
5008	—	19.4	25.7
5010	38.6	21.5	29.2
5025	—	—	24.7
80016	44.7	24.3	34.4
80017	41.9	21.7	31.3
80018	39.6	20.1	29.0
80019 ^b	29.7	15.6	21.1
80020 ^a	28.2	15.3	20.4
80021	40.6	21.4	30.4
80023	43.7	23.5	33.0
80024	37.8	20.2	28.3
80025	40.4	22.3	30.7
80026	38.2	20.7	28.7
80027	39.5	21.1	29.7
80028	40.6	22.2	31.1
80029	44.0	25.0	34.0
80030	40.2	22.1	30.3
80031	39.6	21.8	30.4
80032	36.9	19.6	27.9
80033 ^b	31.9	16.9	22.7
80034	37.2	19.0	27.2
80035 ^a	26.7	14.3	19.0
80036	41.6	23.5	30.9
80037	43.4	22.7	32.1
80038	41.3	22.2	30.8
80039 ^c	35.7	18.3	27.5
80040	42.8	23.5	32.5
101531	38.8	20.4	29.3
101529	42.4	23.0	32.4
<i>M. osgoodi</i>			
5242	25.8	12.4	17.2
5248	25.4	11.8	18.1
<i>Monodelphis</i> sp.			
5002	—	—	23.5*
5003 ^d	—	—	20.6*
5024	—	20.1	26.8

APPENDIX 3

List of Anatomical Terms: On the left are the terms used here; on the right are references and/or Nomina Anatomica Veterinaria (NAV) equivalents.

Abducens Nerve	Nervus abducens (NAV)
Accessory Palatine Artery	(Evans, 1993)
Accessory Palatine Foramen	(Wible and Rougier, 2000); Minor Palatine Foramen (Evans, 1993)
Accessory Palatine Nerve	Nervus palatinus accessorius (NAV)
Ala of Vomer	Ala vomeris (NAV)
Alisphenoid	Os basisphenoidale, Ala (NAV)
Angular Process	Processus angularis (NAV)
Anterior Nasal Notch	(Lillegraven and Krusat, 1991)
Anterior Process of Alisphenoid	(Wible et al., in press)
Anterior Process of Malleus	(De Beer, 1937)
Anteromedial Flange of Petrosal	(Wible et al., in press); Periotic Hypotympanic Sinus (Archer, 1976)
Aqueductus vestibuli	(NAV)
Arteria anastomotica	(Wible, 1987)
Arteria diploëtica magna	(Wible, 1987)
Artery of Pterygoid Canal	(Evans, 1993)
Auditory Tube	Tuba auditiva (NAV)
Basilar Sinus	Sinus basilaris (NAV)
Basioccipital	Os occipitale, Pars basilaris (NAV)
Basisphenoid	Os basisphenoidale, Corpus (NAV)
Body of Mandible	Corpus mandibulae (NAV)
Canal for Sigmoid Sinus	New Term
Capsuloparietal Emissary Vein	(Gelderen, 1924)
Carotid Foramen	Canalis caroticus (NAV)
Carotid Sulcus	Sulcus caroticus (NAV)
Caudal Nasal Artery	Arteriae nasales caudales (NAV)
Caudal Nasal Nerve	Nervus nasalis caudalis (NAV)
Caudal Palatine Foramen	(Evans, 1993)
Caudal Tympanic Process of Petrosal	(MacPhee, 1981)
Cavernous Sinus	Sinus cavernosus (NAV)
Cavum epiptericum	(Gaupp, 1902, 1905; De Beer, 1937)
Cavum supracochleare	(Voit, 1909; De Beer, 1937)
Choanae	(NAV)
Chorda Tympani Nerve	Chorda tympani (NAV)
Cochlear Canaliculus	Canaliculus cochleae (NAV)
Cochlear Duct	Ductus cochlearis (NAV)
Cochlear Fossula	(MacPhee, 1981)
Cochlear Nerve	Nervus cochlearis (NAV)
Condylar Process	Processus condylaris (NAV)
Condylod Canal	Canalis condylaris (NAV)
Condylod Vein	(Evans, 1993)
Coronoid Crest	(Evans, 1993)
Coronoid Process	Processus coronoideus (NAV)
Cranial Accessory Nerve	Radices spinales, Nervus accessorius (NAV)
Crista Parotica	(De Beer, 1937)
Crista Petrosa	(Wible, 1990)
Crus breve, Incus	(NAV)
Crus Commune	(Wible, 1990)
Digastric Muscle	Musculus digastricus (NAV)
Ectotympanic	Os temporale, pars tympanica (NAV)
Element of Paaw	(Klaauw, 1923; De Beer, 1937)
Endolymphatic Duct	Ductus endolymphaticus (NAV)
Entopterygoid Crest	(Novacek, 1986)
Epitympanic Recess	Recessus epitympanicus (NAV)
Ethmoid	Os ethmoidale (NAV)

Ethmoidal Foramen	Foramen ethmoidale (NAV)
Ethmoidal Nerve	Nervus ethmoidalis (NAV)
Exoccipital	Os occipitale, Pars lateralis (NAV)
External Acoustic Meatus	Meatus acusticus externus (NAV)
External Jugular Vein	Vena jugularis externa (NAV)
External Nasal Aperture	Apertura nasi osseum (NAV)
External Occipital Protuberance	Protuberantia occipitalis externa (NAV)
Facial Nerve	Nervus facialis (NAV)
Facial Process of Lacrimal	Os lacrimale, Facies facialis (NAV)
Facial Process of Maxilla	Maxillare, Facies facialis (NAV)
Facial Process of Premaxilla	Os incisivum, Facies labialis (NAV)
Facial Sulcus	(MacPhee, 1981)
Fenestra cochleae	(NAV)
Fenestra vestibuli	(NAV)
Foramen acusticum inferius	Ventral Vestibular Area (Evans, 1993)
Foramen acusticum superius	Facial Canal + Dorsal Vestibular Area (Evans, 1993)
Foramen for Frontal Diploic Vein	(Thewissen, 1989)
Foramen for Inferior Petrosal Sinus	(Wible, 1983)
Foramen magnum	(NAV)
Foramen ovale	(NAV)
Foramen rotundum	(NAV)
Foramen singulare	(NAV)
Fossa for Stapedius Muscle	(MacPhee, 1981)
Fossa for Tensor Tympani Muscle	(MacPhee, 1981)
Fossa incudis	(MacPhee, 1981)
Frontal	Os frontale (NAV)
Frontal Diploic Vein	Vena diploica frontalis (NAV)
Frontal Process of Jugal	Os zygomaticum, Processus frontalis (NAV)
Geniculate Ganglion	Ganglion geniculi (NAV)
Glaserian Fissure	Fissura Glaseri (Klaauw, 1931)
Glenoid Fossa	Fossa mandibularis (NAV)
Glenoid Process of Jugal	(Rougier et al., 1998; Wible et al., in press)
Glossopharyngeal Nerve	Nervus glossopharyngeus (NAV)
Greater Petrosal Nerve	Nervus petrosus major (NAV)
Hamulus	Hamulus pterygoideus (NAV)
Hiatus Fallopii	Petrosal Canal (Evans, 1993)
Horizontal Process of Palatine	Os palatinum, Lamina horizontalis (NAV)
Hypoglossal Foramen	Canalis nervus hypoglossi (NAV)
Hypoglossal Nerve	Nervus hypoglossus (NAV)
Hypophysis	(NAV)
Hypotympanic Sinus of Alisphenoid	(Archer, 1976)
Incisive Foramen	Fissura palatina (NAV)
Incus	(NAV)
Inferior Alveolar Nerve	Nervus alveolaris inferior (NAV)
Inferior Petrosal Sinus	Sinus petrosus ventralis (NAV)
Infraorbital Artery	Arteria infraorbitalis (NAV)
Infraorbital Canal	Canalis infraorbitale (NAV)
Infraorbital Foramen	Foramen infraorbitale (NAV)
Infraorbital Margin	Margo infraorbitalis (NAV)
Infraorbital Nerve	Nervus infraorbitalis (NAV)
Infraorbital Vein	Vena infraorbitalis (NAV)
Infratemporal Crest	Crista infratemporalis (NAV)
Infratemporal Fossa	Fossa infratemporalis (NAV)
Internal Acoustic Meatus	Meatus acusticus internus (NAV)
Internal Carotid Artery	Arteria carotis interna (NAV)
Internal Carotid Nerve	Nervus caroticus interna (NAV)
Internal Jugular Vein	Vena jugularis interna (NAV)
Interparietal	Os interparietalis (NAV)
Intracranial Foramen of Stapes	Foramen intracraniale (Fleischer, 1973)
Jugal	Os zygomaticum (NAV)

Jugular Foramen	Foramen jugulare (NAV)
Lacrimal	Os lacrimale (NAV)
Lacrimal Canaliculus	Canaliculus lacrimalis (NAV)
Lacrimal Foramen	Foramen lacrimale (NAV)
Lacrimal Sac	Saccus lacrimalis (NAV)
Lateral Head Vein	(Wible, 1990; Wible and Hopson, 1993; Rougier and Wible, in press)
Lateral Pterygoid Muscle	Musculus pterygoideus lateralis (NAV)
Levator Labii Muscle	Musculus levator labii superioris (NAV)
Longus Capitis Muscle	Musculus longus capitis (NAV)
Major Palatine Artery	Arteria palatina major (NAV)
Major Palatine Foramen	Foramen palatinum majus (NAV)
Major Palatine Nerve	Nervus palatinus major (NAV)
Malleus	(NAV)
Mandible	Mandibula (NAV)
Mandibular Foramen	Foramen mandibulae (NAV)
Mandibular Nerve	Nervus mandibularis (NAV)
Mandibular Notch	(Evans, 1993); Incisura mandibulae (NAV)
Mandibular Symphysis	(Evans, 1993)
Masseter Muscle	Musculus masseter (NAV)
Masseteric Fossa	Fossa masseterica (NAV)
Masseteric Line	(Evans, 1993)
Mastoid Exposure	Mastoid Process (Evans, 1993)
Mastoid Process	Processus mastoideus (NAV)
Maxilla	(NAV)
Maxillary Artery	Arteria maxillaris (NAV)
Maxillary Foramen	Foramen maxillare (NAV)
Maxillary Nerve	Nervus maxillaris (NAV)
Maxilloturbinal	Os conchae nasalis ventralis (NAV)
Medial Pterygoid Muscle	Musculus pterygoideus medialis (NAV)
Mental Foramen	Foramen mentale (NAV)
Minor Palatine Artery	Arteria palatina minor (NAV)
Minor Palatine Foramen	Foramen palatinum caudale (NAV)
Minor Palatine Nerve	Nervus palatinus minor (NAV)
Mylohyoid Line	Linea mylohyoideus (NAV)
Mylohyoid Muscle	Musculus mylohyoideus (NAV)
Mylohyoid Nerve	Nervus mylohyoideus (NAV)
Nasal	Os nasale (NAV)
Nasal Fossa	Cavum nasi (NAV)
Nasal Septum	Septum nasi osseum (NAV)
Nasolacrimal Canal	Canalis nasolacrimalis (NAV)
Nasolacrimal Duct	Ductus nasolacrimalis (NAV)
Nasopalatine Duct	(Cooper and Bhatnagar, 1976); Ductus incisivus (NAV)
Nasopharyngeal Passage	Meatus nasopharyngeus (NAV)
Nerve of Pterygoid Canal	Nervus canalis pterygoidei (NAV)
Nuchal Crest	Crista nuchae (NAV)
Occipital Condyle	Condylus occipitalis (NAV)
Oculomotor Nerve	Nervus oculomotorius (NAV)
Odontoid Notch	Intercondyloid Notch (Evans, 1993)
Ophthalmic Artery	Arteria ophthalmica interna (NAV)
Ophthalmic Nerve	Nervus ophthalmica (NAV)
Ophthalmic Vein	Vena ophthalmica interna (NAV)
Optic Foramen	Canalis opticus (NAV)
Optic Nerve	Nervus opticus (NAV)
Orbital Fossa	Orbita (NAV)
Orbital Process of Lacrimal	Os lacrimale, Facies orbitalis (NAV)
Orbital Process of Maxilla	Maxillare, Facies orbitalis (NAV)
Orbitosphenoid	Os presphenoidale, Ala (NAV)
Orbitotemporal Crest	Crista orbitotemporalis (NAV)
Orbitotemporal Fossa	Orbita + Fossa temporalis (NAV)

Palatal Process of Maxilla	Maxillare, Processes palatinus (NAV)
Palatal Process of Premaxilla	Os incisivum, Processus palatinus (NAV)
Palatine	Os palatinum (NAV)
Paracondylar Process of Exoccipital	Processus paracondylaris (NAV)
Paraflocculus of Cerebellum	Paraflocculus (NAV)
Parietal	Os parietale (NAV)
Parietal Foramen	(Boyd, 1930, 1934)
Pars canalicularis of Petrosal	(Wible, 1990; Wible et al., 1995, 2001)
Pars cochlearis of Petrosal	(Wible, 1990; Wible et al., 1995, 2001)
Perilymphatic Duct	Ductus perilymphaticus (NAV)
Perpendicular Process of Palatine	Os palatinum, Lamina perpendicularis (NAV)
Petrosal	Os temporale, Pars petrosa (NAV)
Piriform Fenestra	Pyriform Fenestra (McDowell, 1958); Foramen lacerum (NAV)
Posterior Auricular Artery	Arteria auricularis caudalis (NAV)
Posterior Semicircular Canal	Canalis semicircularis posterior (NAV)
Posterior Shelf of Masseteric Fossa	(Marshall and Muizon, 1995)
Posterodorsal Process of Premaxilla	(Wible and Rougier, 2000)
Postglenoid Artery	(Archer, 1976)
Postglenoid Foramen	Foramen retroarticulare (NAV)
Postglenoid Process	Processus retroarticulare (NAV)
Postglenoid Vein	Vena emissaria foraminis retroarticularis (NAV)
Postorbital Ligament	Ligamentum orbitale (NAV)
Postorbital Process	Os frontale, Processus zygomaticus (NAV)
Postpalatine Torus	(Novacek, 1986)
Post-Promontorial Tympanic Sinus	(Wible, 1990); Mastoid Epitympanic Sinus (Archer, 1976)
Posttemporal Foramen (Notch)	(Rougier et al., 1992)
Post-Trigeminal Vein	(Wible and Hopson, 1995; Rougier and Wible, in press)
Posttympanic Crest	(Wible et al., in press)
Posttympanic Process	(Kielan-Jaworowska, 1981; Novacek, 1986); Processus retrotympanicus (NAV)
Postzygomatic Foramen	(Gregory, 1910)
Prefacial Commissure	(De Beer, 1937)
Premaxilla	Os incisivum (NAV)
Presphenoid	Os presphenoidale, Corpus (NAV)
Primary Facial Foramen	(Wible, 1990; Wible and Hopson, 1993)
Promontorium of Petrosal	(Evans, 1993)
Prootic Canal	(Wible, 1990; Rougier and Wible, in press)
Prootic Sinus	(Wible, 1990; Rougier and Wible, in press)
Pterygoid	Os pterygoideum (NAV)
Pterygoid Canal	Canalis pterygoideus (NAV)
Ramus Infraorbitalis	(Wible, 1987)
Ramus of Mandible	Ramus mandibulae (NAV)
Ramus Temporalis of Stapedial Artery	(Wible, 1987)
Rectus Capitis Muscle	Musculus rectus capitis ventralis (NAV)
Rostral Tympanic Process of Petrosal	(Wible, 1990; Sánchez-Villagra and Wible, 2002)
Sacculae	Sacculus (NAV)
Sagittal Crest	Crista sagittalis externa (NAV)
Secondary Facial Foramen	(Wible, 1990; Wible and Hopson, 1993)
Secondary Tympanic Membrane	Membrana tympani secundaria (NAV)
Semicircular Canal	Canalis semicircularis (NAV)
Sigmoid Sinus	Sinus sigmoideus (NAV)
Sphenorbital Fissure	(Gregory, 1910); Fissura orbitalis + Canalis opticus (NAV)
Sphenopalatine Artery	Arteria sphenopalatina (NAV)
Sphenopalatine Foramen	Foramen sphenopalatinum (NAV)
Sphenopalatine Vein	Vena sphenopalatina (NAV)

Sphenoparietal Emissary Vein	(Gelderen, 1924)
Spinal Accessory Nerve	Radices spinales, Nervus accessorius (NAV)
Squamosal	Os temporale, pars squamosa (NAV)
Stapedius Muscle	Musculus stapedius (NAV)
Stapes	(NAV)
Stylohyal	Stylohyoideum (NAV)
Stylomastoid Artery	Arteria stylomastoidea (NAV)
Stylomastoid Notch	Foramen stylomastoideum (NAV)
Subarcuate Fossa	Fossa subarcuata (NAV)
Subsquamosal Foramen	(Wible et al., in press)
Sulcus for Inferior Petrosal Sinus	Sulcus sinus petrosa ventralis (NAV)
Sulcus for Prootic Sinus	(Wible, 1990; Wible and Hopson, 1995)
Sulcus for Sigmoid Sinus	(Wible, 1990; Wible and Hopson, 1995)
Sulcus for Sphenoparietal Emissary Vein	(Wible, 1990; Wible and Hopson, 1995)
Sulcus for Superior Petrosal Sinus	Sulcus sinus petrosa dorsalis (NAV)
Sulcus tympanicus	(NAV)
Suprameatal Foramen	(Novacek, 1986)
Supraorbital Margin	Margo supraorbitalis (NAV)
Superior Orbital Fissure	Fissura orbitalis (NAV)
Superior Petrosal Sinus	Sinus petrosus dorsalis (NAV)
Suprameatal Bridge	Dorsal Boundary of External Acoustic Meatus (Evans, 1993)
Supraoccipital	Squama occipitalis (NAV)
Temporal Fossa	Fossa temporalis (NAV)
Temporal Line	Linea temporalis (NAV)
Temporalis Muscle	Musculus temporalis (NAV)
Temporomandibular Joint	Articulatio temporomandibularis (NAV)
Tensor Tympani Muscle	Musculus tensor tympani (NAV)
Tentorium Cerebelli	Tentorium cerebelli membranaceum (NAV)
Tractus spiralis foraminosus	(NAV)
Transverse Canal Foramen	(Sánchez-Villagra and Wible, 2002)
Transverse Crest of Petrosal	Crista transversa (NAV)
Transverse Frontal Sinus	(Archer, 1976)
Transverse Sinus	Sinus transversus (NAV)
Trigeminal Nerve	Nervus trigeminus (NAV)
Trochlear Nerve	Nervus trochlearis (NAV)
Tuberculum tympani	(Toepflitz, 1920)
Tympanic Process of Alisphenoid	(MacPhee, 1981)
Tympanohyal	Tympanohyoideum (NAV)
Tympanum	(NAV)
Utricule	Utriculus (NAV)
Vagus Nerve	Nervus vagus (NAV)
Vein of Prootic Canal	(Rougier and Wible, in press)
Ventral Condylar Fossa	Fossa condylaris ventralis (NAV)
Vermis of Cerebellum	Vermis (NAV)
Vertebral Artery	Arteria vertebralis (NAV)
Vestibular Fossula	(MacPhee, 1981)
Vestibular Nerve	Nervus vestibularis (NAV)
Vestibulocochlear Nerve	Nervus vestibulocochlearis (NAV)
Vomer	(NAV)
Vomeronasal Organ	Organum vomeronasale (NAV)
Zygoma	Arcus zygomaticus (NAV)
Zygomatic Process of Lacrimal	(Kermack et al., 1981)
Zygomatic Process of Maxilla	Maxillare, Processus zygomaticus (NAV)
Zygomatic Process of Squamosal	Os temporale, Pars squama, Processus zygomaticus (NAV)
Zygomatocmandibularis Muscle	(Turnbull, 1970)
Zygomatocmusculus	Musculus zygomatocmusculus (NAV)